

“The information contained in this report was compiled for the use of the Vermont Agency of Transportation. Conclusions and recommendations contained herein are based upon the research data obtained and the expertise of the researchers, and are not necessarily to be construed as Agency policy. This report does not constitute a standard, specification, or regulation. The Vermont Agency of Transportation assumes no liability for its contents or the use thereof.”

1. Report No.	2. Government Accession No.	3. Recipient's Catalog No.
4. Title and Subtitle Prediction and mitigation of scour and scour damage to Vermont bridges		5. Report Date February 20, 2017
		6. Performing Organization Code
7. Author(s) Anderson, Ian A., Dewoolkar, Mandar M., Rizzo, Donna, M., Huston, Dryver R., Frolik, Jeff, Brand, Matthew, and Howard, Lucas		8. Performing Organization Report No.
9. Performing Organization Name and Address School of Engineering The University of Vermont 301 Votey Hall 33 Colchester Ave. Burlington, VT 05405		10. Work Unit No.
		11. Contract or Grant No. 731
12. Sponsoring Agency Name and Address Vermont Agency of Transportation Materials and Research Section One National Life Drive Montpelier, VT 05633		13. Type of Report and Period Covered Final (2012-2016)
		14. Sponsoring Agency Code
15. Supplementary Notes		
16. Abstract Over 300 Vermont bridges were damaged in the 2011 Tropical Storm Irene and many experienced significant scour. Successfully mitigating bridge scour in future flooding events depends on our ability to reliably estimate scour potential, design safe and economical foundation elements accounting for scour potential, design effective scour prevention and countermeasures, and design reliable and economically feasible monitoring systems, which served as the motivation for this study. This project sought to leverage data on existing Vermont		

bridges and case studies of bridge scour damage, and integrate available information from stream geomorphology to aid in prediction of bridge scour vulnerability. Tropical Storm Irene's impact on Vermont bridges was used as a case study, providing damage information on a wide range of bridges throughout the State. Multiple data sources were combined in an effort to include data, which represents the complex, interconnected processes of stream stability and bridge scour, then identify and incorporate features that would be useful in a probabilistic model to predict bridge susceptibility to scour damage. The research also sought to identify features that could be included in inspections and into a scour rating system that are capable of assessing network-level scour vulnerability of bridges more holistically. This research also sought to review existing scour countermeasures and scour monitoring technologies available in the literature and examine efficacy of new, indirect scour countermeasures and passive scour monitoring techniques.

The specific objectives of this research were to: (1) review the literature and identify methods/technologies that are adaptable to Vermont; (2) analyze Tropical Storm Irene bridge damage information and observations by collecting and geo-referencing all available bridge records and stream geomorphic assessment data into a comprehensive database for identifying features that best represent bridge scour damage; (3) conduct watershed analysis on all bridges, including creation of stream power data to assess if watershed stream power improves the prediction of bridge scour damage; and (4) investigate new scour countermeasures and monitoring technologies, and provide recommendations on implementations.

17. Key Words Scour Tropical Storm Irene Countermeasure Monitoring		18. Distribution Statement No Restrictions	
19. Security Classif. (of this report) Unclassified	20. Security Classif. (of this page) Unclassified	21. No. Pages 142	22. Price

ABSTRACT

Over 300 Vermont bridges were damaged in the 2011 Tropical Storm Irene and many experienced significant scour. Successfully mitigating bridge scour in future flooding events depends on our ability to reliably estimate scour potential, design safe and economical foundation elements accounting for scour potential, design effective scour prevention and countermeasures, and design reliable and economically feasible monitoring systems, which served as the motivation for this study. This project sought to leverage data on existing Vermont bridges and case studies of bridge scour damage, and integrate available information from stream geomorphology to aid in prediction of bridge scour vulnerability. Tropical Storm Irene's impact on Vermont bridges was used as a case study, providing damage information on a wide range of bridges throughout the State. Multiple data sources were combined in an effort to include data, which represents the complex, interconnected processes of stream stability and bridge scour, then identify and incorporate features that would be useful in a probabilistic model to predict bridge susceptibility to scour damage. The research also sought to identify features that could be included in inspections and into a scour rating system that are capable of assessing network-level scour vulnerability of bridges more holistically. This research also sought to review existing scour countermeasures and scour monitoring technologies available in the literature and examine efficacy of new, indirect scour countermeasures and passive scour monitoring techniques.

The specific objectives of this research were to: (1) review the literature and identify methods/technologies that are adaptable to Vermont; (2) analyze Tropical Storm Irene bridge damage information and observations by collecting and geo-referencing all available bridge records and stream geomorphic assessment data into a comprehensive database for identifying features that best represent bridge scour damage; (3) conduct watershed analysis on all bridges, including creation of stream power data to assess if watershed stream power improves the prediction of bridge scour damage; and (4) investigate new scour countermeasures and monitoring technologies, and provide recommendations on implementations.

ACKNOWLEDGMENTS

This work was funded by the Vermont Agency of Transportation (VTrans) and the United States Department of Transportation through the University of Vermont Transportation Research Center (UVM TRC).

Partial support from Vermont EPSCoR with funds from the National Science Foundation Grant EPS-1101317, the National Science Foundation's Graduate Research Fellowship Program (NSFGRFP) through the University of Vermont, and Hydrogologic, Inc. is also acknowledged.

The authors would like to give special thanks to Bill Ahearn, Christopher Benda, Carolyn Carlson, George Colgrove, Callie Ewald, Jeff Wayne Symonds, Pam Thurber, Jason Tremblay, and Nick Wark of Vermont Agency of Transportation for their guidance and feedback during this work.

Professors Arne Bomblies, Richard Downer and Eric Hernandez and Alan Howard of the University of Vermont provided valuable guidance in this work. A number of individuals including Josif Bicja, Jeff DeGraff, Evan Fitzgerald, Matthew Gardner, Scott Hamshaw, Seth Jensen, Aaron Lachance, John Lens, Jessica Louisos, James McCarthy, Jon Olin, Roy Schiff and Kristen Underwood provided resources and input for this work.

Many University of Vermont undergraduate students from Civil, Environmental, Mechanical and Electrical Engineering participated in various aspects of this project, particularly the sensor development. These students worked on the scour sensor development as their independent research or capstone design projects. The authors thank and acknowledge the contributions of these students including Sebastian Downs, Caleb Fields, Joseph Hasselman, Heath Hescoek, Griffin Jones, Connor Lacasse, Albin Meli, Cameron Michaud, Trevon Noiva, Brendan Stringer, Adisun Wheelock and Roy Wu. The authors also thank Mr. Michael Fortney for his contribution to some of the hardware and programming associated with the sensor.

Table of Contents

1	CHAPTER 1.....	9
1.1	INTRODUCTION AND MOTIVATION	9
1.2	OBJECTIVES	12
1.3	ORGANIZATION OF THIS REPORT.....	12
2	CHAPTER 2.....	14
2.1	BRIDGE SCOUR TYPES	14
2.2	METHODS TO COMPUTE SCOUR DEPTH.....	17
2.3	SCOUR RATING SYSTEM	20
2.4	VERMONT BRIDGE DESIGN	22
2.5	SCOUR COUNTERMEASURES	23
3	CHAPTER 3.....	27
3.1	INTRODUCTION	27
3.1.1	<i>Bridge Data.....</i>	<i>29</i>
3.1.2	<i>Rainfall Data.....</i>	<i>30</i>
3.1.3	<i>Stream Geomorphic Data.....</i>	<i>30</i>
3.2	GEOSPATIAL ANALYSIS AND DATA PROCESSING.....	31
3.2.1	<i>Selection of Variables and Analysis Method.....</i>	<i>32</i>
3.3	RESULTS AND DISCUSSION.....	37
3.3.1	<i>Damage Classification and Cost Analysis</i>	<i>37</i>
3.3.2	<i>Rainfall.....</i>	<i>39</i>
3.3.3	<i>Bridge Characteristics</i>	<i>40</i>
3.3.4	<i>Bridge Ratings.....</i>	<i>42</i>
3.3.5	<i>Stream Characteristics.....</i>	<i>45</i>
3.3.6	<i>Logistic Regression and Empirical Fragility Estimate</i>	<i>48</i>
3.4	CONCLUSIONS.....	50
4	CHAPTER 4.....	52
4.1	INTRODUCTION	52
4.2	METHODS.....	55
4.2.1	<i>Data Collection.....</i>	<i>55</i>
4.2.2	<i>Bridge Damage Classification</i>	<i>57</i>
4.2.3	<i>Stream Power Computation</i>	<i>59</i>
4.3	RESULTS AND DISCUSSION.....	60
4.3.1	<i>Damage Distribution.....</i>	<i>60</i>

4.3.2	<i>Empirical Fragility Curves</i>	63
4.3.3	<i>Probability Mapping</i>	64
4.4	CONCLUSIONS	67
5	CHAPTER 5	69
5.1	BACKGROUND	70
5.1.1	<i>Optimization and Sensitivity</i>	70
5.1.2	<i>Bridge Scour and Floodplain Access</i>	71
5.1.3	<i>Differential Evolution</i>	73
5.2	METHODS	75
5.2.1	<i>Study Site and Site Model</i>	75
5.2.2	<i>Scour Prediction</i>	79
5.2.3	<i>Differential Evolution (DE) Optimization and HEC-RAS Modifications</i>	79
5.2.4	<i>Cost Function</i>	81
5.3	RESULTS	82
5.3.1	<i>Flood Wave Mitigation</i>	82
5.3.2	<i>Global Search Results</i>	84
5.4	DISCUSSION	86
5.5	CONCLUSIONS	88
6	CHAPTER 6	90
6.1	INTRODUCTION	90
6.2	METHODS	94
6.2.1	<i>Study Sites</i>	94
6.2.2	<i>Streamflow Return Period Estimates Under Non-Stationary Conditions</i>	95
6.2.3	<i>Estimation of Scour Depths for Sacrificial and Non-Sacrificial Embankments</i>	96
6.2.4	<i>Scour Repair Cost Estimates</i>	98
6.2.5	<i>Hydraulic Modeling Techniques</i>	100
6.2.6	<i>Interviews with Professional Engineers</i>	101
6.3	RESULTS AND DISCUSSION	101
6.3.1	<i>Stream Flows</i>	101
6.3.2	<i>Hydraulic Model Results and Scour Predictions</i>	101
6.3.3	<i>Cost Estimates and Scour Predictions</i>	103
6.3.4	<i>Practicing Professional Engineers' Opinion on the Feasibility</i>	107
6.4	CONCLUSIONS	107
7	CHAPTER 7	109
7.1	LITERATURE REVIEW OF EXISTING TECHNOLOGIES	109

7.1.1	<i>Visual Monitoring Methods</i>	110
7.1.2	<i>Portable Instrumentation</i>	110
7.1.3	<i>Fixed Instrumentation</i>	110
7.2	DEVELOPMENT OF A “SMART ROD” SCOUR SENSOR.....	116
7.2.1	<i>Data Acquisition and Communication</i>	118
7.2.2	<i>Accelerometer Sensors</i>	119
7.2.3	<i>Optical Sensors</i>	121
7.3	DISCUSSION AND CONCLUSIONS	123
8	CHAPTER 8	125
8.1	CONCLUSIONS FROM TROPICAL STORM IRENE CASE STUDY AND DATABASE ANALYSIS WORK .	125
8.2	CONCLUSIONS FROM HYDRAULIC MODELING WORK	127
8.3	CONCLUSIONS FROM SCOUR SENSOR DEVELOPMENT WORK.....	127
8.4	SPECIFIC CONCLUSIONS AND RECOMMENDATIONS TO VTRANS BASED ON THE LITERATURE REVIEW AND RESEARCH	128
9	REFERENCES	131

CHAPTER 1

PROBLEM STATEMENT AND RESEARCH FOCUS

1.1 Introduction and Motivation

Bridge scour is the removal of streambed soil and sediments from the supports of the bridge foundations caused by water induced-erosion. Scour is the leading cause of bridge failure in the United States, with 20,904 bridges listed as scour critical nationwide (Gee, 2008). Hydraulic-caused damage accounts for 52% of bridge failures, with the presumed primary cause being scour (Cook et al. 2015). The increasing occurrences of flood events, and an increase in their magnitude will likely result in greater instances of scour damage to bridges. Scour can be categorized into three main components: long-term aggradation and degradation of the river bed due to erosion and deposition of materials, contraction scour resulting from narrowing of the flow, and local scour caused by a disturbance of the water flow at piers or abutments (Arneson et. al, 2012). In addition to the three scour processes, when designing a new structure, lateral stream migration must be taken into account (Arneson et. al, 2012). The collection of these scour components creates a general category of damage to bridges which encompasses all of the erosive and hydrodynamic related changes to the bridges state.

Current methods for rating and monitoring bridges for scour typically rely on (1) visual inspection, and (2) available scour calculations at the time of bridge design to predict a bridge's vulnerability to scour. Hydraulic and scour calculations are typically conducted during the initial design and construction phase, and rarely updated. These initial scour calculations are then supplemented regularly with direct observations of scour during biannual inspections. For example, the Vermont Agency of Transportation (VTrans) inspection rating system is based on the Federal Highway Administration's National Bridge Inventory coding guide (FHWA, 2015). The National Bridge Inventory scour rating is based on the scour depth in relation to the bridge foundation and scour design calculations. As the scour depth approaches the bottom of the foundation, the bridge becomes at risk of failure and is rated as scour critical. Scour critical bridges require that a plan of action be created, outlining the steps to address the deficient bridges. In Vermont, 815 of the over 4,000 hydraulic bridges have a hydraulic and scour report on file, with approximately 25% of the 2,249 inspected bridges being rated scour critical, or have an unknown foundation. The population of scour critical and unknown foundation bridges would likely increase if the remaining uninspected local bridges were included.

Scour can occur in a variety of ways at a bridge, and act over vastly different temporal ranges. Normal flow conditions can lead to continuous scour at a bridge, but often occurs slowly such that observation and maintenance can prevent major damage. Flood flows have the potential to cause large amounts of scour over short periods of time, faster than repairs can be made, possibly resulting in a bridge

moving from a stable to failed state without much notice. Changes in the stream stability and dynamics can result in a changing scour potential at the bridge below the affected reaches. Two scenarios can be hypothesized in which this system could incorrectly predict scour vulnerability. The first is when design information on the bridge's foundation or hydraulic and scour calculations are not available, as is common on older and smaller local bridges. The second is when hydraulic conditions and scour calculations used in the initial design were never or are no longer valid. Though current design measures may be able to produce a bridge that is robust enough to survive the scour produced by extreme events, thousands of existing bridges across the country are not adequately designed or maintained in relation to scour vulnerability under extreme flood events, and are at risk of premature end of service life. The hidden nature of foundation scour leaves the public unaware as a bridge becomes at risk of failure due to foundation undermining from scour.

Scour is by far the primary cause of bridge failures in the United States (Kattell and Eriksson, 1998). Arneson et al. (2012), FHWA (2015) and others report numerous examples of scour related bridge damage and failure. Regionally, Vermont bridges experienced extraordinary damage on August 28, 2011, when Tropical Storm Irene hit the State of Vermont. Tropical Storm Irene entered Vermont with sustained winds of 50 mph and deposited 100-200 mm (4-8 inches) of rain across the State. Tropical Storm Irene had a rainfall recurrence interval for a twelve-hour storm that exceeded 500 years in some areas and set record flows in nine Vermont streams. Nine other streams had peak flows among the top four on record (USGS, 2011). The flooding and high stream flows that resulted from Tropical Storm Irene were reported to have impacted 223 of Vermont's 251 towns and cities and caused damage or failure to over 300 Vermont bridges (State of Vermont, 2012). Significant number of bridges experienced damage that could be associated with scour. Examples of scour-related damage to Vermont bridges from Tropical Storm Irene are included in Figure 1.1.

Tropical Storm Irene was the second worst flooding event on record for Vermont, after the storm of November 1927, which dropped 150 mm (6 inches) or more of rain over a three-day period (State of Vermont, 2012). Both storms were preceded by a series of higher than average rainfall events, resulting in saturated ground conditions that exacerbated flood conditions. The occurrence of such severe events, those ranging in the 99th percentile of intensity, are happening more frequently, especially over the past three to five decades (Horton, et al., 2014). Climate data show that Vermont is experiencing more extreme events, and that this trend is predicted to continue with more significant floods and major flooding (Frumhoff et al., 2007; Stager and Thill, 2010) demanding more resilient approaches to scour and erosion mitigation.



*Approach scour
(Ludlow, VT).*



Approach scour (Orleans, Vermont)



*Foundation scour
(Dummerston, VT)*

Figure 1.1 – Examples of scour-related damage to Vermont bridges in Tropical Storm Irene (VTrans, 2014)

Successfully mitigating scour-related problems associated with bridges depends on our ability to reliably estimate scour potential, design safe and economical foundation elements accounting for scour potential, design effective scour prevention and countermeasures, and design reliable and economically feasible monitoring systems, which served as the motivation for this study.

The research team discussed with the technical advisory committee (TAC) various possible research directions for this study at the project kick-off and then through follow ups with members of TAC. These discussions led to the focus on identifying and/or developing appropriate tools that are adaptable/relevant to Vermont and utilizing all available data including the Tropical Storm Irene-related data and the Rapid Geomorphic Assessment (RGA) data that are uniquely available for a large number of Vermont streams. A single physics-based model cannot capture all of the highly non-linear, interdependent processes that affect scour; and therefore, a semi-empirical/statistical model/analysis based on field observations would be desirable for a number of reasons. One, the analysis would be inherently able to account for interdependent factors in the aggregate and could lead to probabilistic assessment of risk associated with bridge damage, particularly in extreme flood events similar to Tropical Storm Irene. Since the science of scour prediction on a regional basis is still developing, this analysis could provide the ability to identify the most influential factors for scour damage. Second, this model could account for differences in geomorphic conditions across the state. Third, this analysis can, and probably should, be used beyond the life of this study to refine the predictive tools as a longer climate record develops, and with changes in bridge and roadway design and construction technology. It was determined desirable to analyze available bridge data from Tropical Storm Irene as well as other bridge databases including available bridge inspection records. The TAC suggested a review of countermeasures for scour mitigation and identify/examine techniques appropriate for the conditions specific to Vermont. Regarding scour sensing technologies, although desirable to deploy sensors at select bridge sites, field deployment would depend on the costs of available sensors. The research team suggested exploring development of passive scour sensing technologies as part of undergraduate capstone courses.

1.2 Objectives

This project sought to leverage data on existing Vermont bridges and case studies of bridge scour damage, and integrate available information from stream geomorphology to aid in prediction of bridge scour vulnerability. Tropical Storm Irene's impact on Vermont bridges is used as a case study, providing damage information on a wide range of bridges throughout the state, which can be used to determine the significance of the available data. Multiple data sources are combined in an effort to include data, which represents the complex, interconnected processes of stream stability and bridge scour, then identify and incorporate features that would be useful in a probabilistic model to predict susceptibility to bridge scour damage. The research also sought to work towards identifying features that could be included in inspections and possibly into a scour rating system that is capable of assessing network-level scour vulnerability of bridges more holistically. This research also sought to review existing scour countermeasure and scour monitoring technologies available in the literature and examine efficacy of new, indirect scour countermeasure and passive scour monitoring techniques. The specific objectives of this research were to:

1. provide a comprehensive review of literature and identify methods/technologies that are adaptable to Vermont;
2. analyze Tropical Storm Irene bridge damage information and observations by collecting and geo-referencing all available bridge records and stream geomorphic assessment data into a comprehensive database for identifying features that best represent bridge scour damage;
3. conduct watershed analysis on all bridges, including creation of stream power data and conduct feature selection on the comprehensive database to assess if watershed stream power improves the prediction of bridge scour damage; and
4. investigate new scour countermeasures and monitoring technologies, and provide recommendations on implementations.

1.3 Organization of this Report

This chapter follows with Chapter 2 that presents a concise literature review on bridge scour case studies, methods to compute scour depth, scour rating system, scour countermeasures and scour monitoring technologies.

Chapter 3 presents network-level analysis of Vermont bridges damaged in 2011 Tropical Storm Irene, with focus on scour-related damage. A comparable analysis of damaged and non-damaged bridges identifies significant factors of bridge vulnerability under extreme flood events. Descriptions of the damage

appear as case studies that include pre-storm bridge and stream geomorphology conditions. The georeferenced data include rainfall amounts, damage type and extent, estimated repair costs, bridge characteristics, bridge ratings, and stream geomorphic assessments from a number of sources: VTrans Bridge Inventory System, the State Short Structure Inventory Lists, Regional Planning Commission's Vermont Online Bridge and Culvert Inventory Tool, the Vermont Department of Emergency Management's records of town-owned bridges, and the Vermont Agency of Natural Resources' stream Rapid Geomorphic Assessment data.

Chapter 4 links watershed stream power to the bridge damage from Tropical Storm Irene, develops a process to quantify the hazard at bridges both as a case study and for future storms, and uses stream power as a hazard metric to produce probabilistic predictions of bridge vulnerability. The analysis also offers a comparison between damaged bridges and bridges that were not damaged in Tropical Storm Irene. For this purpose, Specific Stream Power (SSP) and the *event-based* Irene Specific Stream Power (ISSP) are computed for all bridges in the State.

Chapter 5 examines an indirect scour countermeasure/mitigation strategy by restoring floodplain access at a bridge site. Lack of floodplain access at bridges often increases stream velocities, worsening in-stream incision and bank erosion, which in turn increases vulnerability to scour. It is hypothesized that a better access to floodplain at a scour-critical bridge would reduce water flow, velocity and surface elevation leading to decreased scour potential at the bridge. A specific bridge site serves as a test case for this proof-of-concept study that utilizes a steady flow Hydrologic Engineering Center's River Analysis System (HEC-RAS) model of the bridge with a new optimization wrapper based on differential evolution concepts.

Chapter 6 presents another indirect scour countermeasure/mitigation proof-of-concept study that tests the efficacy of using approach embankments as intentional sacrificial "fuses" to protect the integrity of bridges with minimal damage during large flow events by allowing the streams to access their natural floodplain and reduce channel velocities and scour. The study employs steady flow HECRAS models for three specific Vermont bridges on two river reaches. The development of Bayesian streamflow return period estimators using available United States Geological Survey (USGS) stream gauge data enables evaluation of sacrificial approach embankments under non-stationary climatic conditions. Cost-effectiveness of this strategy is also examined.

Chapter 7 documents prototype development of two proof-of-concept, low-cost scour sensors potentially suitable for monitoring scour and redeposition continuously, and communicating the readings wirelessly in real time to stake holders.

Chapter 8 concludes this report with overall conclusions and recommendations to VTrans.

CHAPTER 2

LITERATURE REVIEW

The literature review focuses on five aspects related to bridge scour, the common types and their manifestations, a review of the available literature on equations used to compute the scour depth, the current scour rating system, the Vermont bridge design process, and scour countermeasures.

2.1 Bridge Scour Types

The literature suggests that total bridge scour can be divided into various components that are considered independent and additive, including general scour and local scour. The latter is further subdivided into contraction scour, abutment scour, and pier scour (Briaud et al., 2011). Most research has focused on the three components of local scour. Therefore, this section provides an overview of the local scour evaluation process for contraction scour and pier or abutment scour.

Contraction scour is the erosion of material from the bed and banks across all or most of the channel width, resulting from the contraction of flow area imposed by the bridge abutments and piers, as depicted in Figure 2.1. As flow increases, filling the channel and spilling water onto the flood plains, it often meets conflict at the bridges. Bridge abutments and embankments used to elevate the bridge deck over the river to an appropriate freeboard, creates obstructions to the flow in the floodplain. Common forms used are wing-wall abutments, vertical-wall abutments, and spill through abutments commonly embedded in earthen embankments. Many smaller span bridges also have abutments placed within the channel, causing constriction even in low flows. The blockages caused by abutments in the channel or floodplain force the flow through a smaller section, creating higher velocities and shear stresses. At severally contracted sections, backwater occurs upstream, and large-scale turbulences dominate the flow field. Contraction scour has traditionally been classified as live-bed or clear-water, which reflects the bed material sediment-transport conditions of approaching flows. In the case of live-bed scour, the common assumption is that scour will cease when the load of sediment transported into the contraction is equal to or greater than the load of sediment transported from the contraction. Clear-water scour is the case when no upstream bed movement is occurring.

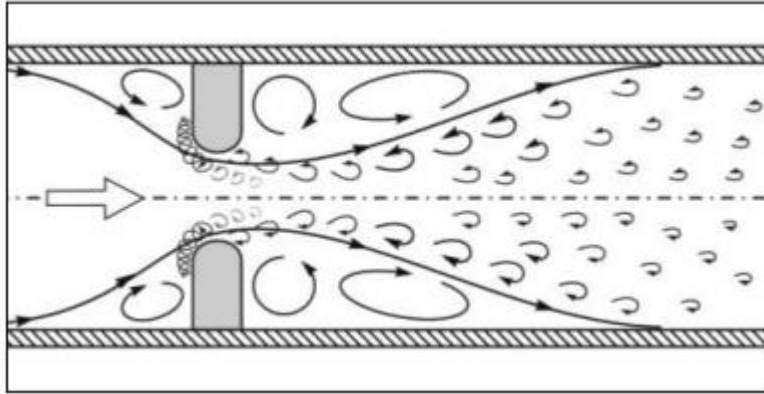


Figure 2.1: Short contraction at a bridge (Ettema et al. 2010)

Local pier or abutment scour is the removal of bed material from around flow obstructions such as piers, abutments, spurs, and embankments caused by the local flow field induced by a pier or abutment, as depicted in Figures 2.2 and 2.3. Abutments are essentially erodible short contractions. High flow velocities and large-scale turbulences around abutments erode the boundary soils. Scour holes typically develop near the end of the abutments, where the wake vortices are the greatest. Geotechnical stability of the embankment is also a key component to abutment scour, if the scour causes geotechnical failure, then the abutment can be treated as a pier.

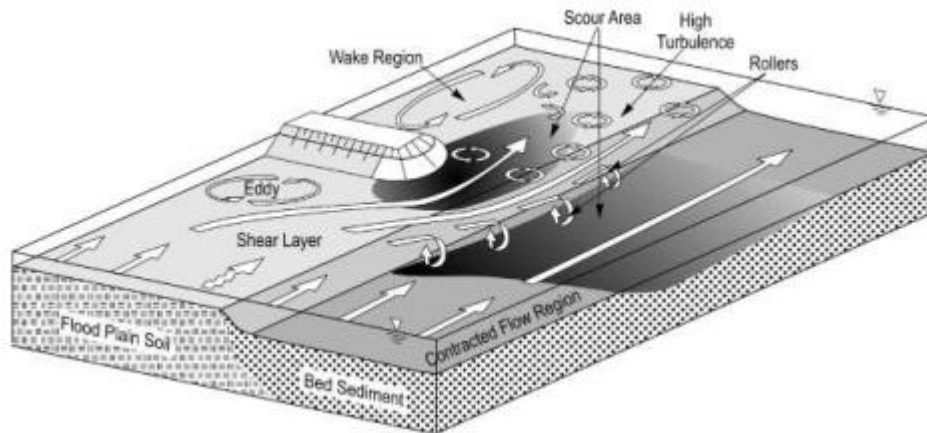


Figure 2.2: Example of the flow patterns and vortices which result in abutment scour (Ettema et al. 2010)

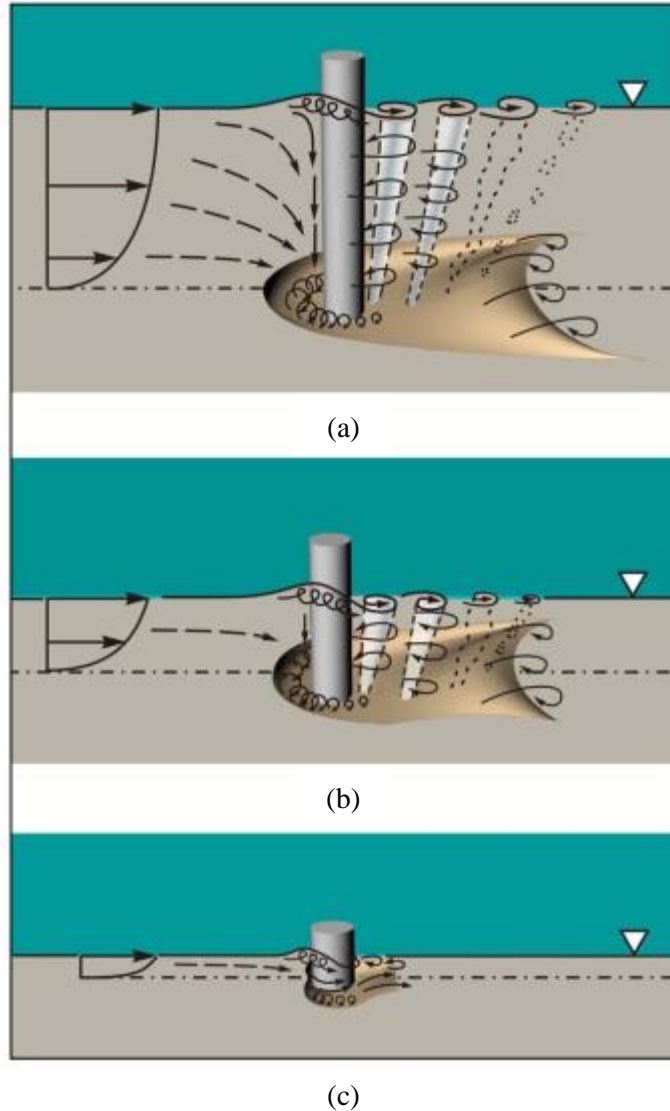


Figure 2.3: Vortices from a pier obstructing flow, resulting in local pier scour at (a) narrow, (b) transitional, and (c) wide pier (Ettema et al. 2011)

Local scour at piers has been studied extensively in the laboratory in single soil layers; however, there is limited field data. The common inverted-frustum scour hole has been seen in single layer sediments. The laboratory studies have been mostly of simple piers, but there have been some laboratory studies of complex piers (Richardson and Davis 2001, Sheppard et al 2011). Often the studies of complex piers are model studies of actual or proposed pier configurations. To understand pier scour, it is necessary to understand the flow field at a pier, and how it changes with pier size and form. Notably, it is an unsteady three-dimensional flow field, interacting with a turbulence structure. The scour forces on the soil are generated by flow contraction around the pier, with a downward flow at the piers face, and vary with pier width and form, and flow depth (Figure 2.3). For narrow piers, (depth/width >1.4) the scour is deepest at the pier face, as downward forces create a scour hole, while lateral contraction forces cause an increase in

velocity and shear stress around the piers sides, causing scour. As the scour develops to a hole fully around the pier, the horseshoe vortices strengthen. Transition piers (depth/width >0.2) function much the same as narrow piers, though they result in shallower scour depths. The reduction in depth lowers the potential for down flow, and increases bed friction in the shallower flow. Wide piers (depth/width < 0.2) have very little down-flow, with most of the scour occurring as the flow turns laterally along the face, and causes contraction on the sides. The deepest scour occurs at the pier flanks.

2.2 Methods to Compute Scour Depth

Traditional scour equations are generally considered to not reflect the present knowledge about scour processes, but rather use the primary dimensions of the foundation width and lengths, flow depth, and sediment size to define the structure and geometric scale of the flow field, and thereby scour depth. Total scour depths at a bridge cross-section are the function of stream hydraulic conditions, sediment transport by flowing water, streambed sediment properties, and bridge structure dimensions. The complex interactions among those variables also complicate the scour development. A large number of studies have been conducted on various bridge scour topics and resulted in several physical and numerical models/equations. Scour calculations are often done as the summation of the multiple scour types, with ultimate scour being the combination of contraction, and local scour, from piers or abutments. The state of the art in bridge scour prediction is outlined in the FHWA HEC-18, updated most recently in 2012.

Contraction scour is a major component of the ultimate scour depth, caused by flow accelerations due to narrowing of the channel cross section, either by natural reductions in the main channel width, or by the blockage in the floodplain, returning flow back to the channel. The literature describes a number of semi-empirical contraction-scour equations that were developed by the use of conservation of flow and sediment in a control volume in conjunction with laboratory derived concepts of sediment transport (Straub 1934, Laursen 1963, Melville 1997, Sheppard and Miller 2006). Researchers through laboratory studies (Froehlich 1989, Melville 1992, Liu et al. 1961, Mueller and Wagner 2005, and Laursen 1980) have found that the transport or lack of transport of sediment in the flow approaching an obstruction or contraction is critical in assessing scour at bridges. Floodplain contraction scour is usually treated separately from main channel contraction scour in compound channels. In this case, one of the difficulties in applying a contraction scour formula is the determination of the discharge distribution between the floodplain and the main channel in the bridge section. Both live-bed and clear-water contraction scour can occur in the field. The former commonly occurs in the main channel of a sand-bed river, while the latter is more likely to be found in a floodplain contraction or a relief bridge located on the floodplain. Contraction scour formulas have been developed analytically for an idealized long contraction as will be described subsequently. In the case of live-bed contraction scour, the limiting condition is the continuity of sediment transport between

the approach-flow section and the contracted section. For clear-water scour, the governing principle is that the depth of scour in the contracted section corresponds to the occurrence of critical velocity there as the scour approaches its equilibrium state. Live bed contraction scour is estimated based on Laursen (1960) equations for long contractions, while clear-water scour is based on Laursen (1963).

Some of the notable studies conducted with the purpose of predicting abutment scour include: Froehlich (1989); Melville (1992); Richardson and Davis (2001); Strum (2006), Ettema et al. (2010); and Chang and Davis (1999). Most of these empirical equations were based on laboratory results and field data and they differ from each other with respect to the factors considered in constructing the scour model, parameters used in the equation, laboratory or site conditions, and so on.

Pier scour is the other possible component to the local scour calculation. The Colorado State University (CSU) equation established by Richardson and Davis (2001) has been the dominant method for prediction of pier scour depth. More recent work by Sheppard et al. (2011) through the NCHRP Project 24-32 has established the Sheppard-Melville method, and has begun to replace the older CSU method for most designs. The newer method is believed to better reflect scour processes, while the CSU method is adapted empirically to scour data. Despite the recent advances in modelling the underlying scour processes at piers, determination of scour depths is made difficult due to factors affecting the flow field, complex pier shapes, arrangements and interactions, and difficulties identifying foundation materials.

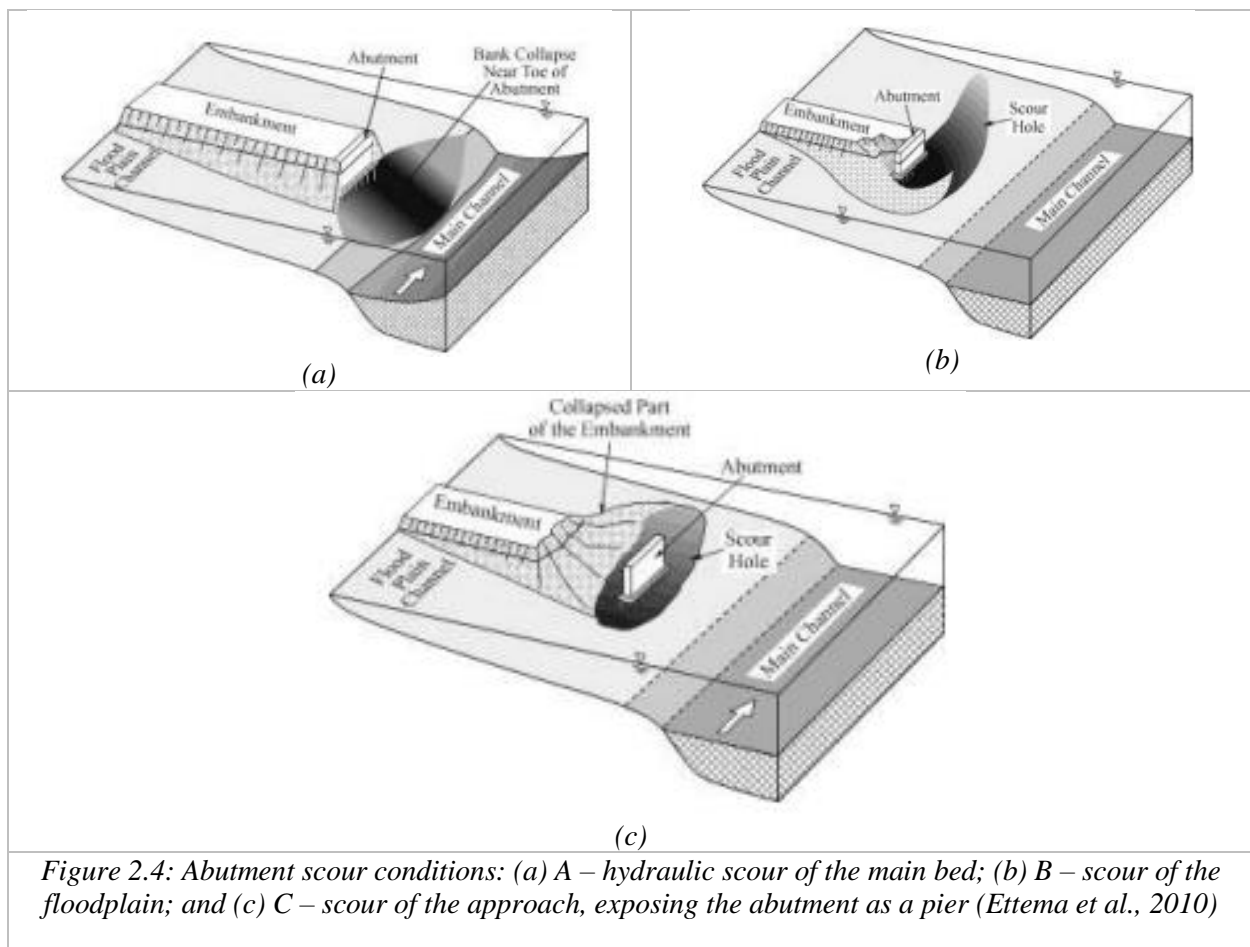
The majority of the methods in HEC-18 were developed by assuming uniform, non-cohesive sediments that are representative of the most severe scour condition, but the erosional resistance of typical soils found at the bridge site is a combination of stratified soils with varying degrees of cohesiveness. The hydraulic parameters used in HEC-18 models are estimated by a one-dimensional hydraulic model such as Water Surface Profile (WSPRO) or Hydraulic Engineering Center's River Analysis System (HEC-RAS) that distributes flow across the approach and bridge opening by conveyance (combination of roughness and flow area); however, the flow distribution at a bridge or in its approach is non-uniform because of cross stream flow caused by channel bed conditions, channel bends, irregular valley topography, and obstructions in the floodplain. The pier scour and contraction scour of some selected models will be discussed here.

The live-bed abutment scour formula developed by Froehlich (1989) and the Highways in the River Environment (HIRE) equation are suggested in HEC-18 (Richardson and Davis 2001). Froehlich's equation is derived from regression analysis applied to a list of dimensionless variables using laboratory data. The HIRE equation is based on field scour data for spur dikes in the Mississippi River obtained by the U.S. Army Corps of Engineers.

Chang and Davis (1998, 1999) presented an abutment scour methodology called ABSCOUR, which has been further developed by the Maryland State Highway Administration (MSHA 2010). ABSCOUR treats abutment scour as an amplification of contraction scour. In addition, the methodology

includes an adjustment/safety factor that is based on the user's assessment of risk and whether the floodplain is narrower or wider than 800 ft (244 m). The full ABSCOUR 9 computer program/methodology includes procedures to refine discharge and velocity distributions and channel setback distances under the bridge; evaluate scour in layered soils; consider the effect of pressure scour; evaluate the slope stability of the embankment; consider degradation and lateral channel movement and other specific concerns. The program is used to integrate contraction, abutment and pier scour and to draw a scour cross-section under the bridge (MSHA 2010).

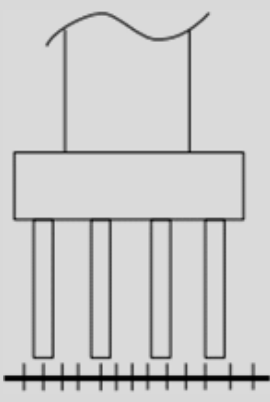
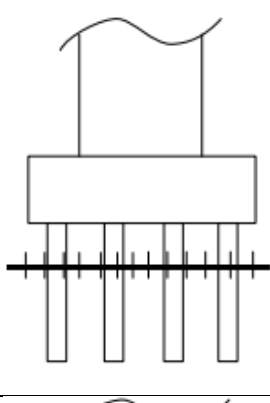
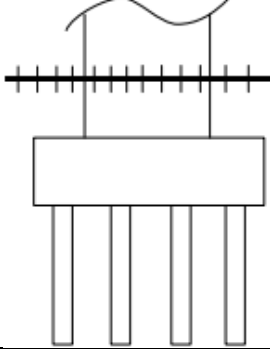
Work resulting from NCHRP24-20 (Ettema et al., 2010) establishes three scour conditions to describe the possible scenarios of abutment and contractions scour (Figure 2.4). This study also related abutment and contraction scour together, treating abutment scour as an amplification of contraction scour, and takes into account geotechnical instability. The three scour conditions are: scour in the main channel leading to undercutting of the embankment and abutment resulting in local collapse, scour in the floodplain around the abutment occurring as clear-water scour, and failure of the approach embankment fully exposing the abutment and resulting in a pier flow field.



2.3 Scour Rating System

The Vermont Agency of Transportation inspection rating system is based on the Federal Highway Administration's NBIS (FHWA, 2015). Vermont's bridge inspections occur on a 24-month basis, with a shorter inspection window for those bridges in need of more immediate attention. As part of the inspection, the scour depth at the bridge is observed. Scour is measured using a variety of techniques from rodding to full underwater inspection when needed. Item 113 of the National Bridge Inventory (NBI) is the Scour Critical Bridge rating, and it details the current status of the bridge regarding its vulnerability to scour. The Scour Critical Bridge rating codes can be seen in Table 2.1 below. The system of scour rating relies on a combination of inspection observations as well as design calculations. The design aspect considers whether the foundation is constructed below the calculated depth of scour for a certain recurrence interval flow. In Vermont, the specific calculated scour depth is either determined during design and construction, or analyzed later as part of a review of scour at bridges. In Vermont, only 882 of the 2,317 hydraulic bridges have a hydraulic and scour report on file. Scour can present itself in a variety of ways at a bridge, and can act over vastly different temporal ranges. Normal flow condition can lead to continuous scour at a bridge, but often occurs slowly enough that observation and maintenance can prevent major damage. Flood flows have the potential to cause large amounts of scour in a short amount of time, faster than any repairs can be made, possibly resulting in a bridge going from a stable to failed condition without notice. As the scour depth approaches the bottom of the foundation, the bridge becomes at risk of failure and is rated as scour critical. Bridge ratings are categorical from 0-9 with an Unknown Foundations (U) category. The scale is not ordinal, instead each rating indicates a specific scenario, not a magnitude of risk. Scour critical bridges are those found to be unstable through either observed scour or have a calculated scour potential greater than the design scour. Ratings of 3 and below are used for scour critical bridges. Bridges with unknown foundations (U) could potentially be added to the scour critical lists. Scour critical bridges require a plan of action be created, outlining the steps needed to address the deficient bridges.

Table 2.1: Scour Ratings Used by VTrans (FHWA, 1995)

Rating	Description	Notes	example
U	No information on the foundation is available – Unknown foundation.	Bridges with U are expected to added to those considered scour critical.	
0	Bridge is scour critical. Bridge has failed and is closed to traffic.	Bridges with ratings 0 through 3 are considered scour critical.	
1	Bridge is scour critical; field review indicates that failure of piers/abutments is imminent. Bridge is closed to traffic.		
2	Bridge is scour critical; field review indicates that extensive scour has occurred at bridge foundations. Immediate action is required to provide scour countermeasures.		
3	Bridge is scour critical; bridge foundations determined to be unstable for calculating scour conditions.		
4	Bridge foundations determined to be stable for calculated scour; field review indicates action required to protect foundations from additional erosion.	Bridges with ratings 4 through 9 are considered non-scour critical.	
5	Bridge foundations determined to be stable for calculated scour conditions; scour within limits of footing or piles.		
6	Scour calculation/evaluation has not been made.		
7	Countermeasures have been installed to correct previously existing scour. Bridge is no longer scour critical.		
8	Bridge foundations determined to be stable for calculated scour conditions; calculated scour is above top of footing. If bridge was screened or studied by experts and found to be low risk, it should fall into this category.		
9	Bridge foundations (including piles) well above flood water elevations.		

2.4 Vermont Bridge Design

The Vermont Hydraulics Manual (VTrans, 2015) outlines the procedures for the hydraulic design of transportation infrastructures crossing streams. Current practice prescribes a minimum freeboard of 1 foot from the low chord to the water surface elevation of the hydraulic design storm. An additional 1 foot is recommended for heavy ice and debris passage. Minimum design frequencies vary based on road classification, with freeways at 1%, principle/minor arterial roads and collector roads at 2%, and local streets at 4% annual exceedance probability (AEP). Analysis of the hydraulic performance of bridge structures is required, with programs such as HEC-RAS, and outlines the process of setting up a model, and contains recommendations for critical parameters for use on VTrans structures. Figure 2.5 is given to aide in selecting flow frequencies for joint probability analysis. The manual outlines the expansion and contraction coefficients of 0.3/0.1 for all cross sections, except the two upstream and one downstream of the bridge, which should be set at 0.4/0.2. Unless significant contraction is present, then it recommends using 0.5/0.3, without defining what significant contraction requires. Peak velocity for use in scour calculations and stone sizing should be taken from the six bridge cross sections, that is the two upstream, the two downstream, and the two internal bridge cross sections. The manual specifically states that HEC-RAS should not be used to calculate scour, but rather used to produce water levels and velocities for external calculations.

Area Ratio $A_R = A_M/A_T$	Frequencies for Coincidental Occurrence							
	10% AEP Design		4% AEP Design		2% AEP Design		1% AEP Design	
	Main Stream	Tributary	Main Stream	Tributary	Main Stream	Tributary	Main Stream	Tributary
$A_R \geq 10,000$	50%	10%	50%	4%	50%	2%	50%	1%
	10%	50%	4%	50%	2%	50%	1%	50%
$1,000 \leq A_R < 10,000$	50%	10%	50%	4%	20%	2%	10%	1%
	10%	50%	4%	50%	2%	20%	1%	10%
$100 \leq A_R < 1,000$	20%	10%	20%	4%	10%	2%	4%	1%
	10%	20%	4%	20%	2%	10%	1%	4%
$10 \leq A_R < 100$	10%	10%	10%	4%	4%	2%	2%	1%
	10%	10%	4%	10%	2%	4%	1%	2%
$1 \leq A_R < 10$	10%	10%	4%	4%	2%	2%	1%	1%
	10%	10%	4%	4%	2%	2%	1%	1%

Note: Shaded values denote design combination for coincidental frequency occurrence. Non-shaded values denote check combination for coincidental frequency occurrence.

Figure 2.5: Vermont Hydraulics Manual recommendations for Joint Probability Analysis (VTrans, 2015)

Scour conditions at the bridge are checked for flows half and a quarter as frequent as the design storm (i.e., if design is 4%, then check at 2% and 1% AEP), as outlined in HEC-18 (Arneson et al., 2012).

Stream geomorphologic change is considered in relation to bridge scour, recommending the Lane calculation outlined in HEC-20 to determine when meanders and braids will form (Lagasse et al., 2012; Lane, 1955). The scour calculations follow Chapter 6 of HEC-18 directly for contraction scour and vertical contraction (pressure) scour. Pier scour, if calculated, follows the HEC-18 procedures outlined in with the CSU and FDOT equations. Abutment scour calculations are not detailed, though the Froehlich (Froehlich, 1989), HIRE equation (Richardson et al., 2001) and the NCHRP 24-20 (Ettema et al, 2010) procedures are mentioned as possible methods. The manual advises that VTrans regards the existing methods as over conservative, and in the absence of their implementation, recommends countermeasures to protect against abutment scour. The footing depth of the abutment is recommended to be placed below the greater of the sum of the contraction and long term degradation (the adjusted thalweg), and 1.8m below the thalweg. If the bridge spans greater than 1.5 the bankfull width, and a geomorphic assessment has determined the stream to be horizontally and vertically stable, the foundations can be raised at a 2H:1V from the edge of the bankfull width.

2.5 Scour Countermeasures

Local scour is a hazard to bridge safety, and the integrity of our transportation system, and can be difficult to predict and detect. Bridge scour countermeasures include systems to monitor, control, inhibit, delay, or minimize stream instability and bridge scour problems. In addition to adequately designing bridges to provide ample flow, and reducing stresses, armoring bridge foundations with countermeasures is often used to increase the resistance to the erosive effects of heavy storm flows. Most bridge scour armoring countermeasures seek to increase the robustness of the bridge foundation support material, acting to prevent or reduce scour erosion. Design selection and installation guidelines were summarized in HEC-23 (Lagasse et al. 2009), providing national guidance on the use of scour countermeasures. Monitoring structures during or after flood events can also be considered an appropriate countermeasure. What follows is a summary of the common armoring countermeasure, monitoring is discussed in Chapter 7.

The most common and widely used countermeasure is the use of riprap, placing rough stone layers over the natural soils, to increase the protection. An extensive review of experiments, model studies, and laboratory tests is provided in Parker et al. (1998). When used properly riprap has an advantage over rigid structures of being flexible and remaining functional even if partial failure occurs. Riprap requires regular inspection and maintenance to ensure functionality, particularly after large storm events, which often displace loose riprap. The ability of the riprap layer to provide scour protection is, in part, a function of stone size, which is a critical factor in terms of shear failure (Lagasse et al. 2009). Common failures in riprap occur when the stones are not large enough to withstand the shear velocities associated with the downstream and horseshoe vortices. Winnowing failure occurs in the absence of a geotextile filter fabric,

allowing for the finer bed materials to be removed through the voids of the riprap layer. Edge failures occur when there is instability at the edges and faces of the coarse riprap layer, causing scour holes and progressive failures toward the bridge foundation. The riprap is undermined from the perimeter in, destabilizing the entire layer. Under high flow events, turbulent flow can often produce forces high enough allowing for transport or translation of the material away from the foundation. Common applications are either on the surface of the bed (Figure 2.6a), in an excavation or existing scour hole (Figure 2.6b), in a depth below the bed level (Figure 2.6c) to prevent scour beyond the application depth. Results in NCHRP 593, (Lagasse et al., 2007) recommend riprap be placed at a thickness twice the d_{50} (median diameter) of the aggregate and a width of twice the pier width in all directions. The riprap layer should be placed in a pre-excavated hole, so that the finished top surface is flush with the existing bed, as to not create additional obstruction, and that geotextile filters should underlie the riprap, but terminate two-thirds the distance from the pier to the edge of the riprap.

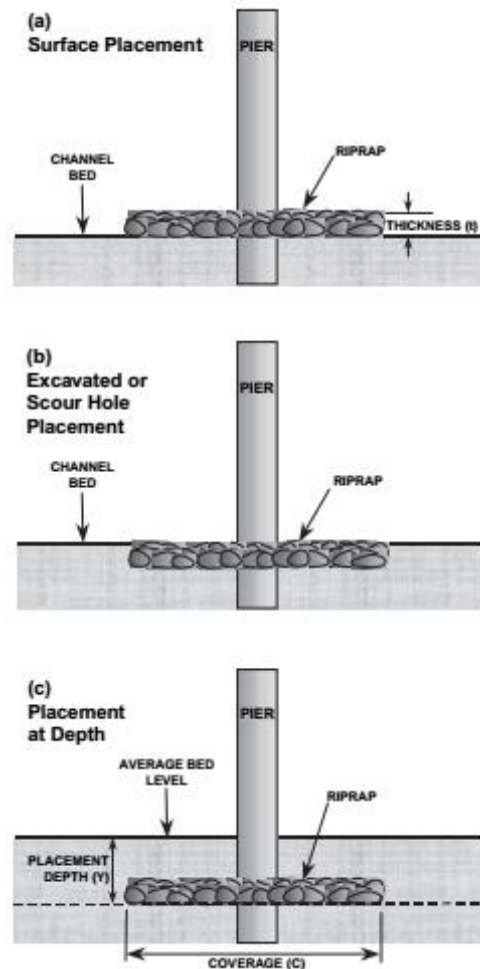


Figure 2.6: Typical riprap application at a bridge pier (Lagasse et al, 2007)

A more advanced and substantial countermeasure would be to partially or fully grout riprap together, to form a rigid defense for the foundation. Grouting riprap produces a larger effective aggregate size, as seen in Figure 2.7. Though not widely used for bridge applications in the United States, it has seen wide application in Europe (Escarameia 1998; CUR 1995). Partial grouting would fill up to 50% of the void space with a highly flowable grout, which when it cures will lock the system together, creating a stable platform to prevent local scour. Fully grouted riprap is often constructed with smaller rocks, allowing for decreased layer thicknesses, and reduced material costs. Partial grouted riprap provides a suitable alternative to fully grouting, as it alleviates the concerns of completely filling the surface voids. Partial grouting increases the stability of the riprap, without sacrificing flexibility, and reduced chances of the entire riprap layer failing through undermining or uplift. Geotextile filters are used to prevent winnowing of the underlying bed material, and is a common recommendation for most well designed countermeasure applications.



Figure 2.7: Partially grouted riprap aggregate (Lagasse et al, 2007)

Results of NCHRP 593 (Lagasse et al. 2007) recommend the partially grouted riprap extend one and a half times the pier width in all directions, and be twice the d_{50} in thickness. When placement is to occur underwater, the thickness should be increased by 50%. The geotextile filter should extend two-thirds of the distance from the foundation to the edge of the riprap. Specifics on grout preparation and admixtures for underwater application can be found in Appendix D of NCHRP 593 (Lagasse et al. 2007). Aggregate sizes below a d_{50} of 9 in. have voids too small to effectively grout, while those with d_{50} above 15 in. are too large to retain grout.

Articulated concrete block (ACB) and Gabion Mattresses systems provide a flexible armor as a local scour countermeasure. ACB systems are made up of prefabricated concrete units that interlock, and

are able to articulate while remaining linked, often tied together by cable. The ACB systems form a continuous mat, as the partially or fully grouted riprap do, but are able to adapt to changing subbase conditions. Specifications and design guidelines for installations and anchoring of ACB systems are provided in HEC-11 (Brown and Clyde 1989). Gabion Mattresses are wire mesh containers filled with rock, often with cells tied together with wire, to create an erosion resistant veneer. Examples of ACB and gabion mattresses can be seen in Figure 2.8. Both gabion mattresses and ACB require less excavation, as they can be placed with smaller depth than riprap armoring, but are prone to undermining and uplift at the periphery. Based on the experiments conducted as part of NCHPR 24-07(2), Lagasse et al. (2006) recommend placement of riprap at twice the width of the pier in all directions, and geotextile extending fully to the edge of the application. The edges of each system must be tied down into a termination trench to prevent failure, and should not be placed at greater than 2H:1V slope.

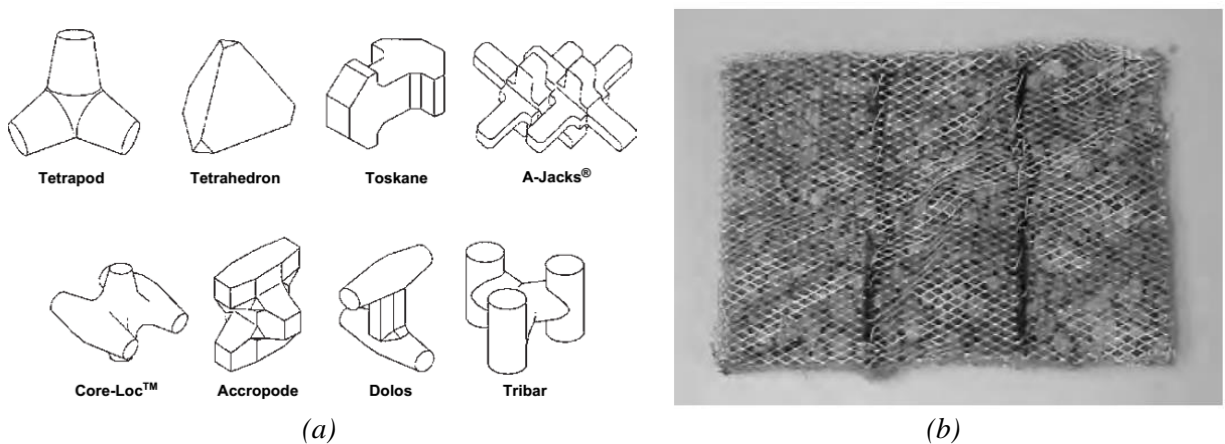


Figure 2.8: (a) Common precast ACB shapes, and (b) a 3-cell gabion mattress (Lagasse et al, 2007)

Geotextiles are an important component of any well designed countermeasure. Geotextile filters are crucial to prevent winnowing through the voids. Geo-containers filled with coarse or fine aggregate can be used beneath riprap armoring to create an additional layer of designed protection, reducing undermining, while still maintaining a flexible and adaptable base. One common problem with geotextile placement underwater is the low specific gravity (0.90-0.96) causing them to float, and be caught as a sail in the flow (Koerner 1998). New geotextiles developed for underwater implementation were created with two layers of non-woven geotextile interlaid with sand, to create a filtering geocomposite, with a desirable specific gravity of 1.5-2, which can sink readily (Heibaum 2002). When placement underwater is needed, sand filled geo-containers are easier to deploy, and create an appropriate filter layer below loose riprap countermeasures.

CHAPTER 3

ANALYSIS OF BRIDGE AND STREAM CONDITIONS OF OVER 300 VERMONT BRIDGES DAMAGED IN TROPICAL STORM IRENE

(An article based on this chapter has been accepted in the journal *Structure and Infrastructure Engineering*. The authors of this article are Ian A. Anderson, Donna M. Rizzo, Dryver R. Huston, and Mandar M. Dewoolkar)

Synopsis:

The 2011 Tropical Storm Irene deposited 100-200 mm of rain in Vermont with a rainfall recurrence interval for a twelve-hour storm exceeding 500 years in some areas. This single hurricane-related event damaged over 300 bridges. The wide range of damage prompted a network-wide analysis of flood, scour, stream and structural conditions. A first step was the assembly of a unique dataset containing information on 326 damaged bridges, 1,936 undamaged bridges and the surrounding stream conditions. Descriptions of the damage appear as case studies that include pre-storm bridge and stream geomorphology conditions. The assembled and georeferenced data include rainfall, damage type and extent, estimated and actual repair costs, bridge characteristics, bridge ratings, and stream geomorphic assessments from a number of sources. The analyses identified significant features of bridge vulnerability under extreme floods. The bridge age and rating assessment characteristics, such as substructure, channel, and structural adequacy ratings, followed by scour, waterway adequacy, and sufficiency ratings, correlated strongly to damage. The stream geomorphic features have promise to supplement future bridge rating systems and in identifying hydraulic vulnerability of bridges. Empirical fragility curves relating probability of meeting or exceeding different bridge damage levels based on channel and waterway adequacy ratings are also presented.

3.1 Introduction

On August 28, 2011 Tropical Storm Irene hit the state of Vermont with a severity that caused major damage throughout the state and impacted 225 of the state's 251 towns and cities (State of Vermont, 2012). Tropical Storm Irene entered with sustained winds of 80 km/h and deposited 100-200 mm (4-8 inches) of rain across the state (NWS, 2011). The greatest rainfall totals were along the higher elevations of the state's mountain ranges (State of Vermont, 2012). At these higher elevations, intense rain caused flash flooding, and progressed to widespread flooding throughout Central and Southern Vermont. The rainfall recurrence interval for a twelve-hour storm exceeded 500 years in some areas, with widespread rainfall in excess of the 100 year recurrence interval where damage was reported. It caused record flows in nine streams. Nine other streams had peak flows among the top four on record (USGS, 2011). This was the second worst state-wide flooding event on record, after the storm of November 1927, which dropped 150 mm (6 inches) or more of rain over a three-day period (State of Vermont, 2012). Both storms were preceded by a series of

higher than average rainfall events, resulting in saturated ground conditions that exacerbated flood conditions. The flooding and high stream flows resulting from Tropical Storm Irene reportedly caused damage or failure to 389 Vermont bridges per Thomas et al. (2013).

Other recent extreme events have caused damage to numerous bridges in other parts of the United States. For example, studies from Hurricane Katrina in 2005 indicate that uplifting and hydrodynamic forces on the superstructure caused the majority of the damage to short and medium span coastal bridges (Okeil and Cai, 2008). An economic analysis of 44 bridges damaged from Hurricane Katrina shows a relationship between surge elevation, damage level and repair costs (Padgett et al., 2008). Subsequent analysis of 262 bridges, of which 36 were damaged, identifies surge elevation as a key factor in determining damage levels from Katrina, and relates it to the estimated likelihood of damage through empirical fragility curves (Padgett et al., 2012). Both of these studies leverage the National Bridge Inventory (NBI) as the primary source of bridge data. Similar bridge infrastructure vulnerabilities have been witnessed at Escambia Bay, Florida during the 2004 Hurricane Ivan (Douglass et al., 2004) and in Hokkaido, Japan during the 2004 Songda Typhoon (Okada et al., 2006). More recently, severe flooding in September 2013 caused the collapse of 30 highway bridges, and damage to an additional 20 bridges in Colorado (Kim et al., 2014).

For some time now, scour has been recognized as the primary cause of bridge failures in the United States (Kattell and Eriksson, 1998) and in other parts of the world providing case studies on bridge damage. For example, Wardhana and Hadipriono (2003) analyzed 503 cases of bridge failures in the United States from 1989 to 2000, and found that flood and scour caused nearly 50% of all failures. Melville and Coleman (1973) report 31 case studies of scour damage to bridges in New Zealand, of which 13, 8, 4 and 6 cases were primarily attributed to pier failure, erosion of the approach or abutment, general degradation, and debris flow or aggradation, respectively. The HEC-18 document (Arneson et al., 2012) mentions numerous examples of scour related bridge damage and failure. During the spring floods of 1987, 17 bridges in New York and New England were damaged or destroyed by scour. The collapse of the I-90 Bridge over the Schoharie Creek near Amsterdam, NY, resulted in the loss of 10 lives and millions of dollars in bridge repair and replacement costs (FHWA, 2015). In 1985, floods in Pennsylvania, Virginia, and West Virginia destroyed 73 bridges. A 1973 national study (FHWA 1973) of 383 bridge failures caused by catastrophic flooding showed that 25 percent involved pier damage and 75 percent involved abutment damage. A second more extensive study in 1978 indicated local scour at bridge piers to be a problem about equal to abutment scour problems (FHWA, 1978; Arneson et al., 2012). The 1993 flood in the upper Mississippi basin caused damage to 2,400 bridge crossings (FHWA, 2015) including 23 bridge failures. The modes of bridge failure included 14 from abutment scour, 3 from pier and abutment scour, 2 from pier scour only, 2 from lateral bank migration, 1 from debris load, and 1 from an unknown cause (Arneson et al., 2012). Arneson et al.

(2012) also reported that the 1994 flooding from storm Alberto in Georgia affected over 500 state and locally owned bridges with damage attributed to scour.

The above case history summary of bridge damage, both coastal and inland, illustrates the vulnerability of existing bridge infrastructure to extreme flooding events. The occurrence of such severe events is expected to increase because of climate change in many parts of the world will shift precipitation patterns (Melillo et al., 2014). For example, extreme rainfall events, those ranging in the 99th percentile of intensity, are happening more frequently, especially over the past three to five decades (e.g., Horton et al., 2014). The effects of Tropical Storm Irene on Vermont bridges therefore provide a uniquely large dataset, where a single hurricane-related extreme flood event caused widespread damage to over 300 bridges in a single state. The network-wide analysis on damaged and statistically comparable non-damaged bridges on a dataset this large is believed to be not available in the literature. This paper presents example case studies including descriptions of the damage and corresponding estimated and actual repair/replacement costs, and feature-based analysis of observed damage. A univariate statistical comparison between damaged and comparable non-damaged bridges identifies an initial set of significant features of bridge vulnerability under extreme events. An ordinal logistic regression further tests those features individually against damage level, revealing features that are correlated to increasing damage. The most significant features may be used to generate fragility curves showing probability for exceeding levels of damage under extreme events for a given feature; and examples are presented.

3.1.1 Bridge Data

To study the effects of Tropical Storm Irene on Vermont's bridge infrastructure, a comprehensive database of all available records on bridges prior to the storm was compiled. The data collection and assembly identified geo-referenced locations and information for all river and stream crossing bridges, including all available inspection data and relevant photographic records. This encompassed 4,761 state- and town-owned bridges from the Vermont Agency of Transportation (VTrans) Bridge Inventory System (BIS). The BIS functions as a record for all bridge inspections conducted in accordance with the Federal Highway Administration's National Bridge Inventory (NBI) coding guide, and contains all bridges, both state- and town-owned over 6 m in span length. For the purposes of this study, we compiled a comprehensive list of all bridge structures, including traditional bridges, stone arches, and open bottom culverts, and applied the general term of "bridge" to all.

Information quantifying Tropical Storm Irene-related damage came from VTrans and the Vermont Department of Emergency Management (VDEM). VTrans provided information on the damage to state-owned bridges. The VDEM collected damage to town-owned bridges for the purpose of applying for Federal Emergency Management Agency (FEMA) repair funding. The damage records were linked to the

comprehensive bridge list to locate and identify the damaged bridges. In some cases, database errors prevented finding a link between the two databases and required further geospatial analysis. This cross-referencing identified 153 bridges in the comprehensive bridge list as having been damaged during the storm. An additional 173 bridges were identified as damaged via a follow-up study of available VTrans online bridge inspection photograph archives, including supplemental inspection photos taken during the post-Tropical Storm Irene recovery. This process identified a total of 326 bridges as having been damaged, with damage ranging from minor streambank erosion to entire bridge collapse. The number of damaged bridges identified in the database (326 bridges) differs from that reported by the VDEM (Thomas et al. 2012, 389 bridges), and is thought to be due to the misclassification of certain culverts as bridges in the higher estimate, as well as rapid and unrecorded post storm bridge repair. Bridges with spans shorter than 6 m were removed from the list, as the analysis relies on inspection records, which are not available for bridges with spans shorter than 6 m. This resulted in 313 damaged bridges available for use in subsequent statistical analysis and feature extraction for comparison with the corresponding 1,950 non-damaged bridges from the comprehensive list of Vermont bridges.

3.1.2 Rainfall Data

The analysis presented here used climate observations collected during Tropical Storm Irene throughout the state of Vermont and surrounding counties in New York, New Hampshire and Quebec (Springston et al., 2012). Ordinary Kriging was used to generate a spatial interpolation of the rainfall measurements over the entire state of Vermont, and provided the average recurrence interval (ARI), using a 12-hr duration storm to match the duration of Tropical Storm Irene (Kiah et al., 2013).

3.1.3 Stream Geomorphic Data

The Vermont Agency of Natural Resources (VTANR) has been quantitatively assessing the hydraulic stability and sensitivity of Vermont streams over the past 15+ years. The River Management Program developed and utilized a set of peer-reviewed stream assessment protocols to collect geomorphic information for over 3,200 km of Vermont streams to create the Rapid Geomorphic Assessment (RGA) database (Kline et al., 2007). The VTANR RGA protocol is a nationally recognized method to provide a measure of stream disequilibrium and stream sensitivity to indicate the likelihood of a stream responding via lateral and/or vertical adjustment to natural or human-induced watershed disturbances (Somerville and Pruitt, 2004; Besaw et al., 2009). The assessments consider each stream on a reach scale, designated as the length of channel considered to be consistent in slope, bed material, and distinguishable in some way from the upstream and downstream sections. The RGA protocols divide into three phases. Phase I compiles existing topographic maps, orthophotos, and local expert knowledge. Phase II comprises field survey

results, and stream stability metrics performed at the reach scale. Phase III is an in-depth assessment on a sub-reach scale, including a detailed field survey and quantitative measurements of channel dimension, pattern, profile, and sediments, used when a specific concern requires greater detail than the Phase II. This analysis uses only the Phase I and II data. In addition to providing an overall RGA (stream reach disequilibrium) score, all information collected during the RGA protocols is available in Arc-GIS (ESRI 2011), including the geometry of the valley and channel reach, watershed and floodplain characteristics, and classification of streambed materials. Additionally, the analysis of damaged bridges included widely available National (and Vermont) hydrography data (i.e., stream-reach characteristics and geomorphology data).

3.2 Geospatial Analysis and Data Processing

The comparison between damaged and non-damaged bridges focuses on two subsets of non-damaged bridges that vary in scale. Selection of the non-damaged bridges began by geospatially indexing the bridge list in Arc-GIS, and identifying the damaged bridges within the state as presented in Figure 3.1a. The two sets of non-damaged bridges used in this analysis include (1) reach scale (Reach-ND), the nearest non-damaged bridge (n = 274), (Figure 3.1b); and (2) watershed scale (Watershed-ND), non-damaged bridges located in subwatersheds that contain the damaged bridges (n = 954), (Figure 3.1c). The Arc-GIS analysis identified the non-damaged bridges nearest to the damaged bridges (reach scale) as well as the subwatersheds with damaged bridges (watershed scale). The reach scale non-damaged bridges were selected using stream flow path distance, rather than Euclidean distance to create one-to-one pairings of damaged and non-damaged bridges that likely experienced equivalent storm-related streamflow impacts. Instances where two damaged bridges share the same nearest non-damaged bridges resulted in fewer non-damaged bridges being included in the Reach-ND set than the damaged bridges.

The watershed scale, which used the USGS (United States Geological Survey) Watershed Boundary Dataset (WBD) 6th level (12-digit) subwatershed for delineation, provides a comparison with non-damaged bridges that are located within similar geographic settings, and were generally exposed to similar storm impacts as the damaged bridges. The USGS WBD is a hierarchical hydrologic unit dataset based on topographic and hydrologic features across the United States that defines the perimeters of drainage areas, including six levels of detailed nested hydrologic unit boundaries (USGS and USDA-NRCS, 2013). The motivation for using watershed and reach scales to identify comparable non-damaged bridges was to ensure that statistical comparisons were more discriminating by providing comparisons of bridges that for a particular scale experienced similar storm impacts and came from geographically and topologically similar settings. Storm impacts differ with location, and the closer a non-damaged bridge is to a damaged bridge, the more likely it is to experience similar storm impacts. The watershed scale was

created to capture non-damaged bridges in the hardest hit regions in the state. The decreased non-damaged data sets also help to reduce the statistical power associated with such a high number of data points, as was the case in the statewide data. A flow chart of the process of collecting and analyzing the bridge database, and the reduction of the data for each dataset being analyzed appears in Figure 3.2.

3.2.1 Selection of Variables and Analysis Method

A Kruskal–Wallis one-way analysis of variance (ANOVA) by ranks was used to compare the damaged and non-damaged bridge data at two scales (i.e., reach and watershed), using the programming environment MATLAB 2012. This non-parametric equivalent of the traditional one-way ANOVA test can accommodate the observed non-Gaussian distributions of some feature residuals that limit the application of a traditional ANOVA (Kruskal and Wallis, 1952; Siegel, 1956). Additionally, the presence of ordinal data types necessitated the use of a non-parametric test. Significant variables from the ANOVA were then tested for correlation to damage state with a multivariate logistic regression.

Table 3.1 summarizes the bridge and stream variable analysis of variance, and lists the resulting means and p-values. Testing was conducted between damaged bridges and each of the non-damaged bridges individually. A small p-value (e.g., less than or equal to some user-defined threshold of say, $p < 0.05$), indicates that it is unlikely (i.e., less than a 5% chance) that the differences observed (i.e., means being tested) are due to random chance. Thus, we could reject the null hypothesis that damaged and non-damaged bridges have similar means. Statistical analysis was conducted on all variables available in the existing databases; however, only those with either intrinsic or statistical significance receive further discussion in the paper. The means for all individual features across all bridges in the state are included as well to assess if the damaged bridges represented typical bridges in the state. The variables in Table 1 separate into three categories: bridge characteristics, bridge rating assessments, and stream geomorphology assessments with the database source identified as VTrans-BIS or VANR-RGA in Table 1.

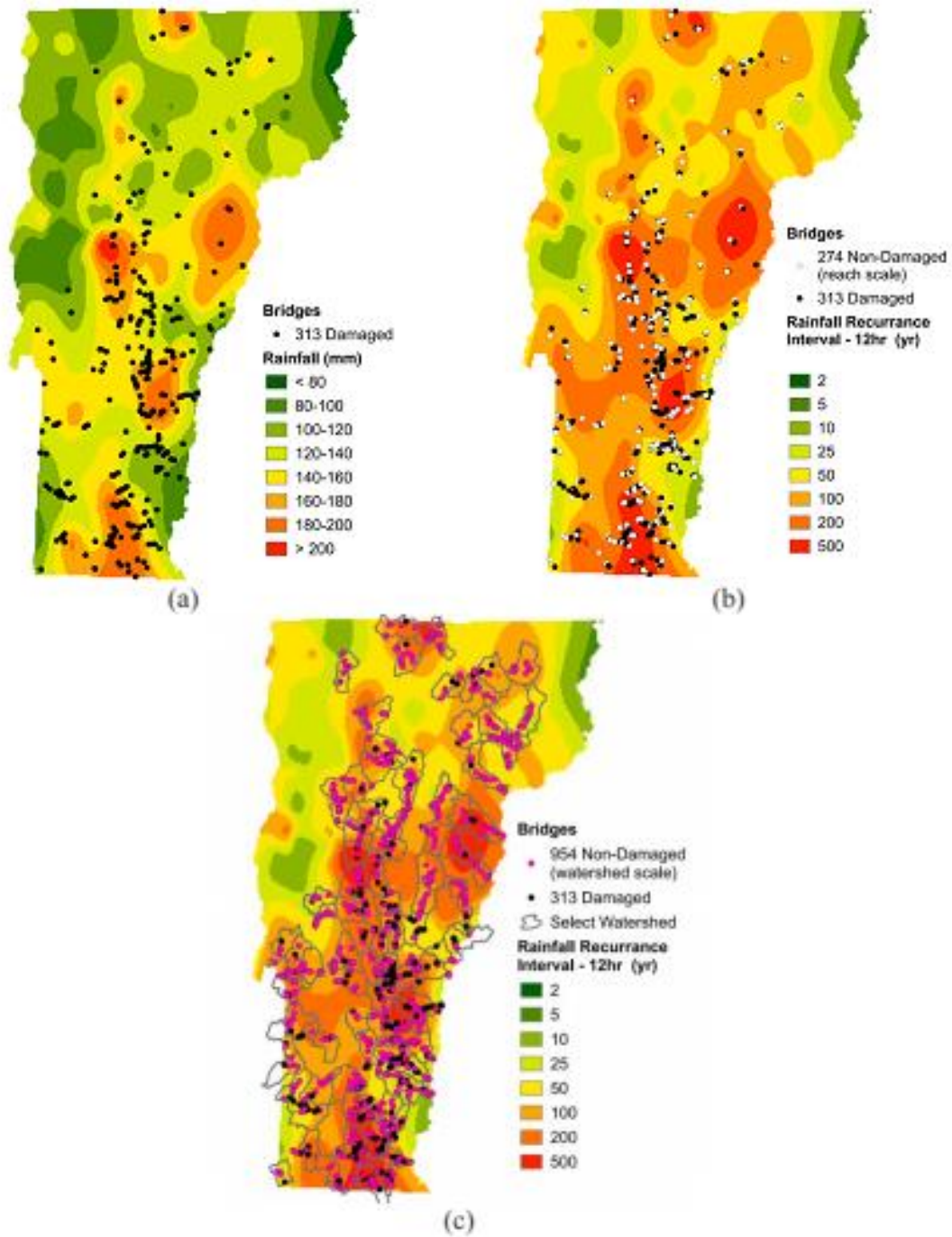


Figure 3.1: Tropical Storm Irene impact on Vermont bridges – (a) Estimated rainfall totals and locations of damaged bridges, (b) Estimated annual recurrence interval, locations of damaged and reach-scale non-damaged bridges, (c) Estimated annual recurrence interval, and locations of damaged and watershed-scale non-damaged bridges

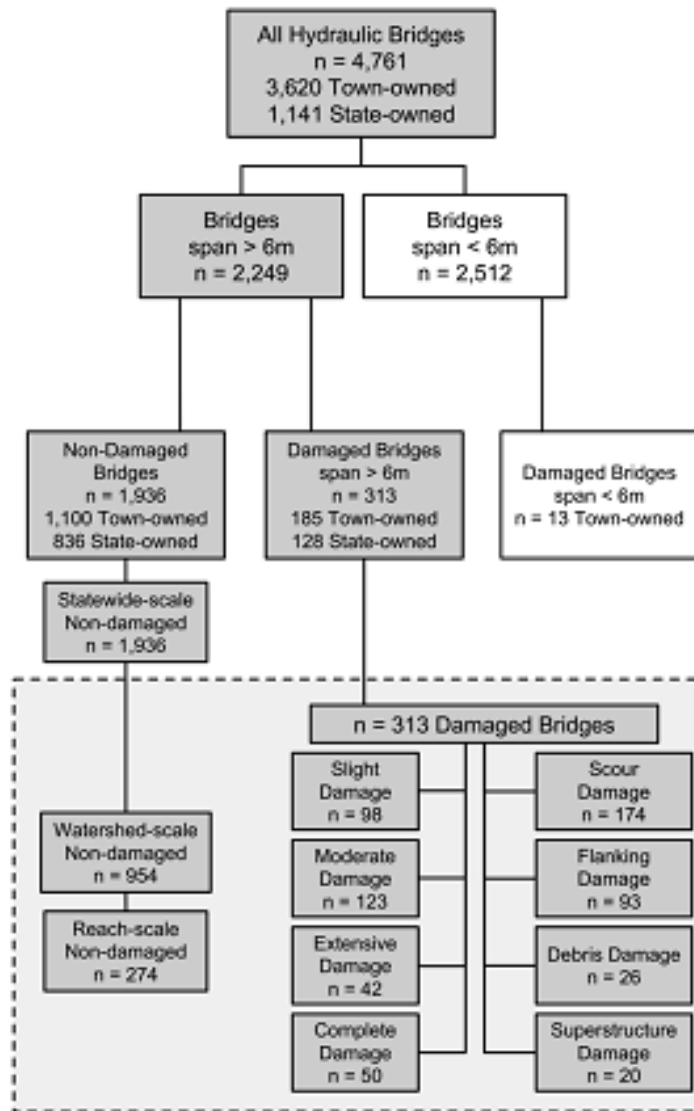


Figure 3.2: Bridge database process chart (the data identified in the boxes without background highlight were not used in the statistical analysis, n denotes sample size)

The variables selected for testing to represent the bridge characteristics from the VTrans BIS include: approach road width, maximum span, span, deck width, vertical clearance, year built, and average daily traffic. The VTrans BIS additionally includes Bridge Ratings Assessments for the deck, superstructure, substructure, channel, scour, waterway adequacy, structural, and state sufficiency ratings. The deck, superstructure and substructure ratings are similar in their method of determining the current condition of the various bridge components, which is scored from 0-9 and U (unknown).

Table 3.1: Variables considered in statistical Kruskal-Wallis analysis (significance indicated in bold, n denotes sample size)

Variable (unit)	Mean				Statistical Significance (p-value)	
	Damaged Bridges (n=313)	Non-Damaged Bridges			Non-Damaged Bridges	
		Reach (n=274)	Watershed (n=954)	Statewide (n=1,936)	Reach (n=274)	Watershed (n=954)
<i>Bridge Characteristics (VTrans-BIS)</i>						
Approach Width (m)	7.5	7.6	7.6	7.8	0.502	0.341
Max Span (m)	17.7	18.4	17.0	17.6	0.876	0.052
Structure Length (m)	23.9	23.8	22.7	24.7	0.496	0.004
Deck Width (m)	78.2	78.7	80.1	81.8	0.415	0.104
Vertical Clearance (m)	34.3	39.8	37.7	38.9	0.018	0.423
Year Built	1948.7	1955.9	1957.2	1957.1	0.010	<0.001
Average Daily Traffic	1392.9	1470.2	1467.1	1791.5	0.828	0.755
<i>Bridge Rating Assessments (VTrans-BIS)</i>						
Deck Rating	6.7	7.1	7.0	7.0	0.004	0.017
Superstructure Rating	6.6	7.1	7.0	7.0	<0.001	0.001
Substructure Rating	6.4	6.9	6.8	6.8	<0.001	<0.001
Channel Rating	6.4	6.9	6.9	7.0	<0.001	<0.001
Waterway Adequacy Rating	6.2	6.6	6.8	6.8	0.002	<0.001
Scour Rating	6.3	6.9	7.1	7.1	0.006	<0.001
Structural Adequacy Rating	39.3	45.3	45.8	45.9	<0.001	<0.001
State Sufficiency Rating	66.0	73.4	75.2	75.5	0.004	<0.001
<i>Stream Geomorphic Assessments (VTANR-RGA)</i>						
Stream Order	3.95	3.92	3.86	4.02	0.715	0.215
Channel Slope (%)	4.1	3.8	4.1	3.6	0.257	0.228
Sinuosity	1.11	1.12	1.16	1.17	0.103	<0.001
Straightening (%)	43.6	36.4	33.0	31.8	0.025	<0.001
Max Depth (m)	1.16	1.17	1.20	1.29	0.619	0.867
Mean Depth (m)	0.80	0.81	0.85	0.93	0.643	0.304
Flood Prone Width (m)	70.7	89.1	102.0	116.3	0.231	0.078
Abandoned Floodplain Height (m)	1.9	1.8	1.8	1.9	0.275	0.165
Width to Depth Ratio	26.5	31.7	24.2	22.3	0.116	0.005
Confinement Ratio	9.4	9.5	10.5	11.0	0.717	0.137
Entrenchment Ratio	3.7	4.1	6.2	7.1	0.701	0.007
Incision Ratio	1.71	1.65	1.58	1.54	0.479	0.038
RGA Degradation Score	9.0	8.8	9.9	10.5	0.901	0.065
RGA Aggradation Score	11.0	10.8	11.0	11.6	0.730	0.882
RGA Widening Score	11.2	10.9	11.6	11.8	0.618	0.197
RGA Planform Score	11.0	11.2	11.1	11.5	0.952	0.940
RGA Rating	0.53	0.52	0.55	0.57	0.788	0.257

The channel, waterway adequacy and scour ratings use descriptive cases of damage to assign values that are roughly ordinal, though the lack of a scale for damage would suggest the data is more likely to be considered nominal. The channel rating assesses the condition of the embankments and channel near the bridge for erosive damage, and rates the condition of any installed countermeasures. The scour rating

evaluates the risk of bridge failure from scour, based on the observed scour compared to the design scour depths. The waterway adequacy rating combines the likelihood of the bridge being overtopped by a flow event with a weighting that depends on the road's level of significance, such that high traffic volume highways would be required to withstand greater storm flows than low volume rural roads. The state sufficiency rating determines the bridge fitness (i.e., sufficiency to remain in service) based on the service it performs using factors derived from over 20 NBI data fields. As a factor in the sufficiency rating, the structural adequacy rating combines the minima of the superstructure and substructure ratings with the reduction in load capacity to determine one component score included in the sufficiency rating.

Variables used to characterize the stream geomorphic assessment include: channel length, bankfull channel width, flood-prone width, maximum depth, mean depth, floodplain height, stream order, sinuosity, straightening percent, confinement ratio, span to channel ratio, width to depth ratio, entrenchment ratio, incision ratio, channel slope, watershed area, specific stream power, RGA degradation score, RGA aggradation score, RGA widening score, RGA planform score, and an overall RGA rating. Details on these parameters may be found in the RGA protocols of Kline et al. (2007). The stream geomorphology parameters apply to an entire stream reach. Therefore, when damaged and non-damaged bridges lie within the same stream reach, they would be assigned the same stream geomorphic assessment values. The analysis uses width, length, depth and floodplain height parameters to determine whether there was a significant difference in stream size for bridges that were damaged. The ratios for sinuosity, confinement, span to channel, width to depth, entrenchment and incision, as well as percentage of the stream reach that was straightened help characterize the geomorphological condition of the stream reach; while the four RGA component scores (i.e., degradation, aggradation, widening and planform) are weighted and combined by experts to assess an overall RGA rating to assess stream reach disequilibrium (i.e., geomorphic stability).

A large number of possible variables from both the BIS and RGA were not included in this parametric analysis, as they are represented by categorical fields and ordinal data with sparse intervals. The most relevant of these variables include the bridge type, foundation type, stream type, bed material, and other fields that may aid in the future evaluation of bridge scour vulnerability.

The variables determined to be statistically significant on the reach scale were additionally tested using a multivariate logistic regression, using the damage level as the dependent variable, to determine which variables contributed to the observed level of damage. An empirical fragility curve was then developed for one of the resulting characteristics as a first step toward risk-based analysis of the bridges.

3.3 Results and Discussion

3.3.1 Damage Classification and Cost Analysis

Bridge damage from Tropical Storm Irene was categorized based on photographic documentation and descriptions in available reports. Bridges damaged included 55% steel beam, 34% concrete slab or beam, and 11% historical steel or wood truss superstructures. Single span bridges made up the vast majority (82%) of bridges damaged, with 12% double span, and the few remaining included 3 and 4 span structures. In cases where photographs were absent, available descriptions were used for damage categorization.

Bridge damage was grouped into four categories: scour, channel flanking, superstructure damage, and debris blockage, with the most prominent type of observed damage determining the category. The majority (55.6%) of bridge damage resulted from scour (e.g., Figure 3.3a). Channel flanking (e.g., Figure 3.3b), the erosion of the approach embankment behind the bridge abutments and specifically not within the channel, was responsible for 29.7% of the damaged bridges. Debris blockage (e.g., Figure 3.3c) was documented at 8.3% of the bridges, at which no other hydraulic damage was observed. Debris accumulation was commonly observed along with the other three types of bridge damage. Superstructure damage (Figure 3.3d) included damage to the deck, guardrails, and siding, and accounted for 6.4% of the reported damage. The majority ($n = 198$) of the 313 damaged bridges were town-owned.

Bridge damage was further categorized into four levels: slight, moderate, extensive and complete. This damage ranking system was based on that proposed in HAZUS (Scawthorn, 2006), and later amended by Padgett et al. (2008). The ranking system descriptions were expanded to include the damage types observed in Tropical Storm Irene, particularly damage from flooded river flow. Slight damage includes: channel erosion not affecting the bridge foundation, superstructure and guardrail damage, and debris accumulation without scour present (Figures 3.4a and b). Moderate damage (Figure 3.4c and d) includes: scour affecting the foundation, but not to a critical state, bank and approach erosion, superstructure damage but not to a critical state, and heavy aggradation. Extensive damage (Figure 3.4e and f) includes: critical scour, with some settlement to a single foundation, but not collapse, full flanking of both approaches, and damage to the superstructure making it structurally unsafe. Complete damage includes cases where the bridge was washed away, collapsed or has significant foundation damage requiring replacement (Figure 3.4g and f). Characterization of the level and type of damage was performed independent of any knowledge of the repair costs. Of the damaged bridges, 30% were categorized as having slight damage, 39% as moderate damage, 14.5% as extensive damage, and 16.5% as complete damage.



Figure 3.3: Damage Type (VTrans, 2014) - (a) Scour damage, Dummerston VT30-B9: scour beneath the concrete spread footing, (b) Channel flanking damage, Jamaica VT30-B40: flanking behind the abutment, (c) Debris damage, Wallingford VT140-B10: debris buildup on a pier, reducing the flow area, (d) Superstructure damage, Montgomery C2001-B5: damage to the sideboards of a covered bridge

Bridges, with their assigned damage level and estimated cost (when available) for repairing the bridge back to its pre-storm condition, are shown in millions of U.S. dollars and U.S. dollars per deck area in Figures 3.5a and b, respectively. The horizontal line and asterisk within each box plot represents the median and mean, respectively; the edges of the box are the 25th and 75th percentiles, and the whiskers extend to the most extreme data points not considered outliers. Outliers are plotted individually. The estimated cost of repair correlates well with damage levels, and when normalized by deck area, shows an increasing trend with average repair cost. When repair costs per deck area are categorized by damage type, the scour damage has significantly greater cost (Figure 3.5c). When a bridge showed only flanking damage, the associated estimated costs of repair were substantially smaller than those associated with scour damage. The average estimated cost of repair for scour, flanking, and superstructure damage were about \$260,000, \$108,000, and \$18,000 per bridge, or \$318, \$120, and \$30 per square meter of deck area, respectively. The completed construction costs for a select number of state-owned bridges rebuilt or remediated following Tropical Storm Irene (n = 12, all with extensive and complete damage) are plotted in Figure 3.5d. In general, the actual repair costs (per deck area) for state-owned bridges appear to be of similar range to the costs of repairs for town-owned bridges estimated for FEMA funding.

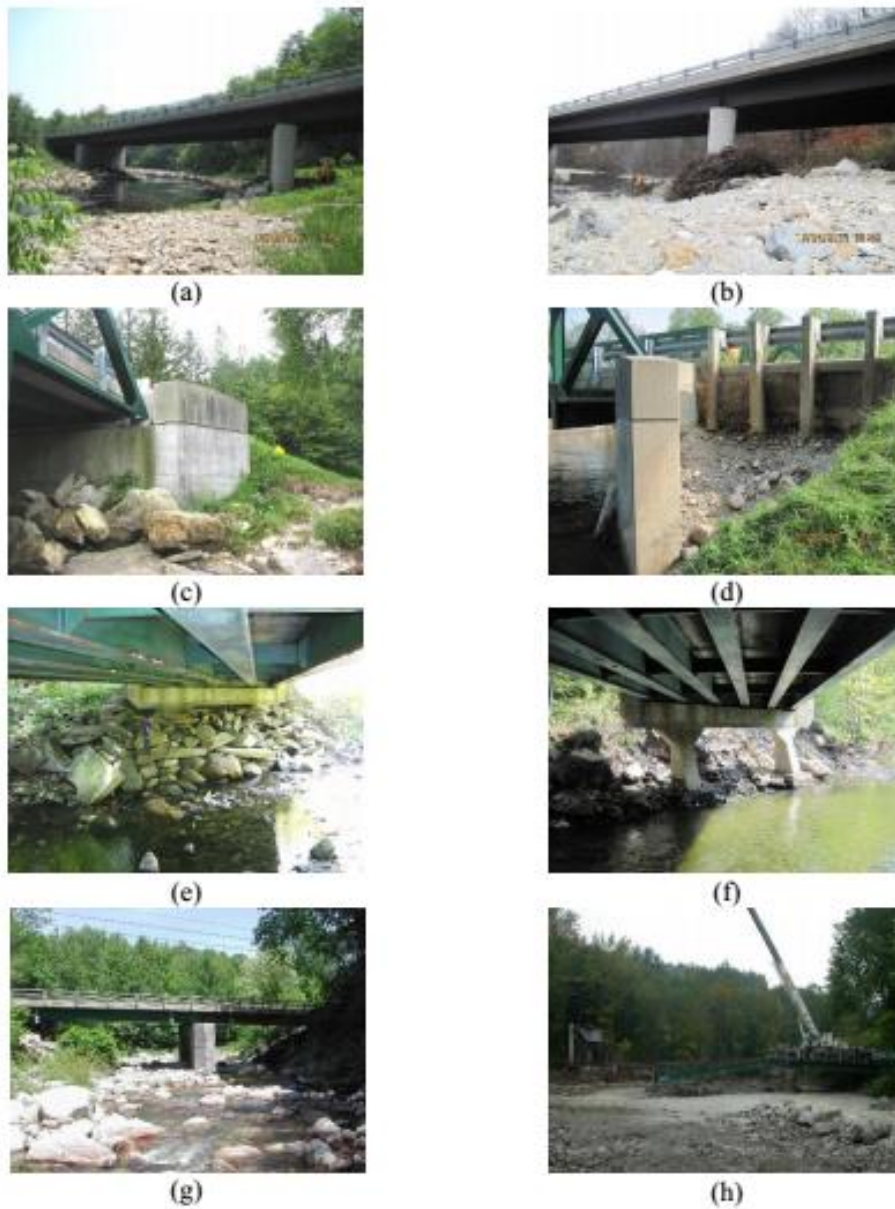


Figure 3.4: Damage Level (VTrans, 2014) – (a) and (b) Slight Damage, Northfield VT12-B61: conditions before and after the storm, (c) and (d) Moderate Damage, Bridgewater C3005-B37: conditions before and after the storm, (e) and (f) Extensive Damage, Cavendish C3045-B35: conditions before and after the storm, (g) and (h) Complete Damage, Rochester VT73-B19: conditions before and after the storm

3.3.2 Rainfall

Figure 3.6 compares the distribution of rainfall and ARI (panels a and b, respectively), for the damaged bridges (n=313) and non-damaged bridges at two different scales – the reach scale (n=274) and watershed scale (n=954). The non-damaged bridges at the reach scale experienced similar storm impacts to the damaged bridges, and were not statistically different ($p = 0.117$, for both rainfall and ARI). The non-

damaged bridges at the watershed scale however experienced a statistically lower storm impacts ($p < 0.001$, for both rainfall and ARI). The watershed scale captured a larger area with greater number of bridges likely bringing the watershed scale mean closer to the global (statewide scale) mean.

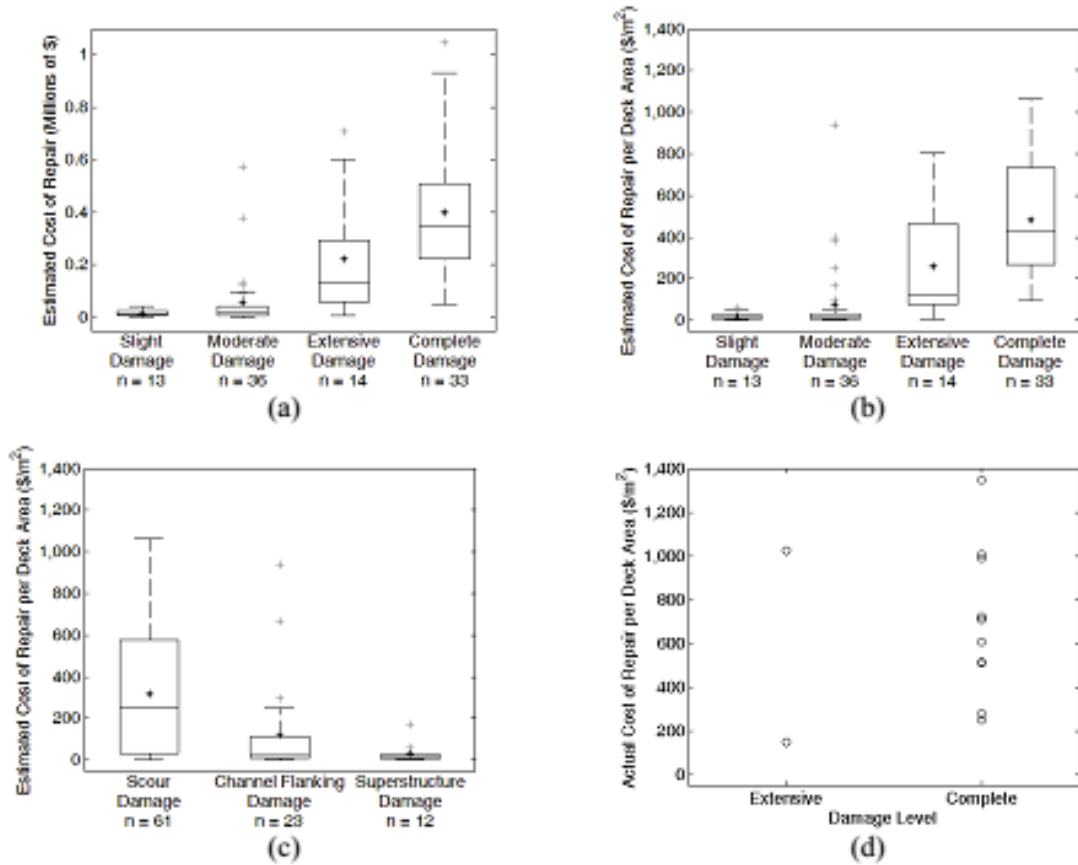


Figure 3.5: Repair cost and cost per deck area for various levels and type of damage – (a) Estimated cost of repair versus damage level, (b) Estimated cost of repair per deck area versus damage level, (c) Estimated cost of repair per deck area versus damage type, (d) Actual cost of repair per deck area of state-owned bridges (n denotes sample size)

3.3.3 Bridge Characteristics

An analysis of the bridges at the reach scale was performed to help identify features important in predicting bridge damage. The p -values in Table 3.1 indicate the probability that the null hypothesis is correct (with significance against the null set at $p < 0.05$) for a given feature, and show that the span and structure length of damaged bridges to be greater when compared to the non-damaged bridges on the watershed scale. The vertical clearance, the distance from the bottom bridge member to the streambed, is significantly lower for the damaged bridges than the non-damaged reach scale (Figure 3.7a), where storm impacts are thought to be the most similar.

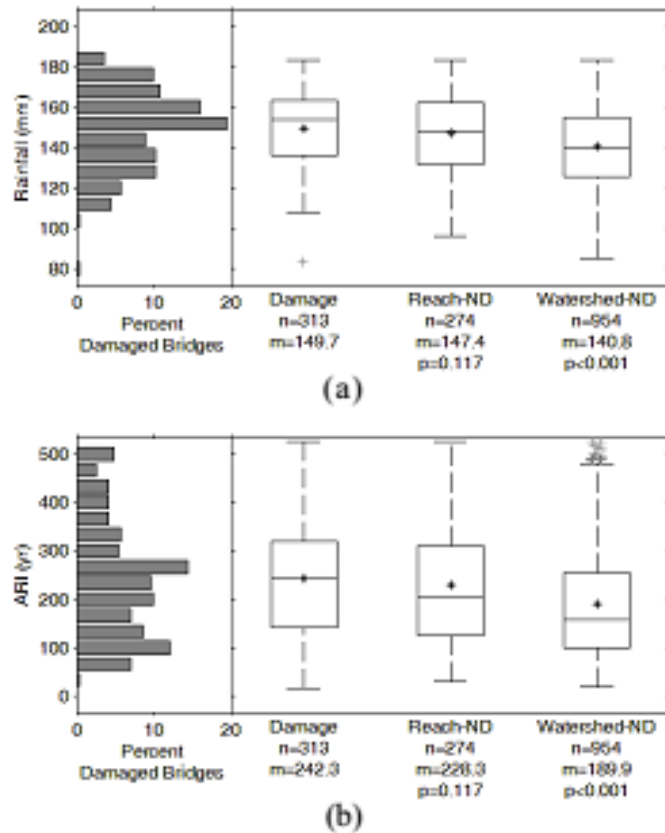


Figure 3.6: Analysis of the rainfall data – (a) rainfall (mm), (b) ARI (yr) (n denotes sample size, m is the mean, and p is the significance value)

Bridge geometry variables are important in that they determine the size and orientation of the bridge to the stream. Scour calculations often include bridge geometry in which the span, width, and clearance play direct roles. The span and clearance of the bridge determine the opening area, where a smaller opening would result in contraction. The width of the bridge indicates the length of contraction, or the length of contact with the stream, where longer widths lead to increased velocities in contraction. A hypothesis is that smaller and lower bridges are more likely to be damaged due to the high and intense flows, and are more prone to debris blockage. The data supports this with respect to vertical clearance, but shows that damaged bridges were longer (in span) than the corresponding non-damaged bridges from the same reach. Bridge geometry could play a more important role if combined and compared to stream size. Channel width is needed to determine if the span is undersized, but that data is not available in the NBI. Likewise, knowing the vertical under-clearance for the bridge would be more useful if it included the depth of flow, to determine freeboard. The current measurement only provides the distance from the low chord to the stream bottom.

A comparison of bridge age shows damaged bridges to be older than non-damaged bridges at both scales (Figure 3.7b). The year built, in which new bridges are generally viewed as more robustly designed, meets the expectation that older bridges were more vulnerable to damage. The significance of age in discriminating between damaged and non-damaged bridges may be due in part to the effort put into managing historic bridges. In particular, many covered bridges were more closely inspected and monitored after Tropical Storm Irene. Bridge age may only reflect regional bridge design and construction practices. Hazard return periods may vary from one region to another, yet bridge age may be a good, holistic parameter because it comprises inherent features (e.g., design standards, storms, construction practices, history of success, major maintenance, etc.) that are not available in existing databases.

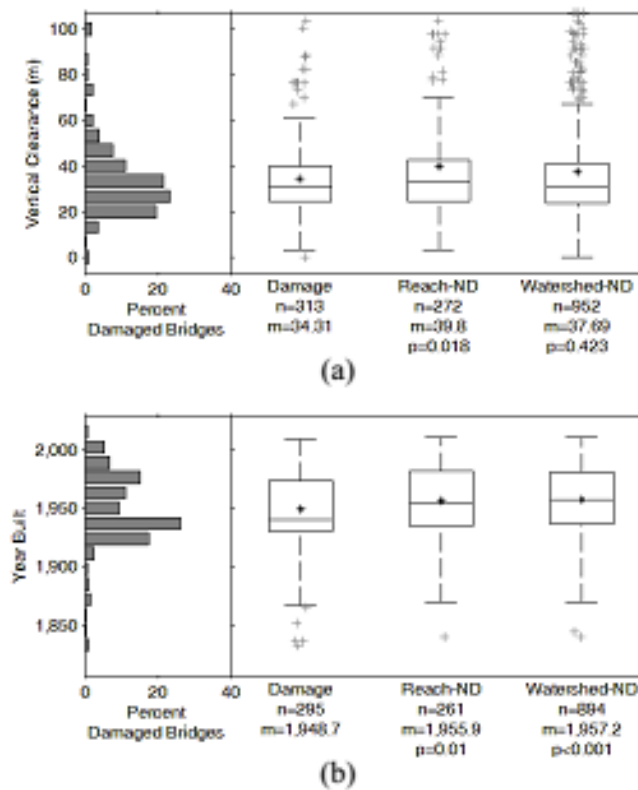


Figure 3.7: Analysis of bridge characteristic variables – (a) vertical clearance (m), (b) year built (*n* denotes sample size, *m* is the mean, and *p* is the significance value)

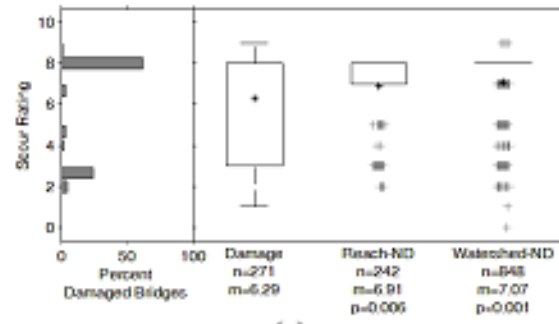
3.3.4 Bridge Ratings

The NBI bridge ratings for damaged bridges were significantly lower than those for both reach and watershed scale non-damaged bridges. The lower ratings prior to the storm show that several damaged bridges may have had preexisting issues, whether from structural deterioration, or prior hydrologic issues.

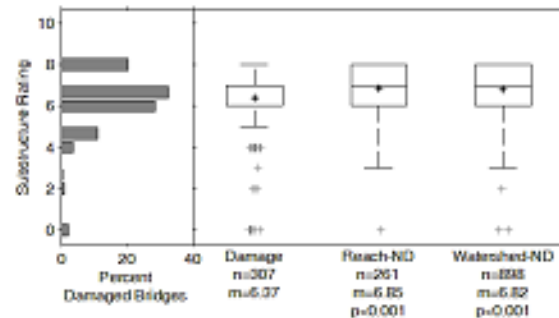
The scour ratings for bridges damaged in Tropical Storm Irene are compared to non-damaged bridges at the reach and watershed scales, both of which are significantly different and higher than the scour

ratings of the damaged bridges as seen in Figure 3.8a. Surprisingly, the majority of damaged bridges (over 50%) had non-critical scour ratings prior to Tropical Storm Irene. Included in the bridge database, 42 damaged and 229 non-damaged bridges were listed as unknown foundation in the scour rating field. However, bridges rated as scour critical (rating of 3 or below) do have a larger proportion of bridges with damage compared to non-damaged bridges at the reach and watershed scales, indicating that a low scour rating may show vulnerability to scour, but a high rating does not necessarily show immunity, particularly during extreme flood events.

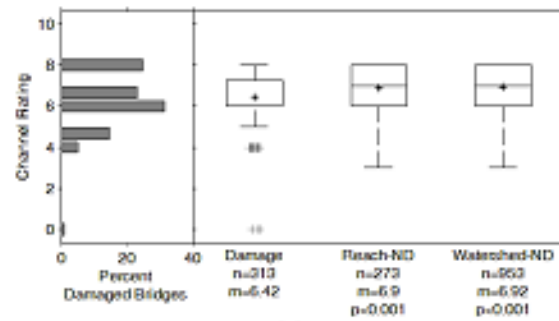
The substructure rating (Figure 3.8b), which rates the structural components of the bridge on an ordinal scale, shows worse ratings for damaged bridges. The channel rating (Figure 3.8c), which accounts for the condition of the embankments and channel protection, indicates that damaged bridges likely had prior occurrences of erosion. The waterway adequacy (Figure 3.8d) rates the likelihood of overtopping of the bridges. The data show that damaged bridges had an increased vulnerability to overtopping. The structural adequacy rating (Figure 3.9a), which takes a load rating reduction factor of the superstructure or substructure, and the state sufficiency rating (Figure 3.9b), which uses as formulated combination of 21 other available parameters in the BIS, shows the greatest difference between damaged and non-damaged bridges particularly at each end of the rating spectrum.



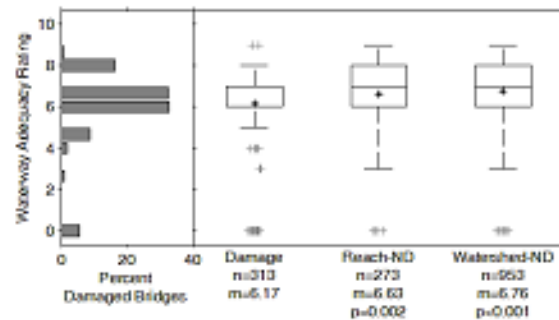
(a)



(b)



(c)



(d)

Figure 3.8: Analysis of bridge ratings – (a) scour rating, (b) substructure rating, (c) channel rating, (d) waterway adequacy rating (n denotes sample size, m is the mean, and p is the significance value)

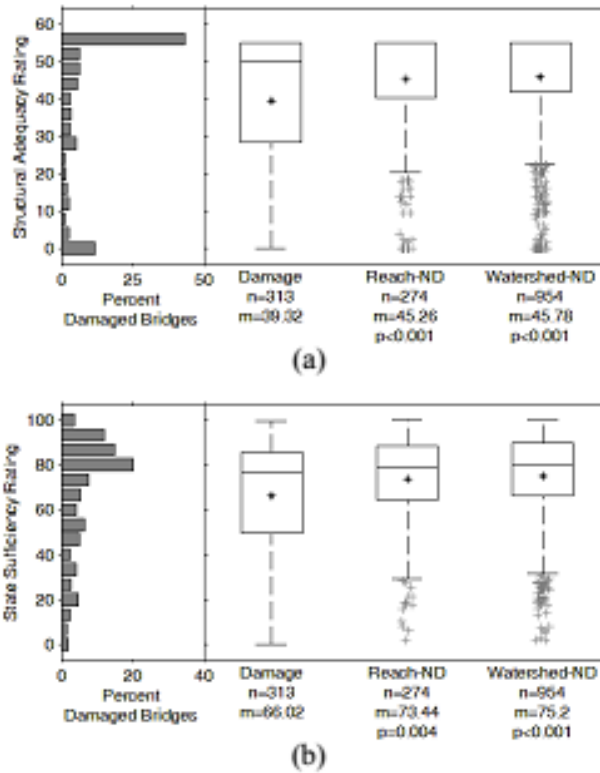


Figure 3.9: Analysis of bridge ratings – (a) structural adequacy rating, (b) state sufficiency rating (n denotes sample size, m is the mean, and p is the significance value)

3.3.5 Stream Characteristics

Stream geomorphic assessment information adds information and expert knowledge about the stream geomorphology that was previously missing from the bridge inventory. The geomorphic data, however, only applies at a stream-reach scale, which given the nearest-neighbor selection of non-damaged bridges at the reach scale, often results in the same stream parameters being applied to the pair of nearest neighbors. This lowers the statistical power of the data and the likelihood that the reach-scale non-damaged bridges will differ statistically from the damaged bridges without a larger sample size. Geomorphic assessments have not been completed across all streams in the state, and so the data was applied only where available. Additionally, a number of geomorphic assessment variables help assess the stream for departure from a reference stream type. Individual reach assessments must take the dominant stream type into account when determining the current condition.

The sinuosity of the stream is significantly lower for damaged bridges than non-damaged bridges at the watershed scale (Figure 3.10a). Additionally, the percentage of straightening was significantly higher for damaged bridges than for both non-damaged bridges at both scales (Figure 3.10b). A stream with low sinuosity and high percentage straightening has fewer degrees of freedom for lateral adjustment, and would

result in an increased velocity in a flood event. The width to depth ratio of damaged bridges was significantly lower than non-damaged bridges at the reach and watershed scales (Figure 3.11a). Lower width to depth ratios for a given stream type are indicative of incision and an associated increase in shear stress and stream power. The entrenchment and incision ratios are significantly different for damaged bridges when compared to the watershed scale non-damaged bridges (Figures 3.11b and c). Lower entrenchment ratios represents a disconnection from the floodplain and increased channelization during flood events. Higher incision ratios indicate bed degradation, as incised streams hold greater flood flows before accessing the floodplain.

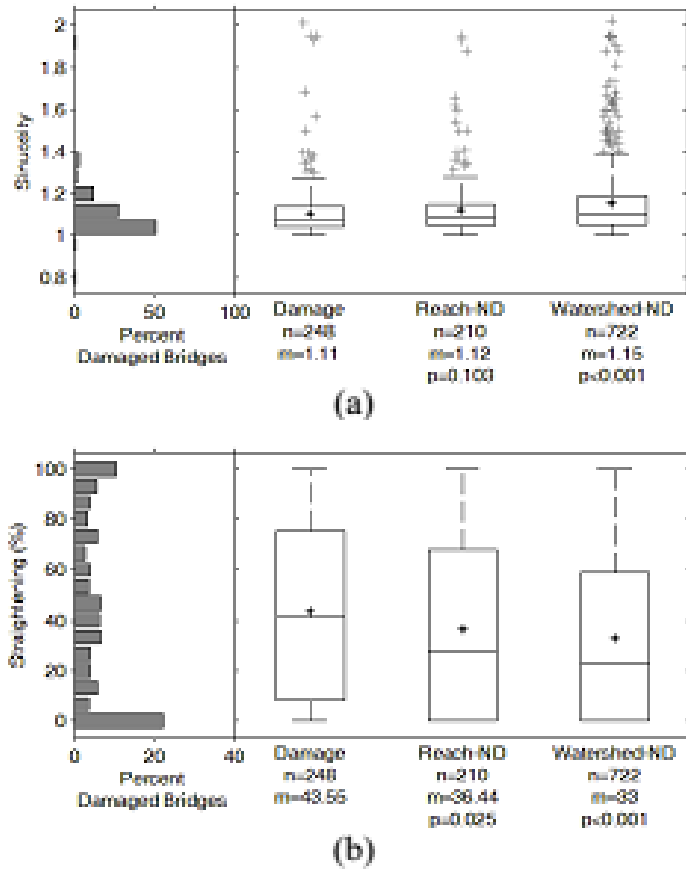
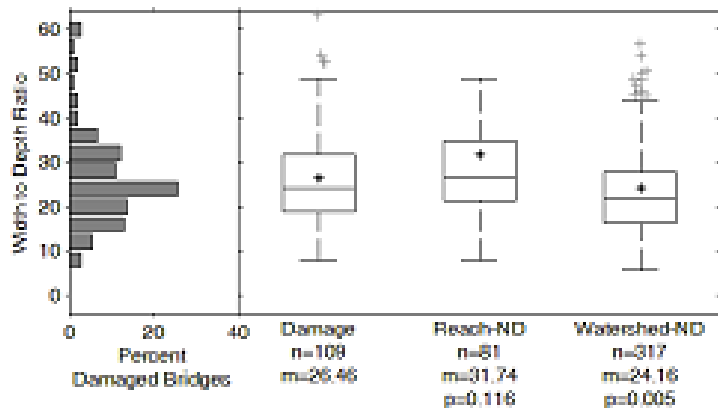
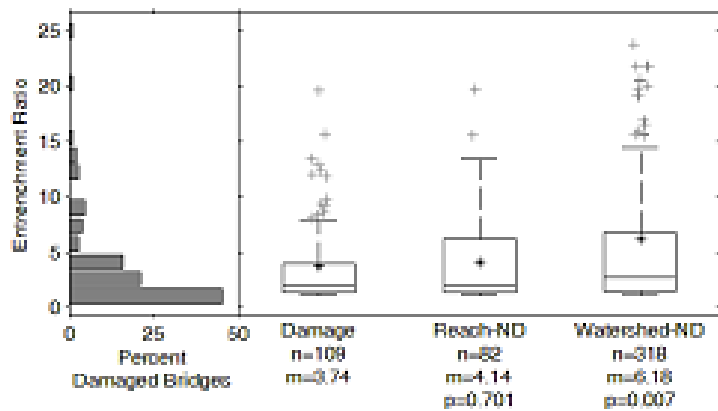


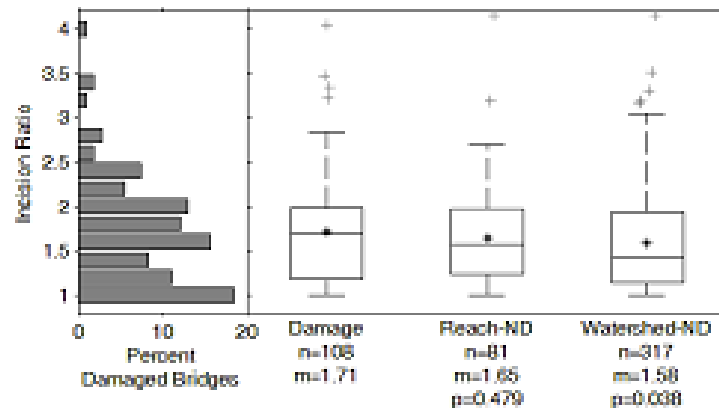
Figure 3.10: Analysis of variables related to stream characteristics - (a) sinuosity, (b) straightening percentage (n denotes sample size, m is the mean, and p is the significance value)



(a)



(b)



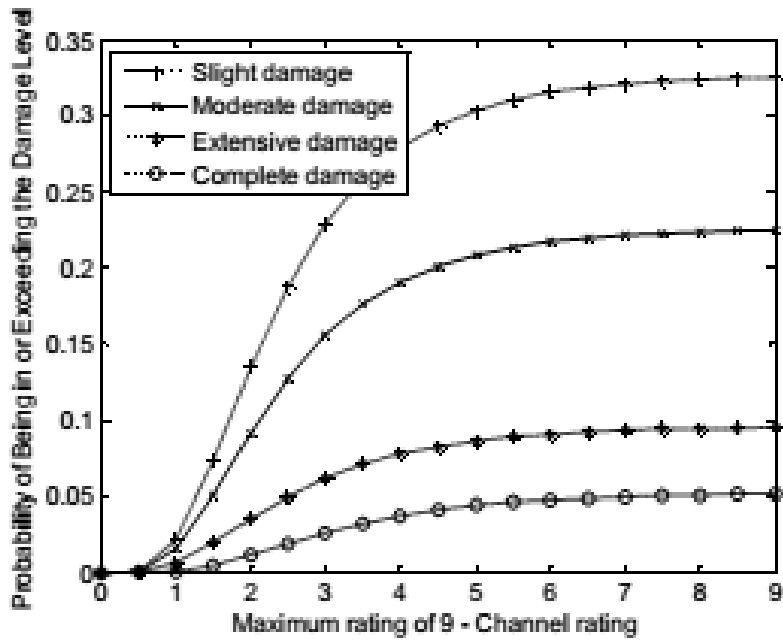
(c)

Figure 3.11: Analysis of variables related to stream characteristics ratios - (a) width to depth, (b) entrenchment ratio, (c) incision ratio (n denotes sample size, m is the mean, and p is the significance value)

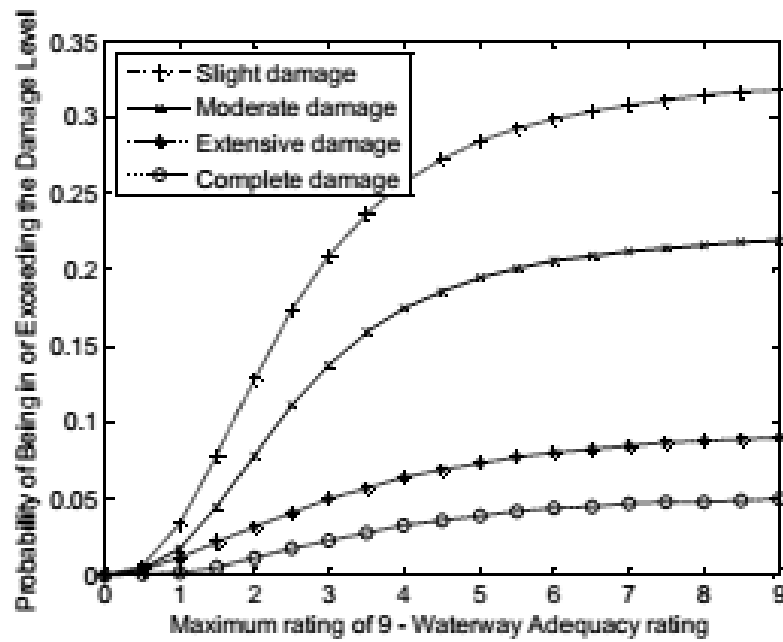
3.3.6 Logistic Regression and Empirical Fragility Estimate

Ordinal logistic regression helped to identify features that discriminate between damage levels at the reach scale. The analysis was conducted on the variables that were identified to be significant in the univariate analysis and were of interest in relating bridge and stream interactions - channel rating and waterway adequacy. The results are consistent with the expectation that a bridge with a lower channel and waterway adequacy rating would be more susceptible to damage, as indicated by their history of channel stability, and flow passage.

Empirical fragility curves were created based on the channel rating and waterway adequacy rating on the watershed scale bridges. For each of these, the ratings are presented as the deduction from the maximum rating of 9. Channel and waterway adequacy ratings were selected because they assess the current bridge and stream interactions. While it would have been advantageous to use the scour rating for this purpose, the values used in the scour rating are not ordinal in nature, but rather are a ranked nominal system, without clear distinctions on the scale. Fragility curves have been applied to empirical bridge damage (Padgett et al., 2012), as well as comprehensively summarized in applications of water resource infrastructure (Schultz et al., 2010). Each damage level is expressed as an individual curve showing the probability of being damaged at or above that level. To create the fragility curves, bridges were separated by damage level, and distributed as a histogram according to the value of each feature. Each distribution is then fit with a lognormal curve. The cumulative distribution function (CDF) of the lognormal fit to each damage level set is estimated at regular intervals to produce the conditional probability curve. The conditional probability is then used to determine the exceedance probability curves, by combining the probability of greater damage into each of the lower damage levels. The finalized fragility curves express the conditional probability of meeting or exceeding the given damage level, as a function of channel rating (Figure 3.12a) and waterway adequacy rating (Figure 3.12b) for the watershed bridges displayed in Figure 3.1c. The probability of damage is scaled depending on the ratio of damaged to non-damaged bridges in a given study area, with the maximum probability equivalent to the ratio of damage to non-damaged bridges being assessed. Probabilistic models of this sort can be the basis of a risk assessment of bridges under extreme flood events in the future. Stake holders would be able to determine the probability of damage exceeding a certain level for each bridge in their inventory under an extreme event similar to Tropical Storm Irene, to assist in determining the overall risk present in the network. In observing the pair of fragility curves, it appears the probability of damages plateaus beyond a rating of 6 (displayed as $9 - 6 = 3$), and that this could be a worthy point of differentiation for at risk bridges in the future. Bridges with poor ratings (potentially below 6) for both channel and waterway adequacy rating would be good candidates for a hydraulic review, to evaluate their vulnerability in flood events.



(a)



(b)

Figure 3.12: Fragility curve for bridge damage given the (a) channel rating, and (b) waterway adequacy rating. The best possible rating in these two categories is 9; therefore, the ratings are subtracted from 9 to reflect that the probability of damage increases with lower channel or waterway adequacy ratings

3.4 Conclusions

The effects of Tropical Storm Irene on Vermont bridges provide a unique, large dataset, where a *single* extreme hurricane-related flood event caused widespread damage to more than 300 bridges across a single state. A total of 326 Vermont bridges were identified as damaged during Tropical Storm Irene, with damage ranging from minor streambank erosion to entire bridge collapse. Of these, 313 bridges with spans greater than 6 m had inspection records available and were considered further. The characteristics of damaged bridges ($n = 313$) were compared statistically to those of non-damaged bridges at the reach scale ($n = 274$) and the watershed scale ($n = 954$).

The collection and georeferencing of hundreds of damaged and non-damaged bridges during a single extreme hurricane-related storm event, in combination with their inspection records and associated stream geomorphic assessments create a unique and significantly useful dataset. To the best of our knowledge such a database is not available in the literature. This database is made available in a spreadsheet format and can be downloaded from: <http://go.uvm.edu/vtbridges-irene-data>.

The damaged bridges included 55% steel beam, 34% concrete slab or beam, and the remaining 11% historical steel or wood truss superstructures. Single span bridges made up the vast majority, 82%, of bridges damaged, with 12% double span, and the few remaining including 3 and 4 span structures.

About 55.6% of the damaged bridges had scour damage, 29.7% had channel flanking, 8.3% had debris damage, and the remaining 6.3% had superstructure damage. When a bridge showed only flanking damage, the associated estimated costs of repair were substantially smaller than those associated with scour damage. The average estimated cost of repair for scour, flanking, and superstructure damage were about \$260,000, \$108,000, and \$18,000 per bridge, or \$318, \$120, and \$30 per square meter of deck area, respectively.

The bridge rating assessment characteristics were all strongly correlated to damage. Channel rating and waterway adequacy rating had strong discriminating power between bridge damage levels.

The analysis indicated that stream geomorphic data have the potential to be used to supplement and enhance the bridge rating systems, and may aid in identifying hydraulic vulnerability. Ratios such as entrenchment, incision, width to depth and straightening show significance at the watershed scale, and indicate that relative measures of a stream's geomorphic condition (disequilibrium) are more important than specific measurements. Vermont was one of the first states to develop and implement a three phase geomorphic assessment of streams, nationally recognized as one of the best overall protocols for assessing stream stability (Somerville and Pruitt, 2004). To the best of our knowledge, this is the first study that links hydrologic stream networks with performance of bridges. As geomorphic data becomes more widely available, the framework presented here could be applied elsewhere.

The analysis identified individual features of the bridge and stream that correlate with underlying damage vulnerability, through comparisons at the stream reach and watershed scales, and outlines a framework to leverage these features to aid in the prediction of bridge vulnerability. Logistic regression identified correlations in the key features and levels of bridge damage, as classified through inspection reports and visual observation by the authors. Empirical fragility curves were created to depict the exceedance probability for a given damage level against the channel and waterway adequacy rating, creating insights that can aid in evaluating bridges vulnerability to extreme events.

CHAPTER 4

STREAM POWER APPLICATION FOR BRIDGE DAMAGE PROBABILITY

MAPPING BASED ON EMPIRICAL EVIDENCE FROM TROPICAL STORM IRENE

(An article based on this chapter has been accepted by the ASCE journal of Bridge Engineering. The authors of this article are Ian A. Anderson, Donna M. Rizzo, Dryver R. Huston, and Mandar M. Dewoolkar)

Synopsis:

On August 28, 2011 Tropical Storm Irene hit the state of Vermont with a severity that deposited 100-200 mm (4-8 inches) of rain across the state and resulted in damage or failure of over 300 bridges. The analysis of available datasets helped identify a set of 313 bridges (greater than 6 m in span) damaged in a single state from a *single* extreme flood event that caused a twelve-hour rainfall recurrence interval that exceeded 500 years in some areas, and 100 years throughout most of the affected areas. Based on available damage reports and photographs, the observed bridge damage was grouped into four levels of severity. This paper links watershed stream power to the observed bridge damage, develops a process to quantify the hazard at bridges both as a case study and for future storms, and uses stream power as a hazard metric to produce probabilistic predictions of bridge vulnerability. The analysis also offers comparisons between damaged bridges and bridges that were not damaged in Tropical Storm Irene. Specific Stream Power (SSP) and the *event-based* Irene Specific Stream Power (ISSP) were computed and found to be both statistically significant at discriminating between damaged and non-damaged bridges, as well as between damage levels. The application of empirical fragility curve analysis for SSP and ISSP produces a probability of damage generated from the results collected from Tropical Storm Irene. Spatially mapping the bridge damage probability from an extreme event like Tropical Storm Irene enables the hazard to be effectively displayed over a broad range of scales (e.g., stream reaches, select watershed and statewide). This, in turn, helps identify problematic reaches, for which bridge placement would be at increased vulnerability. The methodology presented here can be applied to other geographic settings and storm events of interest, and to the best of the authors' knowledge, this is the first investigation comparing site-specific stream power to observed bridge damage at a system level.

4.1 Introduction

Tropical Storm Irene of August 2011 hit the state of Vermont with a severity that caused major damage throughout the state altering the perception of extreme events and their impacts on Vermont's infrastructure. Dropping between 100-200 mm of rain, and causing flooding in 225 of 251 towns across the state, it follows only the devastating November 1927 flooding as the second greatest natural disaster on record in Vermont (NWS, 2011; State of Vermont, 2012). The highest rainfall totals were located over the

Green Mountains running through the center of the state, with estimates of rainfall recurrence intervals exceeding the 500-year storm in some areas, and 100 years through most of the affected areas. The rainfall resulted in extensive flash flooding, setting peak flow records in nine gauged streams, and reaching the top four for peak flows in nine others (USGS, 2011). The flooding and high flows across many of Vermont's rivers and streams caused reports of damage to 389 bridges and hundreds of kilometers of roadway (Thomas et al. 2013). Figure 4.1a displays the location of damaged and non-damaged bridges in the state.

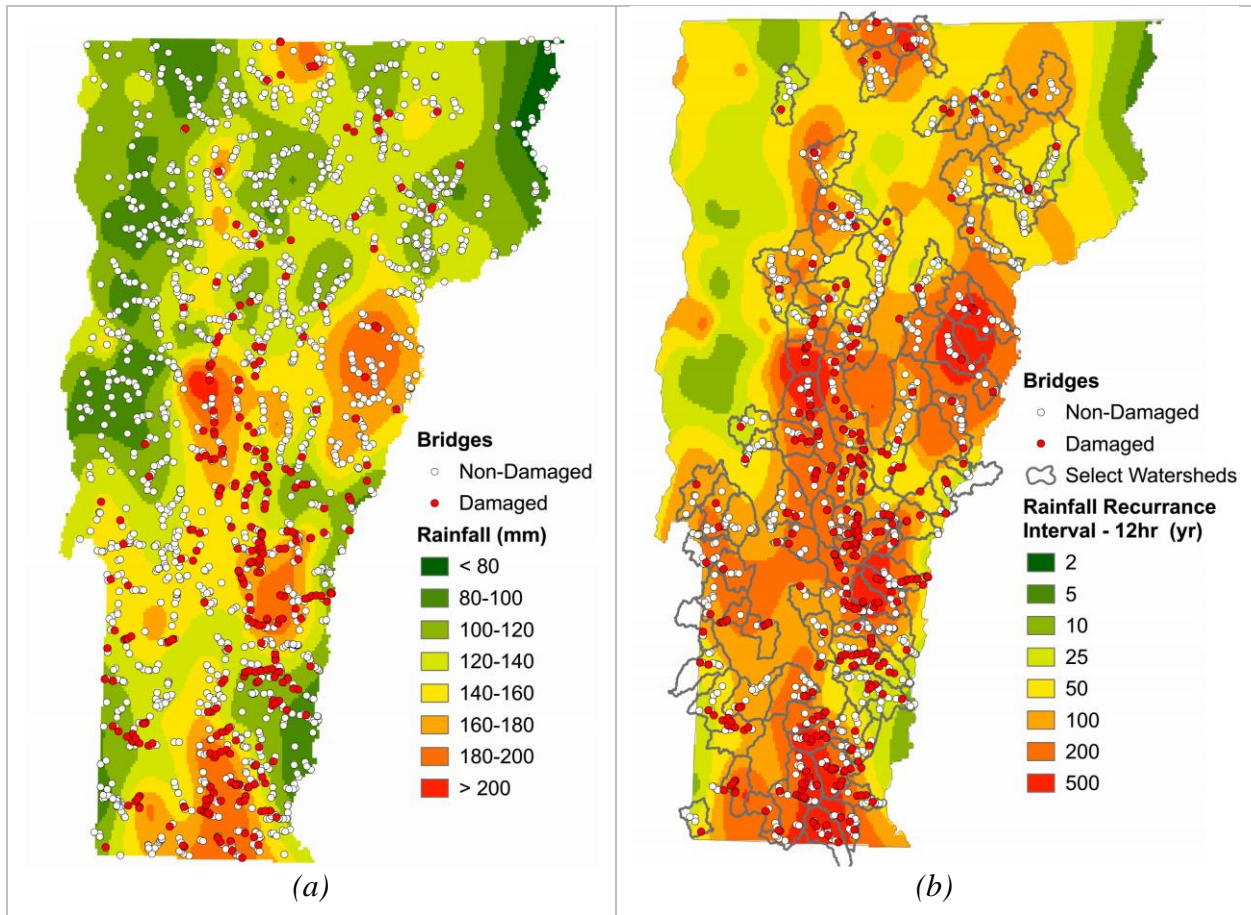


Figure 4.1: Locations of damaged and non-damaged bridges in Tropical Storm Irene (a) state-wide superimposed on rainfall data, and (b) in watersheds where bridge damage was observed superimposed over recurrence interval estimates

Other recent extreme events have caused damage to numerous bridges in other parts of the United States and other countries. For example, uplifting and hydrodynamic forces on the superstructure was responsible for the majority of damage to short and medium span bridges from Hurricane Katrina in 2005 (Okeil and Cai, 2008). An economic analysis of 44 bridges damaged during Hurricane Katrina performed by Padgett et al. (2008) shows a relationship between surge elevation, damage levels, and repair costs. Their subsequent analysis of 262 bridges, of which 36 were damaged, identified surge elevation as a key factor in determining damage levels from Katrina and relates it to the estimated likelihood of damage through

empirical fragility curves (Padgett et al., 2012). Both of these studies used the National Bridge Inventory (NBI) as the primary source of bridge data. Similar bridge infrastructure vulnerabilities have been witnessed at Escambia Bay, Florida in 2004 during Hurricane Ivan (Douglass et al., 2004) and in Hokkaido, Japan during the 2004 Songda Typhoon (Okada et al., 2006). Typhoon-induced extreme precipitation caused severe flooding in August 2009 damaging over 130 bridges in Southern Taiwan (Wang et al., 2014). A series of floods in 2010 and 2011 including a flood associated with category 5 cyclone Yasi caused damage to 89 bridges and culverts in Queensland, Australia, and damaged 47 bridges in Lockyer Valley Region of Queensland in a 2013 flood (Lebbe et al., 2014). More recently, severe flooding in September 2013 caused the collapse of 30 highway bridges, and damage to an additional 20 bridges in Colorado (Kim et al., 2014).

The above case history summary of bridge damage, both coastal and inland, illustrates the vulnerability of existing bridge infrastructure to extreme events. The occurrence of such severe events is expected to increase because of climate change altering precipitation intensities in many parts of the world (Melillo et al., 2014). For example, extreme rainfall events, those ranging in the 99th percentile of intensity, are happening more frequently, especially over the past three to five decades (e.g., Horton et al., 2014). The effects of Tropical Storm Irene on Vermont bridges therefore provide a uniquely large dataset, where a single hurricane-related extreme flood event caused widespread damage to over 300 bridges in a single state.

In this paper, stream power is evaluated as a measure of the hazard. Stream power is the rate of energy (i.e., power) of flowing water against the bed and banks of a river channel, and functionally controls stream dynamics and morphology. Stream power estimates from extreme events were shown to correlate positively with the instances of stream widening in the White River watershed of Vermont (Buraas et al., 2014). Also, Gartner et al. (2015) showed that in the Fourmile Canyon of Colorado, the erosion and deposition correlates with increased power gradients and decreased power gradients, respectively. Stream power generally has been shown to correlate positively to fluvial incision (Seidl and Dietrich, 1992; Anderson, 1994), channel size, mobility and pattern changes (Magilligan, 1992; Rosenbloom and Anderson, 1994; Lecce, 1997; Knighton, 1999), and as an estimate of flood power (Brooks and Lawrence, 1999). Specific stream power (SSP) normalizes total stream power, which is the product of discharge, slope, and the specific weight of water, and normalizes it by the stream width (Bagnold, 1966). SSP allows for the expression of stream power at the unit bed area, rather than the cross-sectional area as is the case in total stream power. Magilligan (1992) and Miller (1990) showed that 300 W/m² provides a minimum SSP threshold to separate reaches with and without large-scale geomorphic change. Stream power calculations have been conducted on multiple scales to support analysis of river systems for various objectives including risk to infrastructure, evaluation of channel stability, and assessment of instream habitats. At the finest scale, stream power has been used to conduct bridge scour analysis in erodible rock (Costa and O'Connor,

1995; FHWA 1999), and relates erodibility indices to local stream power measures. Point-location estimates have been prominent (e.g., Fonstad, 2003; Lecce, 1997; and Magilligan, 1992), with studies that sought to identify transitions in stream power along the longitudinal profile and better understand sediment storage dynamics within a basin. Longer reach-length profiles use continuous distributions of stream power to identify stream power functions through a single fluvial system (e.g. Fonstad, 2003; Reinfeld et al., 2004; and Knighton, 1999). Geographic information systems (GIS), leveraging digital elevation models (DEM), allowed the progression from point- and reach-scale estimates of stream power to network or catchment scale modeling (Finlayson and Montgomery, 2003; Jain et al., 2006; Barker et al., 2008; and Vocal Ferencevic and Ashmore, 2012).

This paper seeks to link watershed stream power to bridge damage from Tropical Storm Irene, create a process to quantify the hazard at bridges both as a case study and for future storms, and use the hazard metric to produce probabilistic predictions of bridge vulnerability. The analysis also offers a comparison between damaged bridges and bridges that were not damaged in Tropical Storm Irene. To the best of our knowledge, this is the first investigation comparing site-specific stream power to observed bridge damage at a network level.

4.2 Methods

4.2.1 Data Collection

To study the effects of Tropical Storm Irene on Vermont's bridge infrastructure, a comprehensive database of all available bridge records prior to Tropical Storm Irene was compiled. The collection and assembly of data identified geo-referenced information for all river and stream crossing bridges in the state, including all available inspection data and relevant photographic records. This process encompassed 4,761 state- and town-owned bridges from the Vermont Agency of Transportation (VTrans) Bridge Inventory System (BIS).

Bridge damage information from Tropical Storm Irene was sparsely recorded, and not available in a singular registry. In order to study the effects of the statewide flooding and storm damage, a comprehensive index of bridges with associated damage was needed. Bridge damage information from the Vermont Agency of Transportation (VTrans) and the Vermont Department of Emergency Management (VDEM) was spatially joined to the VTrans Bridge Inventory System (BIS). Errors in spatial reference limiting the combination of data was corrected by matching identifying features within the databases. The BIS is a statewide database of bridge inspection records in accordance with the National Bridge Inventory (NBI) coding guide, containing all bridges, both state and town owned, with spans over 6 m. The VTrans damage records included State owned bridges damaged in Tropical Storm Irene, while the VDEM list contained town owned bridges and culverts being submitted to Federal Emergency Management Agency

(FEMA) for repair funding. These lists were combined to generate a list of 153 damaged bridges. An additional 173 damaged bridges were identified through review of the VTrans online bridge inspection photograph archives, mainly drawing from post-storm inspection photographs conducted throughout the state. This process identified a total of 326 damaged bridges, which differs from 389 damaged bridges reported by the VDEM (Thomas et al. 2012). The discrepancy is thought to result from the classification of certain culverts as bridges in the higher estimate, as well as rapid and unrecorded post storm bridge repair. Bridges with spans shorter than 6 m were removed from our list of 326 damaged bridges, as they are not present in the BIS. The resulting 313 damaged bridges are included in the subsequent system-wide analysis, and all references to damaged bridges in the sequel refers to the 313. Figure 4.1a displays the location of damaged and non-damaged bridges in the state.

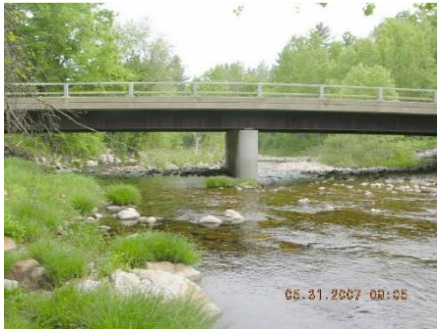
The stream power computations (Section 4) leverage a database of stream metrics developed from Rapid Geomorphic Assessments (RGA) under protocols published by the Vermont Agency of Natural Resources (VTANR). The River Management Program of VTANR has been quantitatively assessing the hydraulic stability and sensitivity of over 3,200 km of Vermont streams for the past 15 years, which feeds into the RGA database (Kline et al., 2007; Kline and Cahoon, 2010). The VTANR RGA protocols are nationally recognized and provide a measure of stream disequilibrium and stream sensitivity to indicate the likelihood of a stream responding via lateral and/or vertical adjustment to natural and/or human watershed disturbances (Somerville and Pruitt, 2004; Besaw et al., 2009). The assessments are conducted on a reach scale, designated as the length of channel considered to be consistent in slope, valley confinement, sinuosity, dominant bed material, and distinguishable from the upstream and downstream river sections in terms of average values of these channel metrics. The RGA protocols are categorized into three phases: In Phase I, stream reaches, and the subwatersheds draining to them, are delineated in ArcGIS with reference to existing topographic, photographic, and geologic information. Phase I also compiles soil and land cover characteristics, and local historical knowledge of channel and watershed modifications; Phase II comprises field survey results, and stream stability metrics performed at the reach scale; and Phase III is an in-depth assessment on a sub-reach scale, including a detailed field survey and quantitative measurements of channel dimension, pattern, profile, and sediments, used when a specific concern is identified, needing greater detail than the Phase II. In addition to providing an overall RGA (stream reach disequilibrium) score, all information collected during the RGA protocols is available in Arc-GIS, including geometry of the valley and channel reach, watershed and floodplain characteristics, and classification of streambed materials. The stream power analysis of this study used the stream reach delineations for Vermont waters developed in RGA Phase I. All of the abovementioned data are georeferenced and available as a single file at: <http://www.uvm.edu/~mdewoolk/?Page=ResearchData.html>.

4.2.2 Bridge Damage Classification

Damage to the 313 bridges affected in Tropical Storm Irene was categorized based on photographic documentation and descriptions in available reports. In cases where photographs were absent, available descriptions were used for categorizing damage into four levels: slight, moderate, extensive and complete. This damage ranking system was based on that proposed in HAZUS (Scawthorn, 2006), and later amended by Padgett et al. (2008). The ranking system descriptions were expanded to include the damage types observed in Tropical Storm Irene, particularly damage from flooded river flows as follows:

- Slight damage includes channel erosion not affecting the bridge foundation, superstructure and guardrail damage, and debris accumulation without scour present. Example bridges with slight damage is shown before and after the storm in Figures 4.2a and b, respectfully.
- Moderate damage includes scour affecting the foundation but not to a critical state, bank and approach erosion, superstructure damage but not to a critical state, and heavy channel aggradation. Example bridges with moderate damage is shown in Figures 4.2c and d.
- Extensive damage includes critical scour, with some settlement to a single foundation, but not collapse, full flanking of both approaches, and damage to the superstructure making it structurally unsafe. Example bridges with extensive damage is shown in Figures 4.2e and f.
- Complete damage includes cases where the bridge was washed away, collapsed or has significant foundation damage requiring replacement. Example bridges with complete damage is shown in Figures 4.2g and h.

Characterization of the damage level was performed independent of any knowledge of the repair costs. Of the 313 damaged bridges, 30% were categorized as having slight damage, 39% as moderate damage, 14.5% as extensive damage, and 16.5% as complete damage. Estimated repair costs were only known for 16, 35, 14 and 34 bridges with slight, moderate, extensive and complete damage, respectively. The mean estimated repair costs for these bridges were about \$46, 35, 194, and 570 per square meter of deck area.



(a)



(b)



(c)



(d)



(e)



(f)



(g)



(h)

Figure 4.2: Bridge damage Level (VTrans, 2014) before (left panel) and after (right panels) the storm - (a) and (b) Slight Damage, Wallingford VT140-B10, (c) and (d) Moderate Damage, Bridgewater C3005-B37, (e) and (f) Extensive Damage, Cavendish C3045-B35, (g) and (h) Major Damage, Rochester VT73-B19.

4.2.3 Stream Power Computation

The calculation of stream power used in this analysis occurs on a broad scale, using widely available data, rather than individual measured observations, to produce comprehensive estimates of stream power. A GIS script was developed to generate the stream power data, which automated the calculation of stream power at any desired point. Total stream power (Ω), also referred to as cross-sectional stream power (Fonstad, 2003) is defined as:

$$\Omega = \gamma \cdot Q \cdot s, \quad (4.1)$$

where γ is the specific weight of water, Q is the discharge, and s is the energy slope. SSP (ω) normalizes the total stream power by the width of the stream to estimate unit-bed-area stream power as:

$$\omega = \gamma \cdot Q \cdot s / b, \quad (4.2)$$

where b is the channel width. The script enables the calculation of stream power for any target point (e.g., bridge or endpoint of a stream reach) using commonly available GIS layers. The process follows those in the literature (Jain et al., 2006; Vocal Ferencevic and Ashmore, 2012, Biron et al., 2013), creating a script that leverages existing GIS tools to process the commonly available data into a stream power estimate. Channel width estimates using regression equations (Jaquith and Kline, 2001) were uniformly applied to calculate SSP for all streams.

The discharge values required for stream power were calculated using regional regression equations for flood discharge at various annual exceedance probability thresholds (Olson, 2014). The discharge used was the bankfull flow (estimated as the 2 year recurrence interval). The regression equations required the drainage area, the basin wetland percentage and the annual rainfall average. The upstream catchment area for each individual target point was determined using both flow accumulation and direction calculations from a 1/3 arc second hydrologically-corrected DEMs of Vermont (VCGI, 2006). The wetland percentages (National Land Cover Database, Homer et al., 2011) and annual rainfall totals (Daly et al., 2012) were averaged using the target point's upstream catchment area. An example illustrating the catchment area for individual bridges is provided in Figure 4.3a.

With the discharge at each target point estimated, the slope in this study was determined based on reach breaks established in the Phase I RGA database. The RGA considers each stream on a reach scale, designated as the length of channel that is considered consistent in slope, valley confinement, sinuosity, and dominant bed material, and distinguishable in some way from the upstream and downstream sections. The target slope for each bridge was selected as the slope associated with the underlying stream reach. Streamlines were extracted from the National Hydrography dataset (USGS, 2013), and the slope was determined by taking the inlet and outlet elevations of the selected reach, and dividing by the shape length (thalweg) to determine the channel slope of the target bridge. Figure 4.3b shows the determination of the slope using the reach delineations, for the same subwatershed shown in Figure 4.3a.

With the discharge and slope calculated at each target bridge and associated reach, the total stream power and SSP can be calculated according to equations 4.1 and 4.2, respectively. Total stream power and SSP for the same subwatershed are presented in Figure 4.3c and d.

In addition to the conventional SSP, which is uniformly based on a 2 yr recurrence interval discharge, an event based stream power was calculated using spatially dependent recurrence intervals based on Tropical Storm Irene rainfall totals, called Irene Specific Stream Power (ISSP). Precipitation observed during Tropical Storm Irene throughout the state of Vermont and surrounding counties in New York and New Hampshire were used to estimate rainfall over the entire state (Springston et al., 2012). These spatial estimates were used to calculate the average recurrence interval (ARI), using a 12-hr duration storm to match the duration of Tropical Storm Irene (Kiah et al., 2013). Figure 4.1b shows the rainfall annual recurrence interval with spatially referenced damaged and non-damaged bridges on the affected subwatersheds. Following SSP in the use of regression equations to estimate discharge, ISSP is a scaled version of SSP. ISSP uses the average rainfall ARI of the catchment area to select a scaled flow estimate, in lieu of measured stream flow estimates. The event-based ISSP provides a stream power measure scaled to the storm intensity, estimating the power present in Tropical Storm Irene. Together, SSP can be used as a measure for identifying the potential high power locations, while the event based ISSP extends upon this analysis, creating a framework of application in identifying high power in an actual storm event.

4.3 Results and Discussion

4.3.1 Damage Distribution

A Kruskal-Wallis one-way analysis of variance was used to compare the effectiveness of using stream power as a discriminatory feature for damaged bridges. This non-parametric equivalent of the traditional one-way ANOVA test can accommodate the observed non-Gaussian distributions of some feature residuals that limit the application of a traditional ANOVA (Kruskal and Wallis, 1952; Siegel, 1956). The set of non-damaged bridges was selected from bridges that were geographically within the subwatersheds with damaged bridges, as seen in Figure 4.1b, creating a dataset of 313 damaged and 951 non-damaged bridges. This geographically-based selection ensures bridges are drawn from spatially-related regions, in which Tropical Storm Irene had notable impacts. A small p-value ($p < 0.05$) indicates significance of the associated feature between the two observed groups used for this analysis. Both SSP (Figure 4.4) and ISSP (Figure 4.5) were significant ($p < 0.001$) when testing between damaged and non-damaged bridges. Each set of figures displays the distribution of the damaged and non-damaged bridges, as well a box plot illustrating the differences between the two. The horizontal line within each box plot represents the median, the edges of the box are the 25th and 75th percentiles, and the whiskers extend to the most extreme data points not considered outliers, set at beyond 2.7 standard deviations. Outliers are plotted

individually, and the asterisks indicate the mean. High values of both SSP and ISSP are correlated with bridge damage, and are a useful parameter to evaluate vulnerability of bridge damage.

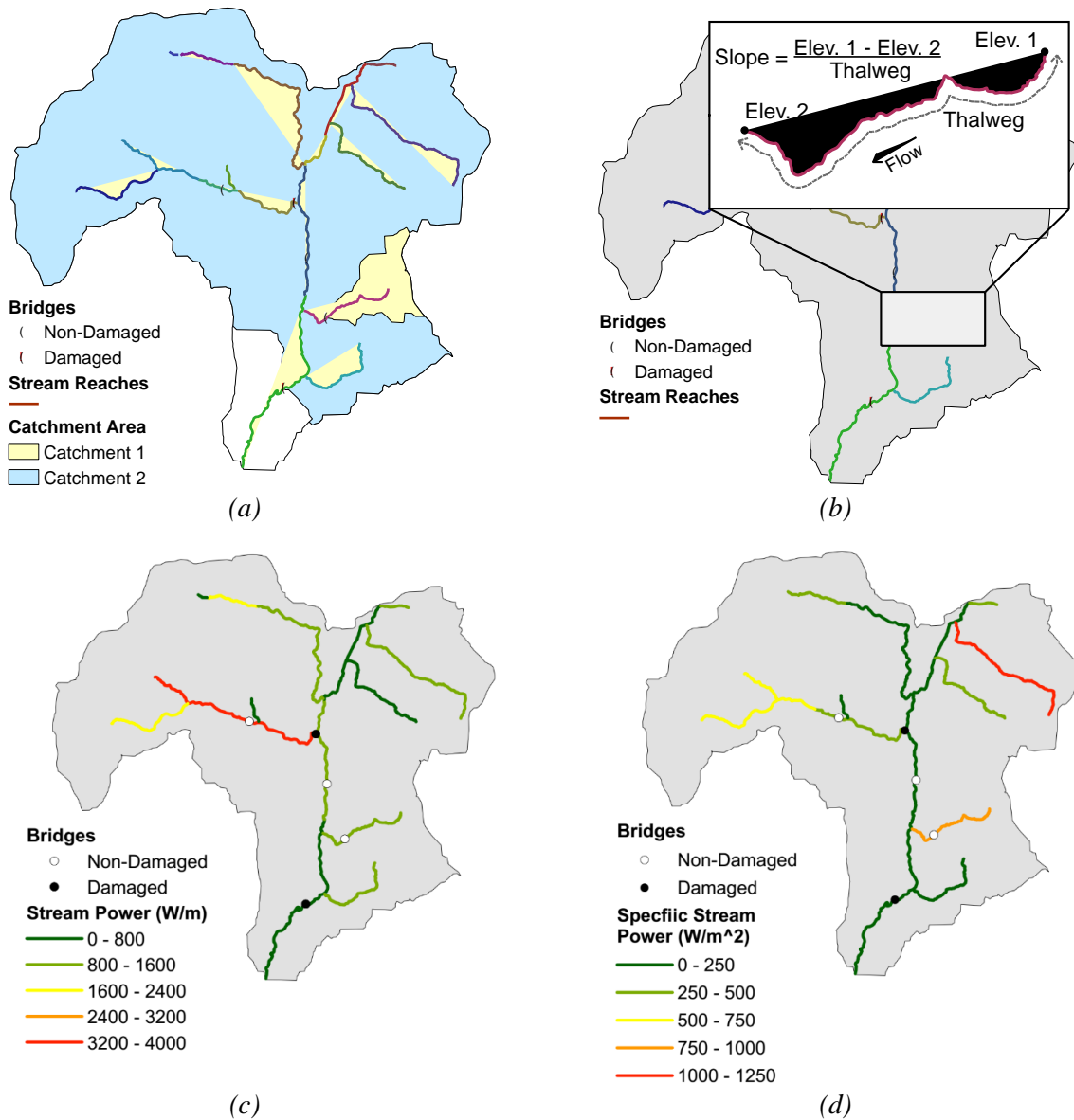


Figure 4.3: Stream power calculation: (a) catchment delineation, (b) slope calculation, (c) stream power, (d) specific stream power

Having determined that both SSP and ISSP are significantly correlated to bridge damage, SSP and ISSP were tested to classify between damage levels using a multivariate logistic regression. Both SSP and ISSP again were significant ($p < 0.001$), this time for distinguishing between the four damage levels used, slight, moderate, extensive and complete. High values for SSP and ISSP were related to increased levels of damage in the bridges affected by Tropical Storm Irene. Since both features were found to be significant at

discriminating between damaged and non-damaged bridges, and between bridge damage levels, both may be good metrics for further probabilistic analysis.

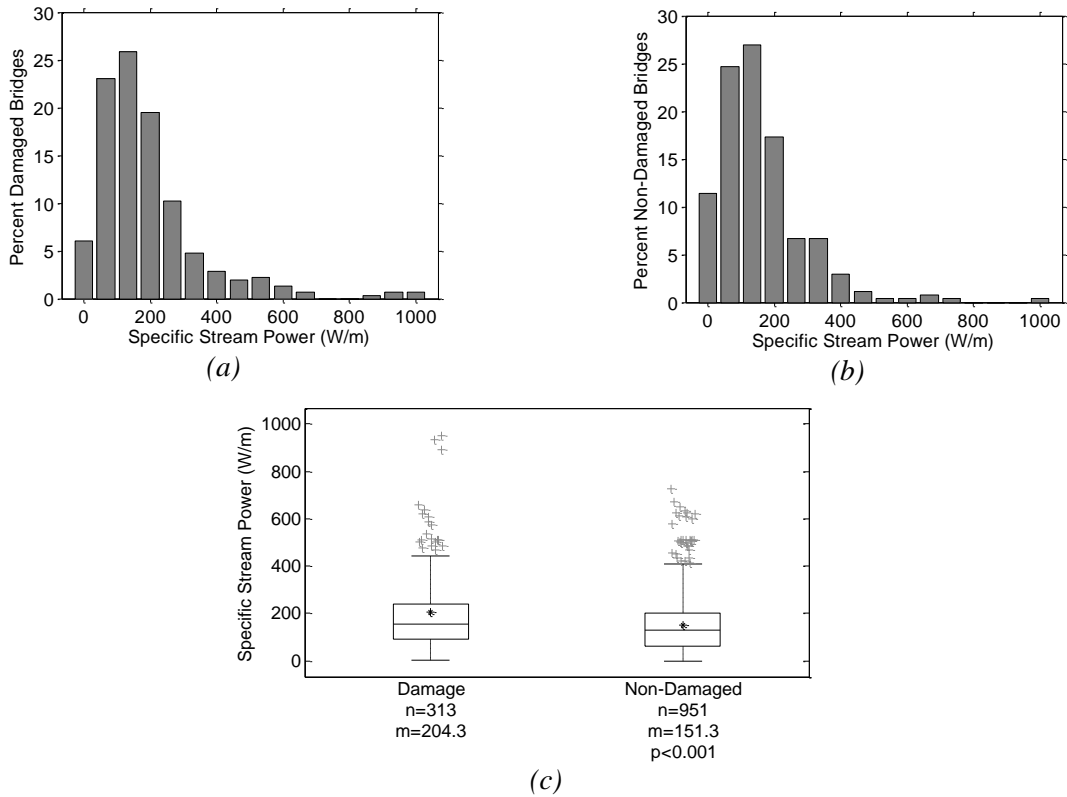


Figure 4.4: Histogram distributions of SSP for (a) Damaged and (b) Non-Damaged bridges, and (c) Kruskal-Wallis (non-parametric) One-way Analysis of Variance on SSP

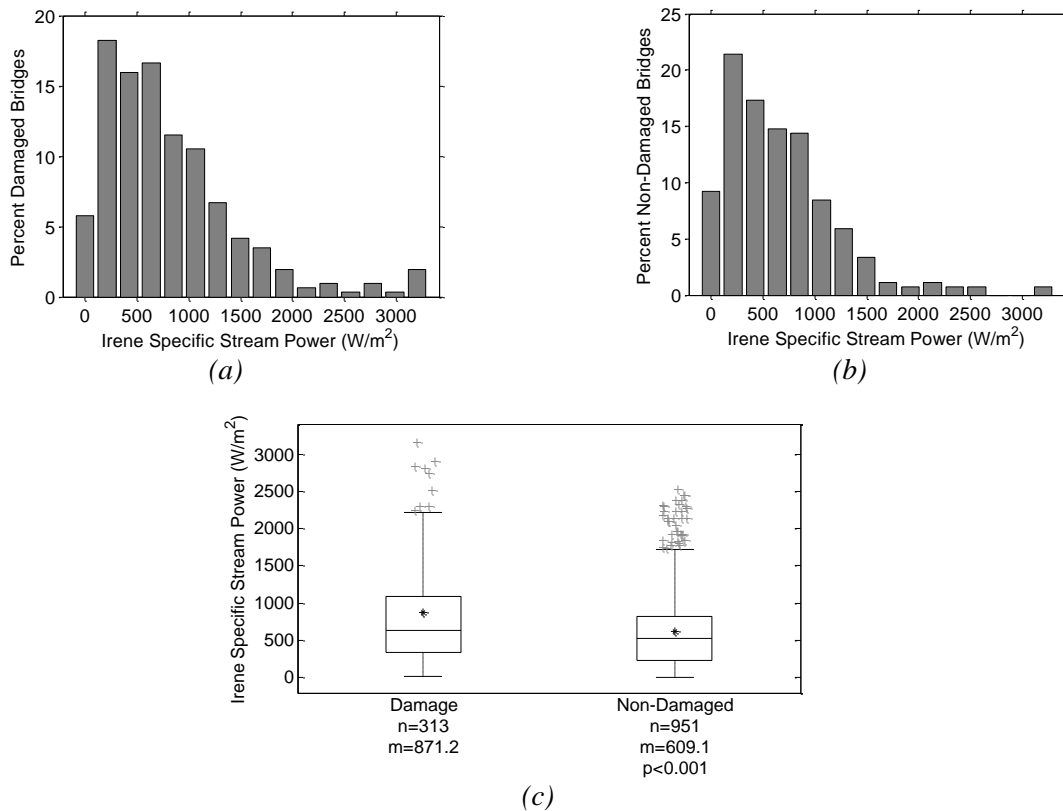


Figure 4.5: Histogram distributions of ISSP for (a) Damaged and (b) Non-Damaged bridges, and (c) Kruskal-Wallis (non-parametric) One-way Analysis of Variance on ISSP.

4.3.2 Empirical Fragility Curves

Given their significance in discriminating bridge damage, both SSP and ISSP were used to create empirical fragility curves from Tropical Storm Irene. Fragility curves have been applied to empirical bridge damage (Padgett et al., 2012), as well as comprehensively summarized in applications of water resource infrastructure (Schultz et al., 2010). Fragility curves in this study express the conditional probability of exceeding a given damage state, over the possible spectrum of steam power values. Each curve represents an individual damage level, and the probability of being damaged at or above that level. To create the fragility curves, bridges were separated by damage level, and plotted as a histogram according to the value of the selected feature. Each set of damaged bridges is then fit with a lognormal distribution. The cumulative distribution function (CDF) of the lognormal fit to each damage level set is sampled at regular intervals to produce the conditional probability curve. The curves are then used to determine the exceedance probability curves, by combining the probability of greater damage into each of the lower damage states. The finalized fragility curves show the conditional probability of meeting or exceeding the given damage state, as a function of SSP and ISSP (Figure 4.6a and b) for the watershed bridges displayed in Figure 4.1b. The

probability of damage is scaled depending on the ratio of damaged to non-damaged bridges in a given study area, with the maximum probability equivalent to the ratio of damage to non-damaged bridges being assessed. The SSP fragility curve provides a tool for determining the current hazard present at a bridge and comparing them between bridges, as a uniform flow recurrence interval was used. The ISSP curves can be used to determine the true bridge vulnerability from Tropical Storm Irene and is useful in identifying bridges with similar exposure to allow for between-bridge comparisons of structural elements or other environmental factors that may have contributed to damage. The process outlined to create SSP and ISSP can serve as a framework for predicting probability of bridge damage using any user-specified storm event.

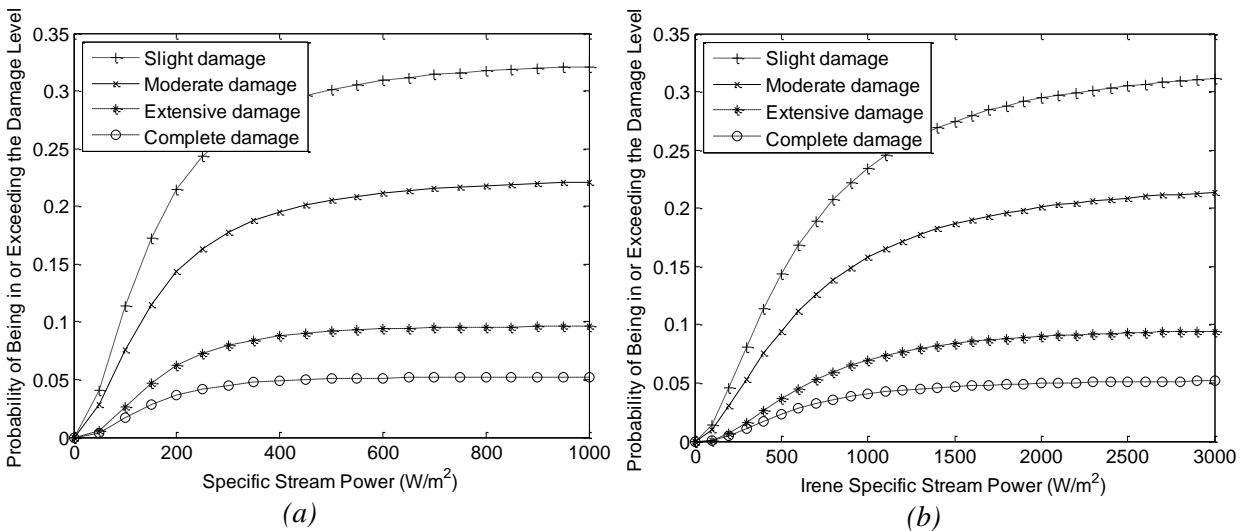


Figure 4.6: Fragility curves of the conditional exceedance probability generated from (a) SSP and (b) ISSP for each of four bridge damage classifications

4.3.3 Probability Mapping

To extend the usefulness of the SSP and ISSP fragility curve analysis, the resulting conditional exceedance probabilities may be mapped to an area, and displayed on a stream-reach network. Using the GIS script created to generate SSP and ISSP measures at bridges and applying it to all 15,261 stream reaches used in this study, a statewide map of SSP and ISSP was created. The stream power measures are used to generate conditional probabilities of damage by interpolation from the SSP and ISSP fragility curves, and scaled to represent the number of damaged to non-damaged bridges in the targeted area. The statewide probability map of ISSP (Figure 4.7), shows the overall probability of damage from Tropical Storm Irene, and shows the effects of geographic watershed differences and identifies locations of stream power differences throughout the state on a consistent measure. The maximum probability of damage in Figure 4.7 is 9.5% corresponding to 215 damaged bridges as having moderate (or greater) damage out of a total of 2,249 bridges. A closer look at Figure 4.7 facilitates comparison of the probabilities of bridge damage between individual watersheds.

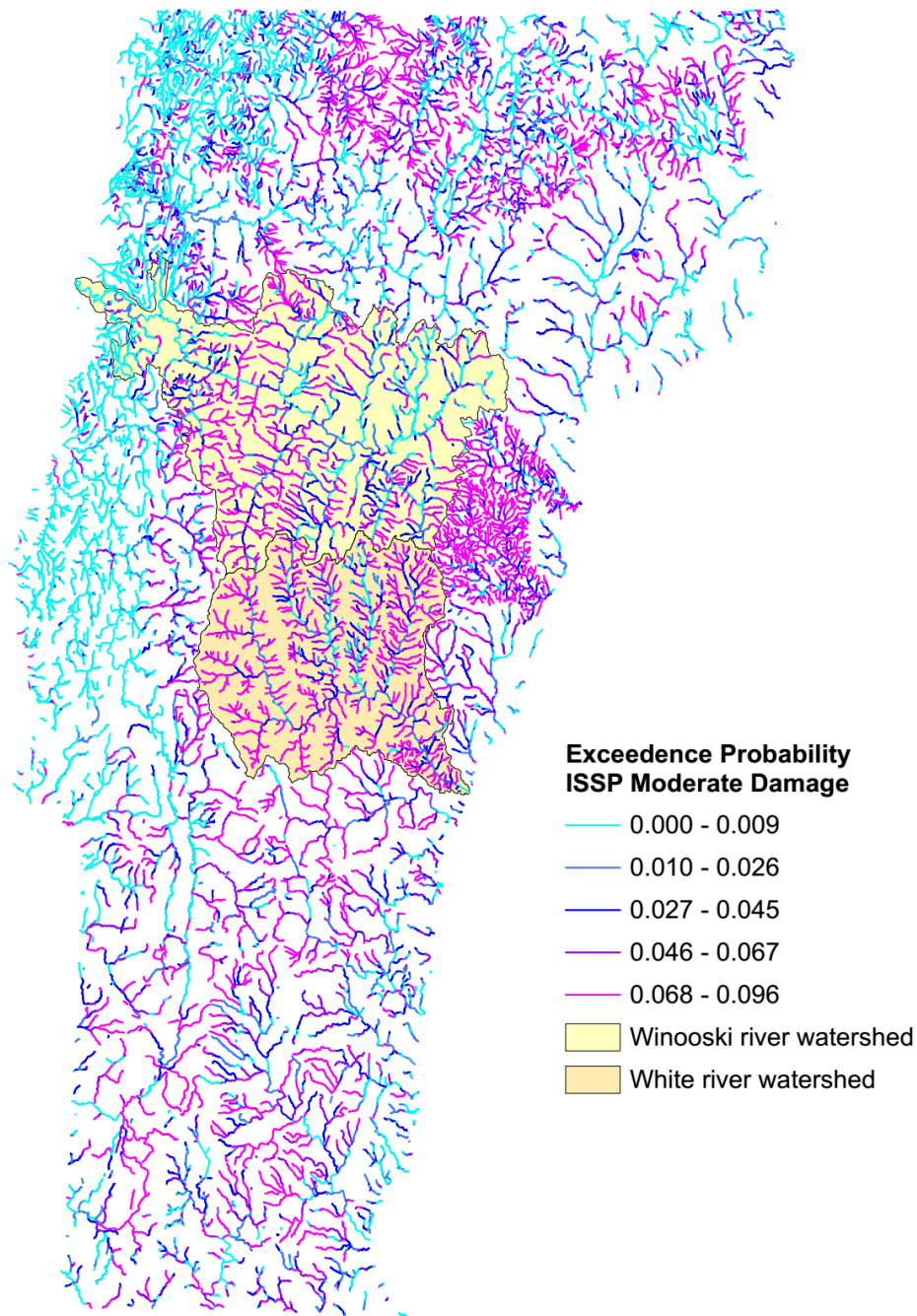


Figure 4.7: Probability map for the state of Vermont generated from ISSP.

For analysis focused in a single watershed, the probability of damage can be scaled to the total number of bridges in the selected watershed. For example, the probability maps (Figure 4.8a, 8b, 8c, and 8d) show the Winooski River and White River watershed, with each stream reach showing the maximum probability of damage in the Winooski watershed of 7.5 % corresponding to 23 damaged and 306 total bridges, and in the White River watershed of the 29% corresponding to 53 damaged and 180 total bridges.

Because the exceedance probabilities in Figure 4.8 are calculated on the watershed scale, color references from one watershed to another are not consistent, and should not be compared. Rather, the exceedance probability can be compared in various stream reaches and sub-watersheds to others within the containing watershed, to observe differences in the spatial hazard evident from Tropical Storm Irene. The SSP probability maps (Figure 4.8a and c) help show the uniform vulnerability based on stream power differences, with areas of high probability indicating vulnerability to the bridge infrastructure in those locations. The ISSP maps (Figure 4.8b and d) illustrate the prevailing hazard from Tropical Storm Irene in those locations to bridges and likely other transportation infrastructure, showing the increased effects of high rainfall on bridge damage. We observe that some areas, which appear to have high damage probability (upper right corner of Figure 4.8c), lack any recorded bridge damage, suggesting that additional bridge and hydrogeologic characteristics not considered in this analysis (e.g., surficial geology) may be necessary to differentiate vulnerability; this will be the focus of continued work. The expected trend of higher exceedance probability of damage (thus, higher stream power measures) in the steeper headwaters and tributaries, are reduced in the flatter and broader valley floor streams, as flow progresses downstream. Though the two pairs of maps are very similar, there are particular differences in which individual reaches are rated differently.

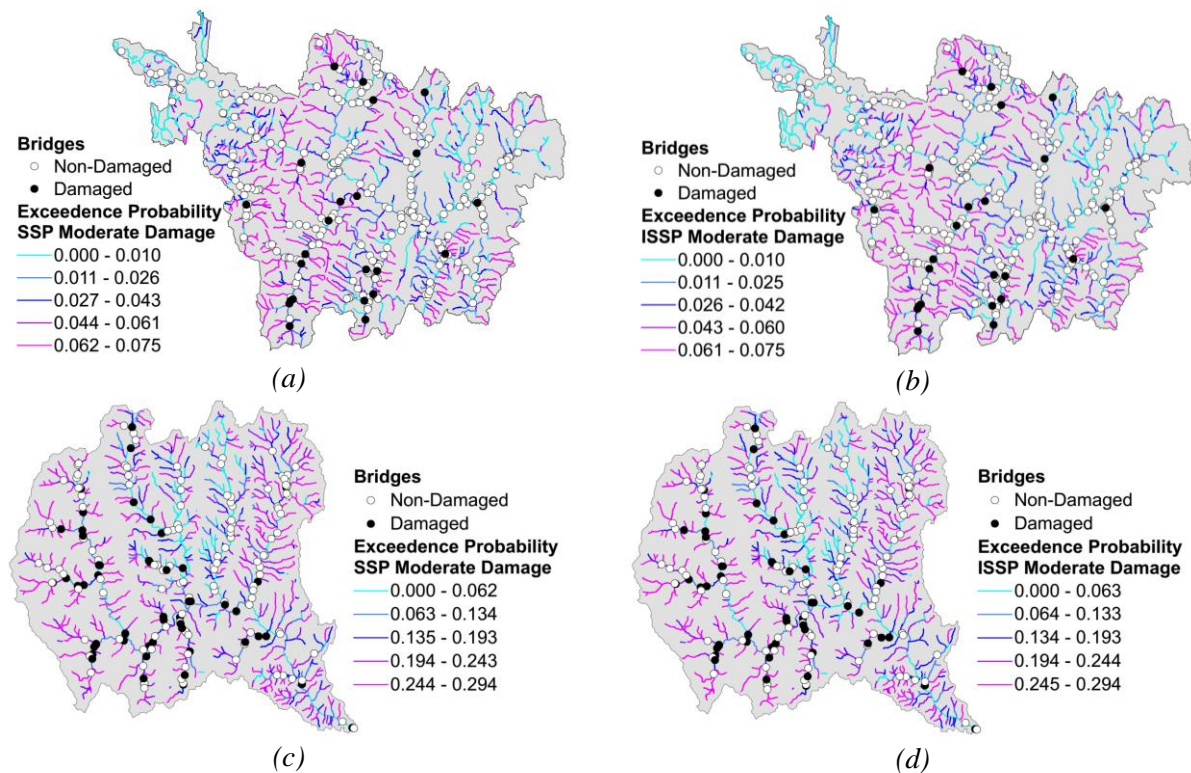


Figure 4.8: Probability Map for the White River Watershed generated from (a) and (c) SSP and (b) and (d) ISSP

4.4 Conclusions

This paper assimilated data and categorized the observed damage to 313 Vermont bridges from Tropical Storm Irene into four levels of severity, showed a linkage between bridge damage and stream power, and quantified and displayed the hazard statewide at the bridges and stream reaches used in this study. The application of empirical fragility curve analysis for stream power produced a probability of damage generated from the results collected from Tropical Storm Irene. With the implementation of probability mapping, the hazard to bridges from an extreme event like Tropical Storm Irene could be effectively displayed over a broad section of stream reaches, both at select watershed and statewide scales. The following specific conclusions are drawn from this work:

- 1) A GIS script was created and implemented to generate stream power measures statewide for the studied bridges and stream reaches in Vermont, including the use of a scaled stream power value to correspond to the magnitude of the storm impact.
- 2) Specific Stream Power, and the event-based, Irene Specific Stream Power were found to be both statistically significant at discriminating between damaged and non-damaged bridges, as well as between bridge damage levels from Tropical Storm Irene.
- 3) The resulting spatial probability maps allowed for visual display of vulnerable reaches, for which bridge placement would be at increased hazard. Further application of event-based SSP probability maps could be generated using rainfall ARI in future climate simulations to produce the probability of bridge damage for a hypothetical climate scenario.

The approach presented here could be implemented in other geographic regions. The method of estimating SSP and ISSP, and the calculation and expression of bridge hazard through fragility curves and probability maps could be useful in creating a screening tool for damage prediction. The methodology, and automated scripts used allow for rapid implementation in future applications, thus not limiting this work to Vermont. The Tropical Storm Irene database used here for the 313 damaged bridges experienced rainfall recurrence intervals ranging between 10 and 500 years, indicating that this methodology could be evaluated for a wide range of design flows for any watershed beyond the borders of Vermont.

As far as we know, this is the first investigation comparing site-specific stream power to observed bridge damage at a system level, and represents a fundamental breakthrough in the prediction of flood related bridge damage.

Future studies expanding upon this work could apply the probability maps to create a risk based inventory screening tool, to aid in decision making relating to transportation infrastructure planning. The complex interactions between the inherent bridge and site vulnerability cannot solely be explained through stream power, or any single variable. Future research seeks to leverage the full database of features to

identify which underlying characteristics in addition to the stream power play the most significant role in bridge damage vulnerability. Identifying these features requires the development of new feature selection techniques (i.e., genetic algorithms, learning system classifiers), which until recently were not widely available. The total cause of bridge damage also very likely includes a combined occurrence of high stresses, hydrogeologic instability, and vulnerable bridge infrastructure.

CHAPTER 5

HEURISTIC ASSESSMENT OF BRIDGE SCOUR SENSITIVITY USING DIFFERENTIAL EVOLUTION: CASE STUDY FOR LINKING FLOODPLAIN ENCROACHMENT AND BRIDGE SCOUR

(An article based on this chapter has been published as a technical paper in the journal of Environmental Systems Research. The authors are Lucas J. Howard, Ian A. Anderson, Kristen L. Underwood, Mandar M. Dewoolkar, Larry M. Deschaine and Donna M. Rizzo)

Synopsis:

Stakeholders are often required to make judgments and decisions about the tradeoffs between multiple competing objectives inherent in any engineering design. Design optimization can provide decision support for such situations, but often prescribes that only a single design solution be selected for a given set of preferences. The purpose of this study is to frame an objective function for assessing how the sensitivity of one objective relative to another varies in space and to demonstrate the method using a real site, with spatially-dependent floodplain access and bridge scour as the objective tradeoffs. Bridge scour is a widespread and expensive infrastructure problem, and the proposed methodology provides the ability to assess how the sensitivity of bridge scour to floodplain access varies at different locations in a river reach.

The site chosen for demonstration purposes was the Lewis Creek in the vicinity of the Quinlan Covered Bridge in Charlotte, VT. Differential Evolution (DE) was wrapped around an existing HEC-RAS model. The decision variables corresponded to floodplain access at locations up and downstream of the bridge; the objective function was constructed so that optimal solutions may be interpreted as relative salience of floodplain access to bridge scour. Multiple weightings of the objectives were used to verify that the rank-order of locations was robust. The optimal DE solutions for all weightings resulted in the same sensitivity ranking of locations, providing evidence that the analysis is not dependent on a particular choice of stakeholder objective weightings.

For systems with spatially dependent variables that impact a constraint or objective of interest to stakeholders, a tool for identifying locations where that variable has a particularly strong or weak impact (e.g. where floodplain access is more or less important for bridge scour) has obvious advantages. This study demonstrates a method for conducting such a sensitivity analysis using a numerical optimization scheme. On the real test site, the sensitivity ranking was consistent across multiple stakeholder weightings, providing evidence that the technique is robust, and one that can be used at multiple stages of design. This work demonstrates the utility of a novel interpretation of optimization results in which locations are ranked according to the relative sensitivity of competing objectives.

5.1 Background

5.1.1 Optimization and Sensitivity

The use of numerical optimization techniques to address real-world environmental and engineering problems, and provide decision support to stakeholders is a common strategy (Rios and Sahinidis, 2012). Optimization has been coupled with process-based models of varying complexity to minimize the cost of groundwater remediation or monitoring (Deschaine et al., 2013), to design the shape of a radio antenna for satellites (Hornby et al., 2011), to optimize the control of hydroelectric power plants, and for many other applications (Bartholomew-Biggs et al., 2002; Jeongwoo and Papalambros, 2010; Marsden et al., 2004; Mugunthan et al., 2005; Shlomi et al., 2010).

These applications all represent “design optimization problems” in which multiple objectives from various stakeholders must be translated into a single objective function (also known as cost or fitness functions) that can be reduced to a scalar value (i.e. cost or fitness) that “adequately” represents the design performance. Stakeholder constraints, preferences, and objectives are encoded in this cost function. In cases with multiple competing objectives, there is no single optimal solution (Jeongwoo and Papalambros, 2010). As a result, a number of numerical optimization methods found favor, generically referred to as evolutionary computation (e.g. genetic algorithms, evolutionary algorithms, simulated annealing, and differential evolution). These techniques, inspired by the concepts of natural selection in biological evolution, are able to effectively explore the tradeoffs between competing objectives resulting in, sets of non-dominated solutions (Fowler et al., 2015; Xu and Lu, 2011) where the design performance in one objective cannot be improved without decreasing its performance in other objectives. Since multiple stakeholders’ place varying importance on the different objectives and prioritization of constraints (Fowler et al., 2015), there are tradeoffs between the objectives (Fowler et al., 2015; Kurek and Ostfeld, 2013) with, for example, increases in contaminant cleanup time being weighed against monetary cost. In such cases, the two or more objectives can be combined into a total, scalar, cost or fitness function to create a single-objective problem (Kurek and Ostfeld 2013). The set of design variables that optimize (i.e. minimize or maximize) this function then corresponds to the optimal design solution.

Sensitivity analysis can also be performed subsequent to, or concurrently with, optimization (Harsha Choday and Roy, 2013) in engineering applications (Liou et al., 2013; Mesfin and Shuhaimi, 2010). These analyses typically quantify the sensitivity of the objective function to changes in design variables (Guerra-Gómez et al., 2013), near the optimal solution or otherwise (Liou et al., 2013), providing information about the marginal impact of changes in the design – potentially valuable information for designers and other stakeholders.

In this work, we use optimization as a tool to assess sensitivity rather than to find an optimal design. The goal is to wrap optimization around a process-based fluvial model to provide insight into the system behavior and visualize the spatial relationship between variables and competing objectives. More specially, in cases where an objective is comprised of two or more variables that are functions of space, the proposed method ranks locations according to the sensitivity of the objective to that variable. It does so, not by assessing sensitivity near an optimal solution, but instead by interpreting “optimal” results as indicative of relative—not absolute—sensitivity. Thus, the goal is to ordinally rank locations to provide decision support information.

Such an approach has significant advantages. It limits the need to explicitly weight competing objectives, since it does not prescribe a set of “best” designs, but indicates where, spatially or temporally, a particular variable is more or less important to a given objective. The approach suggested here may be used in the more preliminary stages of planning to provide information about system behavior and guide design criteria development.

In this work, the proposed method is applied to a real hydrologic system — a 1,025 m stretch of a river and a fixed bridge location. Using floodplain access (a spatially-dependent quantity) and bridge scour (the objective), we wrap an evolutionary algorithm around a widely-used, process-based fluvial model to rank locations up and downstream of the bridge according to the impact of floodplain access or encroachment on predicted scour at the bridge’s abutments. These results are relative, and the method may be generically applied to this kind of system to aid in the optimal placement of new bridges or to direct the efficient removal of floodplain encroachments to mitigate bridge scour risk.

5.1.2 Bridge Scour and Floodplain Access

Bridge scour is the removal of streambed soil and sediments from the supports of bridge foundations caused by water-induced erosion. Scour is the most common cause of bridge failures in the United States (Katell and Eriksson 1998; Arneson et al., 2012) and other parts of the world. For example, Melville and Coleman (1973) report 31 case studies of scour damage to bridges in New Zealand. In another study, Wardhana and Hadipriono (2003) analyzed over 500 cases of bridge failures in the United States from 1989 to 2000 and found that nearly 50% of the failures were related flood and scour. The HEC-18 document mentions numerous examples of scour related bridge damage and failure. It also reports that flooding in 1993 caused the failure of 23 bridges in the upper Mississippi basin at an approximate cost of \$13 million and in the following year, flooding was responsible for \$130 million in damage to bridges in Georgia including about 180 bridges in need of replacement (Arneson et al., 2012). More recently, Tropical Storm Irene damaged over 300 bridges in Vermont and 61 % of the affected bridges had scour-related damage (Anderson et al., 2014). The average cost of repairing the scour damage from Tropical Storm Irene

has been estimated at about \$240,000 (or about \$310 per square meter of deck area) (Anderson et al., 2014). Arneson et al., (2012) estimated the cost of a total bridge failure to be 2–10 times the cost of the bridge itself. The available case studies have indicated that repairing a scour-damaged bridge after-the-fact is onerously expensive, and remediating scour-critical bridges may be more economical in the long run.

The bridge repair and replacement costs mentioned above include only the direct costs of repair. If a bridge must be closed for repairs or fails altogether, there are cascading secondary costs due to lost time and decreased productivity of travelers, not to mention the very real risk of injuries and fatalities if scour damage results in unexpected and sudden bridge failure. When these secondary costs are considered, the total average cost of a single bridge failure is estimated at \$13 million (Briaud et al., 2014) – and over 23,000 bridges were classified as critical in 2011 in the United States, representing nearly 5 % of all bridges (Arneson et al., 2012). Given that scour is the leading cause of bridge failure and that hundreds of bridges are expected to experience flooding in excess of the 100-year flood annually (Arneson et al., 2012), the scale of this infrastructure management problem is clear.

Floodplain constriction is a key factor in scour damage risk (Anderson et al., 2014) as floodplains are vital to the attenuation of flood waves during storm events (Luke et al., 2015). Thus, from the perspective of bridge scour, increases in channel flow, velocity and water surface elevation can lead to increased scour potential. The linkage between bridge scour and floodplain access is complicated by the fact that roads and bridges are often placed near or across rivers and streams cutting them off from their natural floodplains. Lack of floodplain access often increases stream velocities, worsening in-stream incision and bank erosion, which in turn increases vulnerability to scour. Developing smart remediation strategies that reduce stream velocities and bridge scour during large storm events and help ameliorate the tradeoffs between human infrastructure needs and protection of the natural environment is critical for long-term sustainability. Mitigating scour risk by restoring floodplain access (i.e. regions adjacent to the stream channel which may become inundated during high-flow events) away from the bridge would help attenuate flood waves and result in smaller peak stage and discharge during storm events, which has obvious benefits that extend beyond bridge scour mitigation. Increased floodplain access may be beneficial in two ways: by decreasing backwaters, increases in water elevation upstream of constrictions, and decreasing peak flow velocities created downstream of constriction.

The importance of floodplain constriction by bridge structures is fairly well understood and various works have investigated these effects or calculated bridge scour at abutments in the floodplain (Kouchakzadeh and Townsend 1997). Additionally, there have been studies which describe the use of fuse plugs for flood mitigation (Jaffe and Sanders, 2001; Pugh, 1985; Schmocker et al., 2013). Fuse plugs allow access to floodplains during high flow events, and work on the assumption that increased floodplain access will result in non-local attenuation, i.e. attenuation of the flood wave away from the fuse plug. However, to

the best of our knowledge, prior research investigating the impacts of floodplain constriction (other than bridge structure constriction) on scour has not been published. A tool that can assess the relative sensitivity of bridge scour to floodplain access at different locations in a river reach has obvious benefits for this scenario.

In addition to mitigating scour at existing bridges, consideration of floodplain access is important when planning the location of new bridges. An understanding of the relative sensitivity of floodplain access at different locations has the potential to be very powerful. As previously mentioned, a bridge itself constitutes floodplain encroachment and becomes essentially part of the hydraulic and hydrologic river system. Whether the engineering problem at hand is to mitigate risk for a bridge at a fixed location, optimal placement of a new bridge to minimize scour risk within design constraints, or best placing an unavoidable encroachment when flexibility exists, understanding the sensitivity of scour to floodplain access at different locations both up and downstream of the bridge (existing or proposed) is key.

5.1.3 Differential Evolution

Evolutionary computation (EC) is a class of numerical optimization techniques using biologically analogous concepts (Figure 5.1). EC methods use “populations” of candidate solutions that are recombined, mutated and reproduced using a form of trial and error that attempts to optimally maximize (or minimize) a global fitness (or cost) function.

Differential Evolution (DE) is a stochastic, population-based EC algorithm designed for global optimization of real-valued functions with multiple variables (Rios and Sahinidis, 2012). These design variables specify a design solution that is evaluated by combining one or more objectives into a scalar-valued objective function. This function can then be optimized. It is often referred to as a cost function when the design problem is framed as a minimization problem or a fitness function when framed for maximization in the context of evolutionary algorithms. For this work, minimization was chosen and the function to be optimized will be referred to throughout as the cost function. Generally, constraints can be treated either as additional objectives to be minimized with penalty terms added to force convergence to feasible solutions (Bartholomew-Biggs et al., 2002). They can also be enforced explicitly, with the search limited to feasible regions of the search space (Storn and Price, 1997).

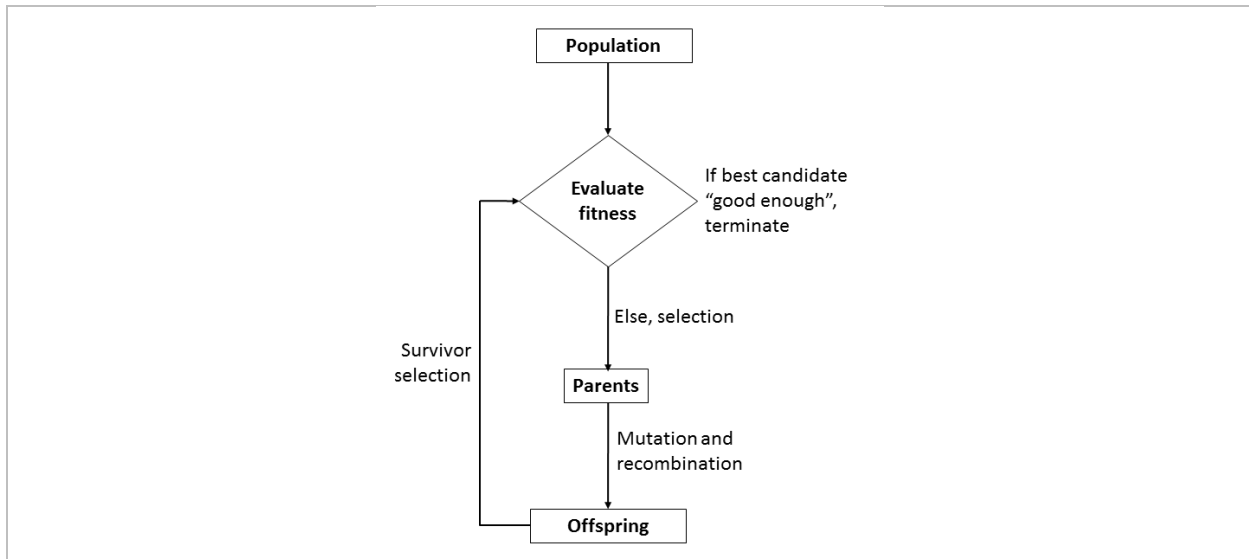


Figure 5.1: A flow chart of a generic evolutionary computation algorithm, in which a population of candidate solutions is initialized, a set of offspring candidates produced, and a new set of potential solutions is chosen for the next generation based on fitness

DE is an evolutionary algorithm, which solves real parameter and real value problems (Storn and Price, 1997). The DE algorithm begins with initialization of the population, selected from a uniform distribution that covers the entire parameter space. Individual candidate solutions are modified using biologically-analogous mutation and crossover operations to explore the search space. These operations are controlled by two parameters, the crossover fraction and the mutation factor. Details on the mechanisms of the algorithm are described by (Storn and Price, 1997). In a general sense, the algorithm creates a set of potential solutions referred to as the population. These candidates are then perturbed, and their fitness (cost) evaluated to determine how suitable they are. The next generation is then chosen from any combination of the original population and the perturbed "offspring" based on their fitness scores. DE has been shown to outperform many other evolutionary algorithms on standard benchmark and real-world problems (Vesterstrom and Thomsen, 2004).

DE has been successfully used on a cost function containing an implicit weighting of multiple objectives, resulting in a significantly improved design (Hornby et al., 2011). These kinds of tradeoffs encoded in a cost or fitness function have been discussed and utilized in applications including satellite antenna design (Hornby et al., 2011), optimizing the performance and operation of hydroelectric power plants (Li et al., 2015), and optimal management of groundwater remediation and management (Deschaine et al., 2013; Rizzo and Dougherty, 1996). Sensitivity of the cost function to changes in the design variables near the optimum (Dougherty and Marryott, 1991) is one way to evaluate relative sensitivity. However, interpretation of the optimal values of the decision variables themselves as relative sensitivity has not been proposed to the best of our knowledge.

5.2 Methods

5.2.1 Study Site and Site Model

The selected study area is the Lewis Creek channel and adjacent floodplain in the vicinity of the historic Quinlan Covered Bridge in Charlotte, northwestern Vermont (Figure 5.2). The study reach is 1,025 m long. The upstream drainage area of the river at this location is approximately 180 km². The Lewis Creek watershed spans the Northern Green Mountain and Champlain Valley biogeophysical regions in northwestern Vermont. The region is characterized by a humid, temperate climate, with mean annual precipitation reported as 1074 mm (Olson, 2014) and mean annual temperature recorded as 7.8°C (NOAA 2016). Mean annual runoff (488 mm) comprises 45% of the precipitation (USGS, 2010), and surface waters drain to Lake Champlain. Land use in the Lewis Creek watershed is estimated as 62% forested, 26% agricultural and 8% developed (Troy et al., 2014).

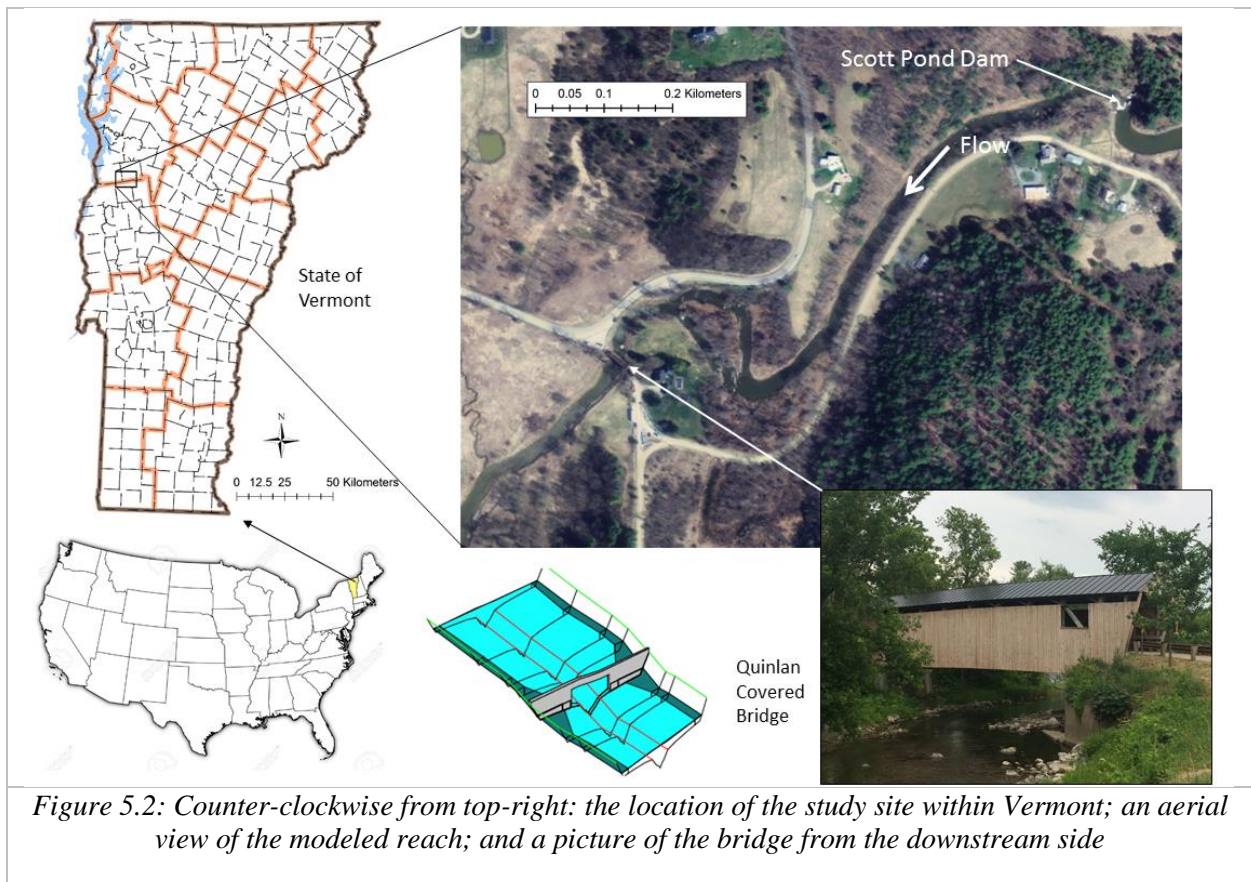
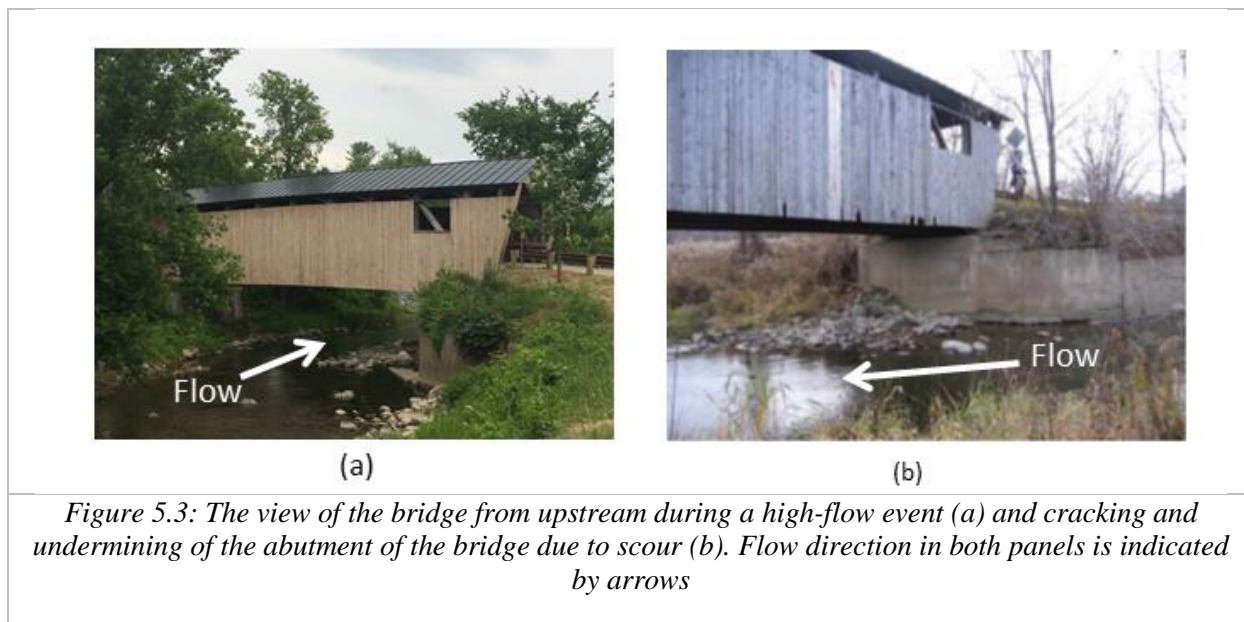


Figure 5.2: Counter-clockwise from top-right: the location of the study site within Vermont; an aerial view of the modeled reach; and a picture of the bridge from the downstream side

Mean annual flows in the Lewis Creek are estimated as 3.1 m³/s, based on historic records for a nearby US Geological Survey gaging station located nearly 6.5 180 km downstream with a drainage area of 199 180 km². The peak flow recorded since 1990 is 133 m³/s on 27 April 2011 (USGS, 2010). Regionally, the study reach of the Lewis Creek is located at the transition from a semi-confined valley to a much broader alluvial valley. In the upper half of the study reach the channel is constrained along the north

bank by a moderate to steep, forested, valley wall and is vertically disconnected from the floodplain along the south bank which has been cleared and modified to accommodate a gravel road and light density residential development. In the lower half of the reach, the valley setting is more open and the degree of channel incision below the floodplain is less pronounced. Riparian areas are partly forested and partially in hay and lawn.

The Quinlan Bridge span (Figure 5.3) is less than the natural bankfull width of the Lewis Creek channel, and the bridge is oriented at a sharp angle to the Lewis Creek. Flows are constricted through the bridge span leading to upstream aggradation and scour of the bridge abutments. Roads in vicinity of the bridge are elevated above the floodplain and both laterally and vertically constrain the channel and floodplain on approach to the bridge. Ice jams regularly cause localized flooding upstream and downstream of the bridge, threaten the integrity of the abutments of this historic bridge, and subject a nearby residential property to inundation and fluvial erosion hazards (SMRC, 2010).



In 2010, an analysis of the bridge was contracted to provide recommendations on several alternatives to existing conditions for the purpose of reducing the risk of further damage. Mitigation scenarios considered included lowering adjacent roads, lowering the floodplain, removing berms and realigning the bridge (SMRC, 2010). To perform the analysis, a HEC-RAS (Hydrologic Engineering Center-River Analysis System) model was built, calibrated and validated. HEC-RAS is a widely-used river and stream modeling software (Goodell, 2014) designed and distributed by the U.S. Army Corps of Engineers (USACE.) It supports modeling of many hydraulic structures, including bridges, and simulations of alternatives provide the predicted physical variables needed (such as velocity and stage) to evaluate scour and erosive potential for proposed scenarios. HEC-RAS was used to evaluate and compare multiple scenarios related to encroachment as a proof of concept.

The reach modeled by Milone and Macbroom, Inc. is 1,025 m long and drops approximately 5.8 m in elevation through the reach. The model extends from just upstream of the Scott Pond Dam (which operates in a run-of-river mode) to just downstream of the bridge, and is comprised of 13 cross sections. Eight of the 13 cross sections are labeled in Figure 5.4. The model geometry shows the cross sections in plan view (Figure 5.4a) as well as a cross section of the river along its length (Figure 5.4b). Only these Eight cross sections include floodplain access modifications for the proof-of-concept presented in this work, as increasing floodplain access was not physically realistic at all locations. The cross sections are labeled with XS₁ representing the most upstream cross section and XS₈ the most downstream. The bridge is between XS₆ and XS₇.

Flow magnitudes for various return periods were calculated by Milone and MacBroom using USGS streamflow gaging data from Lewis Creek, #04282780 (USGS, 2010), and regression equations (Olson, 2002). Normal depth was used as a downstream boundary condition based on the original survey. The analysis of alternatives was primarily done using steady-state simulations, but a sediment transport analysis was performed to investigate the potential impact of erosion and sedimentation for the proposed alternatives. The latter requires a quasi-unsteady analysis in HEC-RAS in which a transient event is modeled using a series of steady flows.

For steady flow simulations in HEC-RAS, stage and flow are calculated using energy losses between user-defined cross sections. For transient simulations, it solves the full 1-D St. Venant equations; HEC-RAS version 4.1, used for the Quinlan model, provides support only for 1-D modeling. The recently released version 5.0 provides support for 2-D flow modeling, however our data did not support 2-D simulations. In this work, transient simulations were used with an upstream hydrograph as a boundary condition. The hydrograph was constructed by scaling the quasi-unsteady hydrograph built by Milone and MacBroom for the sediment transport model so that peak flow corresponded with the design (50-year) flow. HEC-RAS routes this flow through the reach and provides hydraulic variables at the bridge for a given scenario.

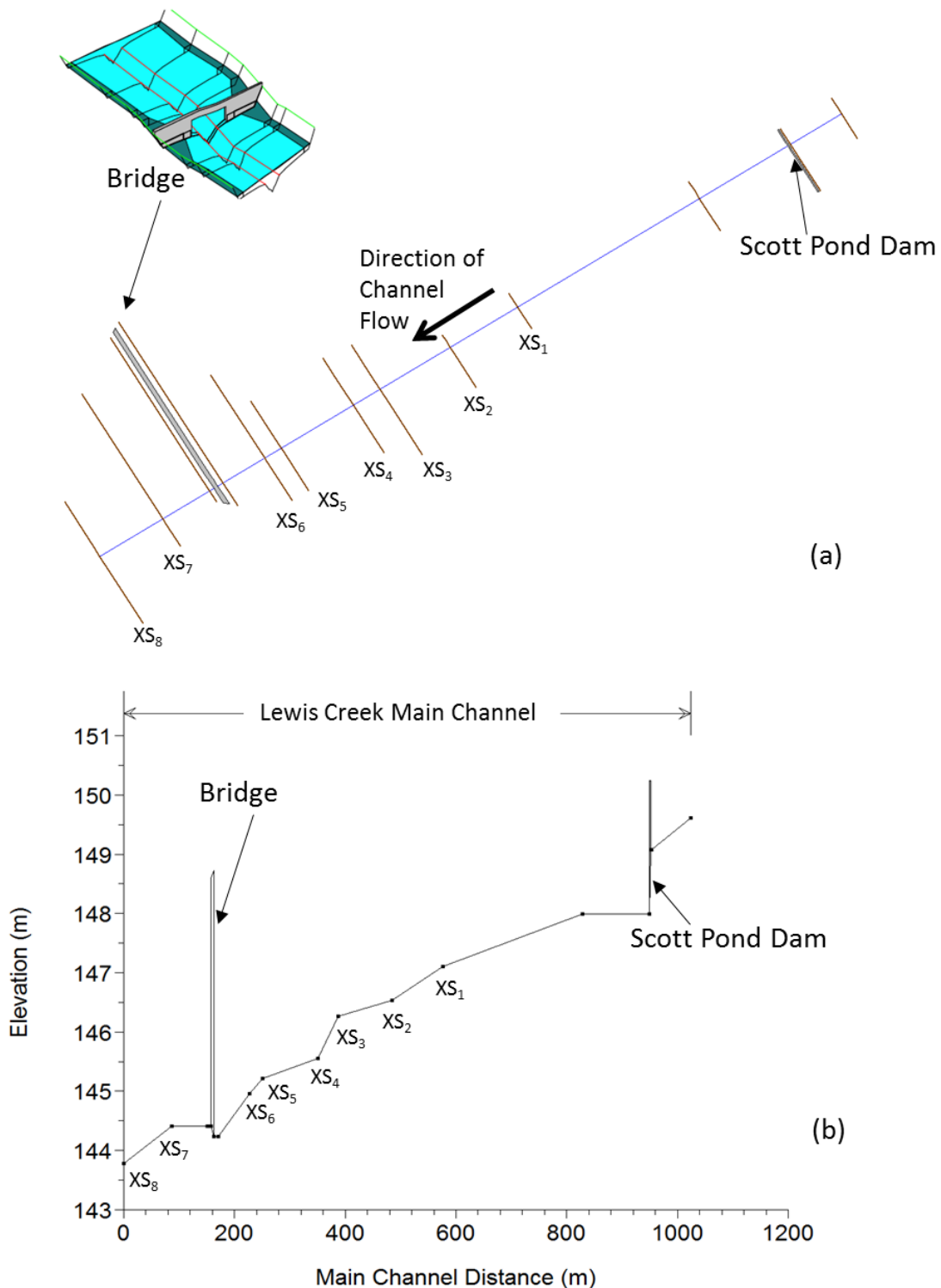


Figure 5.4: The model geometry of the Quinlan bridge is shown with its 13 cross sections (a). The direction of flow is from the upper-right to the lower-left. In (b), a side view of the modeled reach is shown. The Scott Pond Dam can be seen to the right and the bridge to the left. An arbitrary local datum was used for both horizontal and vertical coordinates.

5.2.2 Scour Prediction

Models such as HEC-RAS provide the means to predict physical variables, such as flow, stage or velocity. These variables, in turn, can be used in empirical scour equations as described by the Federal Highway Administration (FHWA) in HEC-18 (Arneson et al., 2012).

Scour predictions were calculated in post-processing using the results of HEC-RAS simulations. The following contraction scour equation is selected for this work, and is one of many outlined by the FHWA in HEC-18 (Arneson et al., 2012):

$$Y_s = 4Y_o \left(\frac{V_o}{\sqrt{gY_o}} \right)^{\frac{1}{3}} (0.55)K_1K_2, \quad (1)$$

where Y_s is the scour depth [m], Y_o is the water elevation at the bridge [m], V_o is the flow velocity [m/s], gravitational acceleration [m/s^2], and K_1 and K_2 are the skew and abutment coefficients, respectively.

Generally, the scour equations are overly conservative (Sheppard et al., 2014). However, for the purposes of evaluating bridge scour relative to a number of proposed scenarios, referred to here as *relative scour risk*, it is reasonable to interpret higher contraction scour values as corresponding to increased scour risk. While our results used the contraction scour equation, the methodology and the subsequent interpretation of the results would not change if a different scour equation was selected. As these equations are empirical, their validity is constrained to the range of data used to derive them.

When combined with the HEC-RAS model developed by Milone and MacBroom, Inc., Eq. (1) provides the needed hydraulic parameters, and enables scenarios to be evaluated and compared on the basis of bridge scour risk.

5.2.3 Differential Evolution (DE) Optimization and HEC-RAS Modifications

This design challenge can be formulated as a multi-objective optimization problem. To demonstrate the application of a method for evaluating the location-dependent sensitivity of bridge scour to floodplain access and constriction, the Quinlan Bridge HEC-RAS model geometry was modified. The modified geometry represents this stretch of the Lewis Creek as having the maximum amount of floodplain access possible. The design flood was initially (and artificially) constricted entirely to the channel, thus providing no floodplain access up or downstream of the bridge. This is a noteworthy departure from current standard engineering methods and research, as the modified model does not reflect any proposed or hypothetical scenario. Optimization with DE was then used to find the most efficient removal of encroachments to minimize bridge scour at the Quinlan Bridge. To efficiently mitigate scour risk, different magnitudes of encroachment removal may be needed depending on the location; scour sensitivity to floodplain access can be inferred from these optimal encroachment removal values and locations ranked by their impact on scour. Locations that require more extensive encroachment removal to reduce scour are more salient.

Once the modifications to the HEC-RAS model were implemented, a DE optimization algorithm was wrapped around the model to impose floodplain constriction, enable HEC-RAS simulations, and post-process the calculated contraction scour results without using the graphical interface. Floodplain area was modified and HEC-RAS simulations then used to predict scour. Python code was written to provide this functionality using the HEC-RAS API [Application Program Interface (Goodell, 2014)] and the ability to read and write to the HEC-RAS text files. In this work, the DE implementation in the Python library, SciPy, based on the description given by Storn and Price (1997), was wrapped around the combined HEC-RAS/cost function framework.

DE has several parameters that are user-defined. For this application, the crossover fraction was set to 0.7 and the mutation factor sampled from a uniform distribution in (0.5,1) every generation. The population size was 10. Because DE is a stochastic method, optimization was repeated using random restarts to verify consistent convergence. For each of three values of the weighting parameter β from Eq. (4), batch runs of 10 random restarts were performed.

Removal of encroachments on both the left and right side of the channel (facing downstream) was defined along eight cross sections for a total of 16 variables. These variables are defined over a range from 0 to 1, with 0 indicating no floodplain access (full constriction) and 1 indicating full floodplain access (no constriction). This is shown graphically in Figure 5.5, with \vec{x} being a vector whose components represent flood access corresponding to the left or right side of a particular cross section.

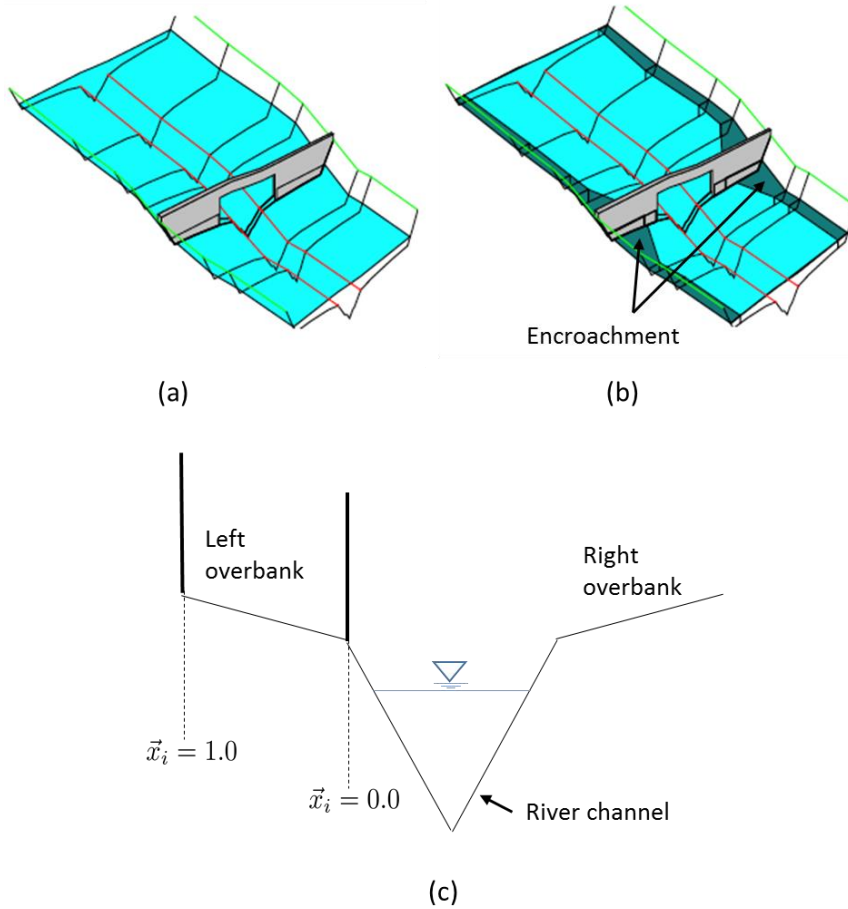


Figure 5.5: HEC-RAS modeled bridge with no encroachments (a), with encroachments (b), and schematic showing removal of floodplain constrictions. For the location corresponding to the i^{th} component of the decision vector, $\vec{x} = 0$ specifies no relaxation of the constriction, i.e. no flow is permitted to access the floodplain. $\vec{x} = 1$ specifies full floodplain access, i.e. no encroachments.

5.2.4 Cost Function

Construction of the cost function is key, particularly when multiple objectives are involved or when constraints are being enforced using penalty terms, to ensure that solutions meet the constraints and specifications of the real-world problem. A cost function was constructed to combine and weight the two competing objectives (floodplain access and bridge scour) into a scalar value as follows:

$$f(\text{floodplain access}, \text{scour}) = \text{floodplain access}_{sum}^2 + (\text{scour} - \text{scour}_{min})^2 \quad (2)$$

with *floodplain access* a vector of unitless floodplain area values, *scour* the scour in meters, and scour_{min} the user-defined threshold scour value. An optimal solution is one with low floodplain access (i.e. few built encroachments) and reduced bridge scour. These objectives are inversely correlated, so the tradeoffs between them are defined by a set of pareto optimal (non-dominated) solutions. The cost function weights

and combines these objectives into a scalar function to be minimized. Written with more succinct notation, Eq. [2] becomes:

$$f(Y_s, \vec{x}) = (\sum_i \vec{x})^2 + (Y_s - Y_{s_min})^2 \quad (3)$$

The cost function is equal to the sum of the squares of the floodplain access parameters, \vec{x} , where i is an index for location) and the amount of bridge scour Y_s over baseline scour Y_{s_min} as determined by a simulation with fully open floodplains. It is a function of the entire set of floodplain access parameters encoded in \vec{x} and the scour, which is an implicit function of \vec{x} since the level of scour depends on the hydraulic behavior given a specified floodplain access scenario.

If the goal were to perform design optimization and identify a single floodplain design that maximizes encroachment along the eight selected channel locations while minimizing scour at the bridge, rather than evaluate sensitivity of individual locations along the channel, weighting parameters could be added to each term in equation [3] to define the tradeoffs between the two stakeholder objectives. For the purposes of performing a sensitivity analysis, weights that determine the relative importance of objectives are not necessary because the optimal values of floodplain access will be evaluated relative to one another. In other words, they will be used to rank locations according to sensitivity and their absolute values will not be considered. To test this assumption, equation [3] was modified with a weighting factor, β , as follows:

$$f(Y_s, \vec{x}) = (\sum_i \vec{x})^2 + \beta(Y_s - Y_{s_min})^2 \quad (4)$$

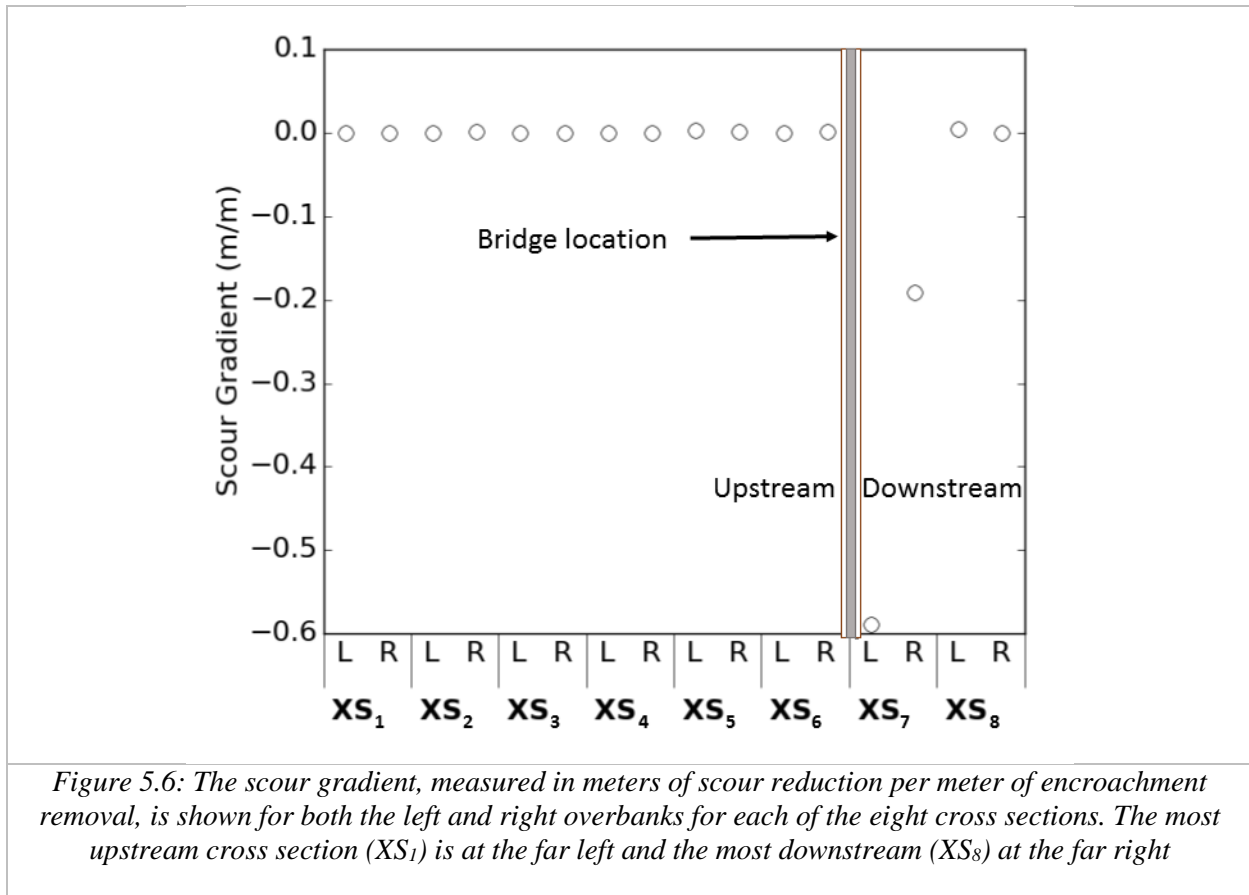
Larger values of β implicitly place greater weight on scour reduction, while values closer to zero weight minimization of floodplain access more heavily. Optimization was performed using values of β that relatively weight the two objectives over two orders of magnitude.

5.3 Results

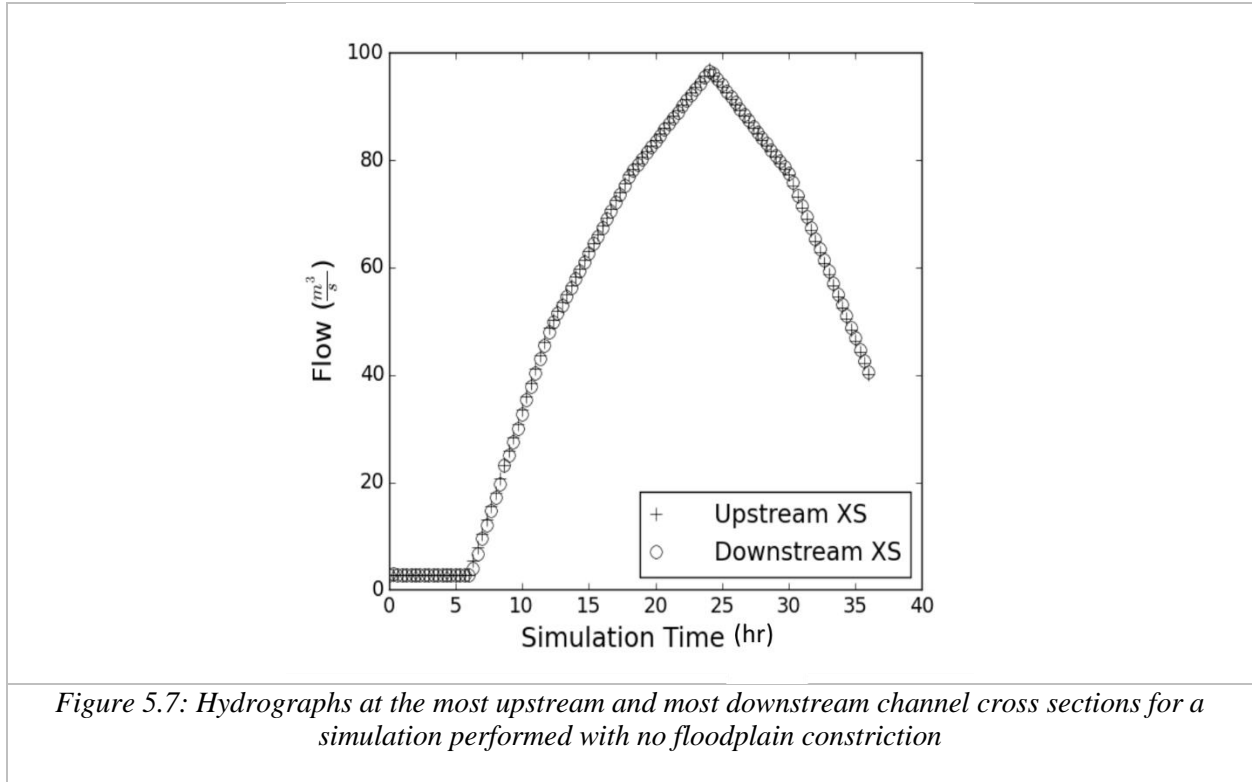
5.3.1 Flood Wave Mitigation

An initial exploratory investigation of system behavior was performed to guide future testing. The scour gradient was calculated using a one-sided finite difference approximation and defined as the rate of change of scour with respect to changes in floodplain access (Figure 5.6). All sixteen components of the gradient are shown in terms of the physical locations they represent. Labels “XS₁”, and letters “L” and “R” in a cross section for example, refer to the left and right overbanks, respectively, of the first cross section, XS₁. The figure shows the approximate partial derivative of scour with respect to the corresponding component of \vec{x} . Figure 5.6 identifies only XS₇, the location immediately downstream of the bridge, as

having any noteworthy effect on bridge scour; all other locations have a negligible impact on simulated bridge scour.



To complement this finding, the up and downstream hydrographs for the 50-year design storm for a simulation reflecting maximum floodplain access were plotted to assess the extent of flood wave attenuation and the role of naturally available floodplain access in the system. These hydrographs are shown in Figure 5.7. There is no discernible difference between the up and downstream hydrographs, and therefore, no flood wave attenuation. This simulation reflects the maximum amount of floodplain access, so no other plausible scenario would result in increased flood wave attenuation. The most likely explanation for this result is that the reach is simply not long enough and does not have sufficient storage volume in the floodplains. Scour potential is increased by increasing flow velocity and increasing water surface elevation. If upstream floodplain access does not attenuate flood waves, and there is no corresponding decrease in flow velocity, then bridge scour for the design flood will be controlled by backwaters created by downstream constriction. When viewed together, the scour gradient and hydrograph data provide convincing justification for focusing only on the two variables corresponding to cross section 7 (X_7^R and X_7^L , the unitless encroachment parameters at the right and left side, respectively, of cross section 7) given the trivial impact that other locations have on bridge scour.



5.3.2 Global Search Results

The optimal results generated by applying DE to three cost functions representing different weightings of objectives ($\beta = 0.1$, $\beta = 1$ and $\beta = 10$) are shown in Figure 5.8 in coordinates normalized by the size of the floodplain. The results in unnormalized coordinates are shown in Figure 5.9. For the purpose of sensitivity analysis, the ranking of two variables (i.e. the amount of left and right floodplain access at cross section 7) should be independent of weighting; all solutions should be on the same side of the line defined by $y = x$. Optimal solutions below and to the right of the 45° line correspond to solutions where $X_7^R < X_7^L$. Solutions above and to the left of this line correspond to solutions where $X_7^R > X_7^L$. Optimal solutions for all three cost functions fall on the same side of the $y = x$ line and indicate the same sensitivity ranking of variables.

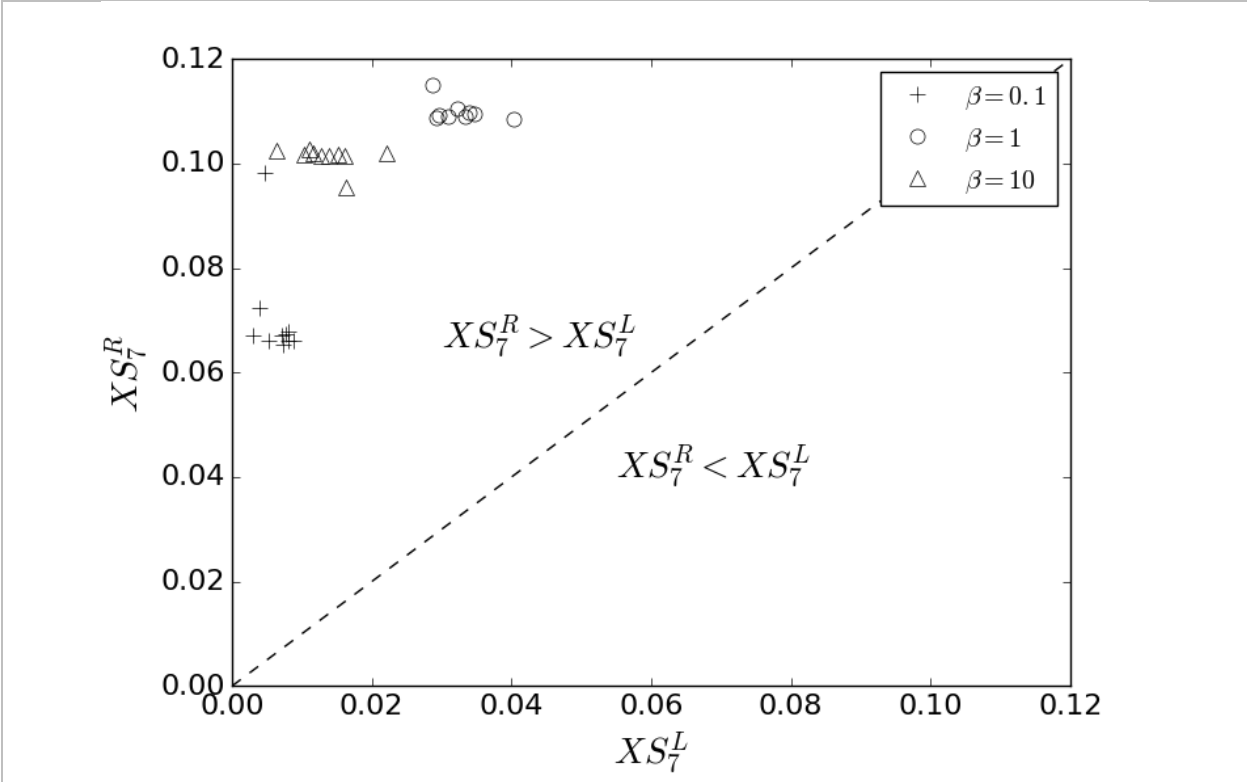


Figure 5.8: Optimization results in the normalized coordinates for all three weightings of the two objectives

The results of all ten batch runs for all three cost functions are shown together in Figure 5.8 to confirm consistent convergence of DE. DE performs its search for optimal solutions stochastically, so to increase confidence in the optimal results produced by DE, random restarts were performed on all three cost functions. There is no way to ensure that the location it converges to is a true global optimum; thus, random restarts (with different pseudo random number generator seeds) that converge to the same optimal solution increase the chances of finding a globally optimal solution or provide evidence that the initial results are not local sub-optimal solutions. For each cost function, the results are clustered in the same region of the search space, indicating that convergence was consistent and representative of globally optimal solutions.

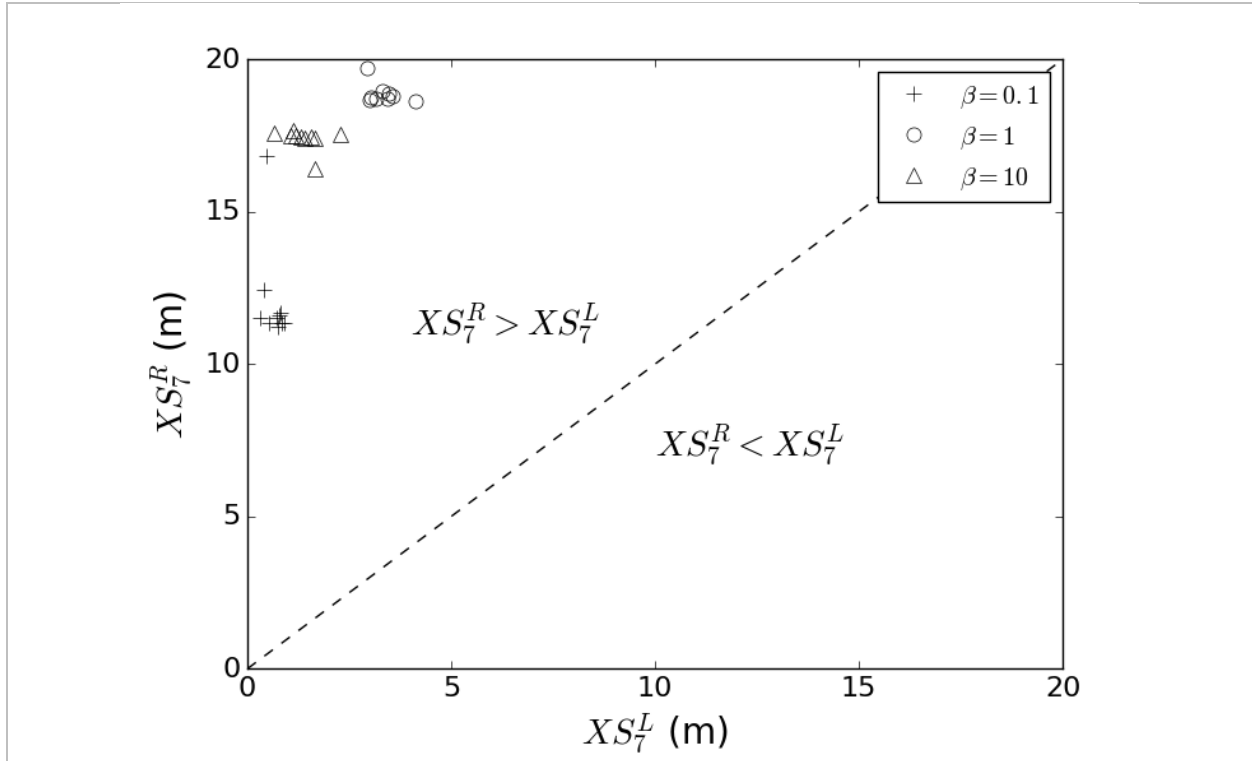


Figure 5.9: Optimization results in the unnormalized coordinates for all three weightings of the two objectives

5.4 Discussion

The implemented methodology provides a framework for decision support in the form of a sensitivity analysis. Using optimization and a process-based model, the proposed methodology assesses the spatial variability of the impact of one objective on a system constraint. The system in this case is a river channel and the constraint of interest is contraction scour at a fixed bridge location. For demonstration purposes, optimization was performed using DE to minimize a cost function that increases with increasing bridge scour (the constraint) and increasing floodplain access (the spatially-dependent design variable). The desired outcome is a ranking of floodplain access by location in terms of impact on bridge scour under a defined design flow (i.e., flood of 50-yr return interval). We interpret the optimal connected floodplain at a specific cross section of a river as an indicator of the relative impact of floodplain access at that location to bridge scour.

Optimization performed on this system results in a set of spatially dependent optimal floodplain access values as the connected floodplain shape (plan view width) is changed to optimize the objective function. The proposed method is distinct from the design optimization process, instead leveraging numerical optimization and a constructed cost function to evaluate the relative spatial sensitivity of one objective with respect to another. Although it is straightforward to rank locations according to their

respective optimal values, the interpretation of this information as relative sensitivity is not. The optimization process performed in this work provides evidence that this is a reasonable interpretation.

The scour gradient was earlier defined as the rate of change of scour with respect to changes in floodplain access at specific locations along the channel. The gradient at maximum constriction can be easily interpreted as relative sensitivity by noting that locations where the scour is reduced more per unit of increased floodplain access have a greater impact on bridge scour. These results suggest that bridge scour at the Quinlan Bridge system is controlled primarily by a backwater created by downstream constrictions. This implies that upstream reach storage effects at this particular site do not significantly mitigate the design flood wave. The up and downstream hydrographs at maximum floodplain accessibility confirmed this interpretation, showing very little flood wave mitigation between the top and bottom of the reach (Figure 5.7). The gradient results (Figure 5.6) also indicate that only the cross section immediately downstream of the bridge had any noteworthy effect on bridge scour, and that scour was more sensitive to floodplain access on one side of that cross section than the other. The finding that only downstream floodplain constriction causing backwater has an impact on bridge scour is specific to floodplain access and is a result of insufficient upstream storage area in the floodplains. The channel is vertically disconnected from much of the study reach at the stage of the 2-year flood – significantly lower than the 50-year design storm used for performing the sensitivity analysis. This may partially explain the lack of floodplain storage (and resultant negligible flood wave attenuation).

Optimization of the cost function was consistent for all three cost functions (values of weighting parameter β) with identical rankings of the two salient decision variables. Optimization resulting in identical ranking of variables for all three values of β indicates that the sensitivity analysis is roughly independent of the weighting of the objective terms in the cost function. A result of this finding is that the method does not rely on a precise weighting of objectives by stakeholders – the sensitivity analysis is identical across objective weights. While the site in question does not have upstream sensitivity, in a reach with more salient locations (i.e. more locations where floodplain access impacts bridge scour) the method could be applied analogously to rank more than the two locations ranked in this work.

The reliability of the underlying model itself is important when assessing the reliability of the sensitivity analysis. In this work energy losses and erosive effects, due to sharp changes in direction of the stream channel, cannot be modeled using the 1-D St. Venant equations solved in HEC-RAS 4.1. In their report, Milone and MacBroom noted the sharp turn in the stream immediately preceding the bridge. One of the bridge scour mitigation measures briefly considered was to realign the stream and straighten its approach to the bridge. However, from a stream geomorphic perspective it was judged to be both prohibitively expensive and ultimately ineffective.

However, this sharp turn in the stream channel must be considered in terms of its impact on the sensitivity results. A picture of the sharp approach is shown in Figure 5.3a. Without a more detailed representation of the site physics (e.g. a 2-D model), it is difficult to determine the extent to which the 1-D HEC-RAS modeling approach oversimplifies the bridge scour and erosion dynamics. Two-dimensional modeling, such as that now available in HEC-RAS 5.0, would be a logical next step to confirm the sensitivity findings of this work, and to evaluate the site itself as a candidate for further study using 2-D models. However, even without this 2-D analysis there are good reasons to trust the results. The backwater-controlled scour is dependent on lack of floodplain storage volume, a detail that is not affected by not modeling potential 2-D energy loss effects. Thus, the conclusion implied by the sensitivity analysis that downstream floodplain access is more salient to bridge scour mitigation than access upstream is a direct result of this finding, and it is therefore likely that substituting a 2-D model would not substantively change the sensitivity analysis. Even if there are noteworthy erosive effects not captured in the 1-D model, these would be more relevant to accurate and quantitative prediction of bridge scour at the site than the sensitivity analysis presented in this work.

In general, the proposed methodology is independent of either model or optimization technique. It requires that there be an objective of interest (in this case floodplain access) that impacts another objective or constraint (in this case bridge scour). A model, capable of simulating different scenarios and calculating these objective(s) and constraint(s), must exist. If the competing objectives are functions of space, then a ranking with this method may be performed, provided the model is not too computationally expensive for the chosen optimization algorithm. The latter was not the case for this application. If the model were more computationally expensive or the search space much larger, an alternative optimization algorithm may be warranted. However, this does not materially impact the interpretation proposed in this work, and the relative ease of the optimization makes it unlikely that different algorithms would produce different results.

5.5 Conclusions

This work presents a new approach to applying DE optimization to engineering challenges, and tests that approach on a real site. The technique involves constructing a cost function in such a way that the multi-objective ``optimal' results do not represent an optimal design in the traditional sense of minimizing a collective set of two or more constraints, but rather represent the sensitivity of a given constraint or objective of interest with respect to a second objective or constraint – a novel interpretation of optimization results. Because optimal decision variable values are assessed relative to one another and do not represent a specific design or reflect stakeholder-defined preferences of objectives, the need to specify the relative importance of objectives is relaxed. The constraint used to demonstrate the approach was bridge scour with respect to floodplain access, and the system was a river system comprising natural channel geometry and

built structures (a bridge). The use of DE on constructed cost functions representing different weightings of the two objectives provided the same rank-order of reach locations with respect to their floodplain access impact on predicted bridge scour; ancillary testing using a finite difference scour gradient supports the proposed interpretation. Also of interest is that the sensitivity analysis is somewhat independent of objective weighting, which potentially reduces the stakeholder burden of deciding how to weight competing objectives. Instead, this approach focuses analysis on elements of the system's behavior that can be used to guide the design of floodplain infrastructure, remediation efforts, or the placement of new bridges. Applying this approach to other rivers would focus attention on locations where increased floodplain access would result in the most efficient use of resources, and applying it to other systems with spatially-variable components which have functional relationships with objectives of interest to stakeholders may provide similar decision support information.

CHAPTER 6

USE OF SACRIFICIAL EMBANKMENTS TO MINIMIZE BRIDGE DAMAGE FROM SCOUR DURING EXTREME FLOW EVENTS

(An article based on this chapter is in review with the journal of Natural Hazards. The authors of this article are Matthew W. Brand, M.W., Mandar M. Dewoolkar and Donna M. Rizzo)

Synopsis:

The leading cause of bridge failure has often been identified as bridge scour, which is generally defined as the erosion or removal of streambed and/or bank material around bridge foundations due to flowing water. These scour critical bridges are particularly vulnerable during extreme flood events, and pose a major risk to human life, transportation infrastructure, and economic sustainability. Climate change is increasing the intensity and persistence of large flow events throughout the world, further straining bridge infrastructure. Retrofitting the thousands of undersized and scour-critical bridges to more rigorous standards is prohibitively expensive. This research tested the efficacy of using approach embankments as intentional sacrificial “fuses” to protect the bridge integrity and minimize damage during large flow events by allowing the streams to access their natural floodplain and reduce channel velocities. This countermeasure concept was evaluated using the Hydrologic Engineering Center's River Analysis System (HEC-RAS) models. Steady flow models were developed for three specific bridges on two river reaches. Streamflow return period estimators for both river reaches were developed using Bayesian analysis and available United States Geological Survey (USGS) stream gauge data to evaluate sacrificial embankments under non-stationary climatic conditions. Fuse placement was determined to be a cost effective scour mitigation strategy for bridges with suboptimal hydraulic capacity and unknown or shallow foundations. Additional benefits of fuses include reductions in upstream flood stage and velocity.

6.1 Introduction

Scour is the primary cause of bridge failures in the United States (Kattell and Eriksson, 1998) and other parts of the world. Melville and Coleman (1973) report 31 case studies of scour damage to bridges in New Zealand, which were primarily attributed to pier failure (13 cases), erosion of the approach or abutment (8 cases), general degradation (4 cases), and debris flow or aggradation (6 cases). The Federal Highway Administration (FHWA) Bridge Scour Evaluation Program reports that as of 2011, the United States has over 23,000 (4.7%) scour critical bridges, and over 40,000 (8.3%) bridges with an unknown foundation (Hydraulic Engineering Circular 18 (HEC18) by Arneson et al. 2012). Between 1969 and 1991, more than 1,000 bridges failed; 60% of those failures were due to scour (Briaud et al., 1999). Wardhana and Hadipriono (2003) analyzed 503 cases of bridge failure in the United States from 1989 to 2000 and found that the leading causes of bridge failure relate to flood and scour. HEC 18 provides several examples of

scour related bridge damage and failure in the United States. For example, during the 1987 spring floods, 17 bridges in New York and New England were damaged or destroyed by scour. Failure of the I-90 Bridge over the Schoharie Creek near Amsterdam, NY in 1987 resulted in the loss of 10 lives and millions of dollars in bridge repair and replacement costs (FHWA 2015). In 1985, flooding in Pennsylvania, Virginia and West Virginia destroyed 73 bridges. A 1973 national study (FHWA 1973) of 383 bridge failures caused by catastrophic floods showed that 25 percent involved pier damage and 75 percent involved abutment damage. A second more extensive study in 1978 indicated local scour at bridge piers to be a problem about equal to abutment scour problems (FHWA 1978; Arneson et al. 2012). The 1993 flood in the upper Mississippi basin caused damage to 2,400 bridge crossings (FHWA 2015) including 23 bridge failures (Arneson et al., 2012). The analysis of over 300 Vermont bridges damaged in 2011 Tropical Storm Irene indicated that about 56% of the damaged bridges had scour damage, 30% had channel flanking, and the remaining 14% had superstructure and debris damage (Anderson et al., 2017a).

As part of the Third National Climate Assessment, Walsh et al. (2014) concluded that some regions of the United States are experiencing an increase in the frequency and intensity of heavy downpours and hurricane-level storms due to non-stationary weather conditions. The Northeast United States has seen the largest increases in heavy precipitation with a 71 percent increase in precipitation during heavy storm events (Karl et al., 2012); this problem is compounded by the fact that storm events are persisting longer than in the past, further increasing flooding hazard through persistent wetness and lack of ground surface infiltration capacity during long periods of rainfall (Guilbert et al., 2015). The recent increase in extreme rainfall events and persistence leads to non-stationary streamflow return period estimates. The latter refers to the observation of parameters (e.g., watershed streamflow parameters such as mean or variance) that change with time. This can lead to infrastructure that does not meet necessary design criteria throughout time. The Northeast United States is not alone in experiencing this phenomenon; numerous studies show that flooding risk is increasing throughout the world in places such as China (Fu et al., 2013), England (Fowler et al., 2005), India (Rajeevan et al., 2008), and Switzerland (Schmocker-Fackel and Naef 2010). This leads to more devastating and frequent flooding events, further strain on infrastructure and an increased need for cost-effective scour mitigation for bridges. Retrofitting the thousands of existing undersized and scour critical bridges to the current standards is prohibitively expensive.

Adding complexity to the linkages between bridge scour and damage is the fact that roads and bridges often encroach rivers and streams floodplains, which can significantly restrict stream-flow area. Lack of floodplain access thus often increases stream velocities, worsening in-stream incision and bank erosion, and in turn, increasing bridges' vulnerability to scour. Developing smart mitigation strategies that reduce stream velocities and bridge scour during large flow events helps to balance the tradeoffs between human infrastructure needs and protection of the natural environment for long-term sustainability.

This research studies the efficacy of using approach embankments as intentional sacrificial fuses to minimize bridge damage by reducing potential scour. A sacrificial approach embankment design allows streams to access their floodplain during high-flow events, reducing channel velocities, and correspondingly, the potential destruction associated with bank erosion and bridge scour. An example of a fuse operating during normal and high flow events is shown in Figure 6.1. During normal flow events, the embankment is sufficiently armored such that it does not wash away. However, during high flow events, the embankment is quickly eroded and allows the river access to its floodplain. This reduces the velocities underneath the bridge by channeling flow around the bridge and into the floodplain. This concept can prove effective for both existing and new bridges as a scour countermeasure technique.

A very limited amount of research was found on the use of sacrificial embankments in hydraulic bridge design; however, there is a significant body of work on fuse-plugs for earth- and rock-filled dams. A fuse-plug spillway, as defined by the United States Bureau of Reclamation (USBR), is a form of auxiliary spillway consisting of a low embankment specifically designed to be overtopped and washed away during a large flood. The first physical hydraulic model study of fuse-plugs was performed by the USBR to determine their usefulness for flood control dams in 1980s. The report (Pugh, 1985) concluded that a properly designed fuse-plug embankment would predictably wash out when a large flood needs to pass through the reservoir.

A detailed hydraulic analysis of fuse-plug designs performed for a canal in Switzerland by Schmocker et al. (2013) found fuse-plugs to be useful in smaller applications, such as along a river or canal. They tested two, scaled, fuse-plug designs in a flume, one with a large inclined clay core and a second having sandy fill with a small clay core. Both designs performed as expected and eroded away in a quick and controlled manner. The authors recommended the sandy fill fuse-plug design over the inclined clay core because of its comparative ease of construction and equivalent performance.

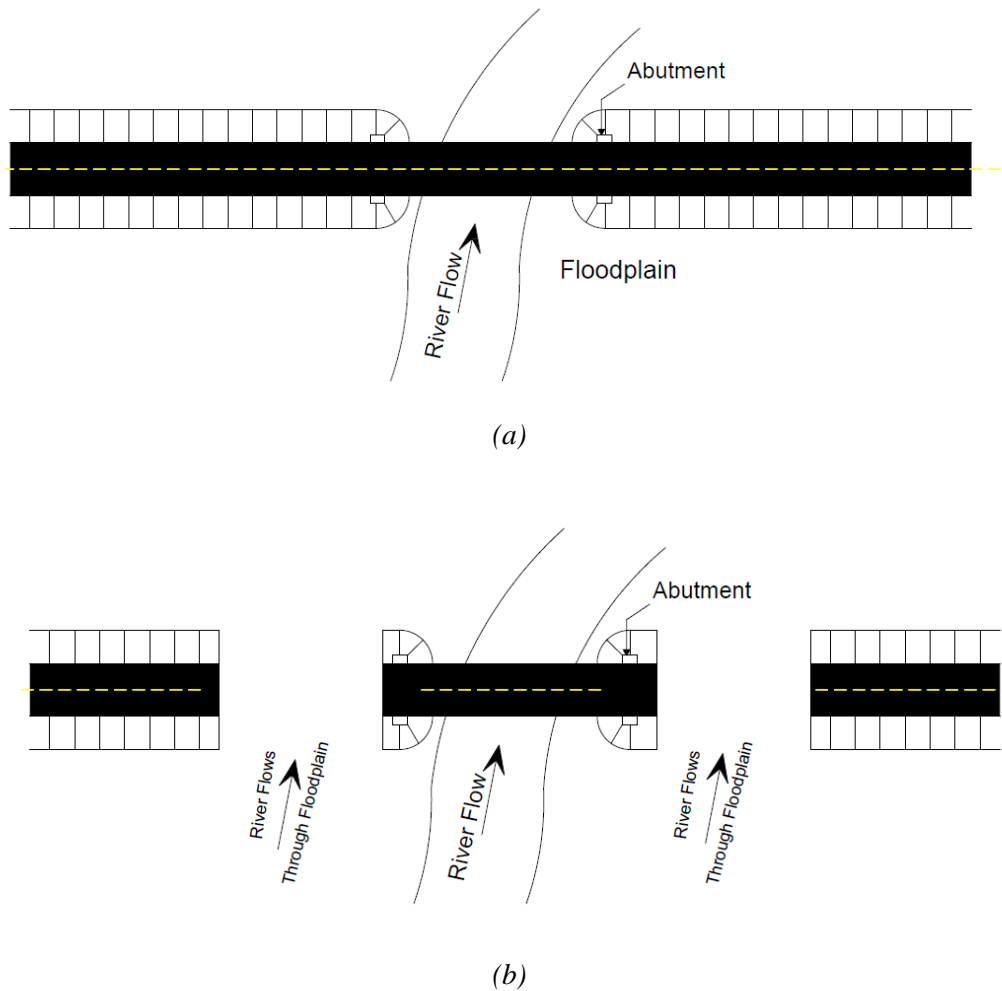


Figure 6.1: Concept of a sacrificial approach embankment (a) Plan view of bridge under normal flow conditions and (b) during large flow events when fuse is activated to allow access to floodplain.

In May of 2011 at the New Madrid Floodway on the Mississippi River near Cairo, Illinois, a fuse-plug along the Mississippi River was activated when the United States Army Corps of Engineers detonated a forward levee to allow the Mississippi access to a large floodplain during a storm reducing the stage of the flood upstream of the breach. Luke et al. (2015) studied the impacts of detonation after the storm and determined that the fuse-plug reduced the flood stage by 0.8 m and was a significant factor in minimizing damage to Cairo. Luke et al. (2015) suggest that future hydraulic modeling studies on breach geometries and floodplain activation techniques would be useful to the New Madrid Floodway and others with similar geometries. In addition, other researchers have proposed similar mechanisms to reduce flood stage and velocities by purposefully breaching key levees as a flood mitigation technique (Jaffe and Sanders, 2001). Translating fuse-plug designs from a levee situation to a sacrificial embankment situation is feasible because levee and bridge embankments share many of the same design characteristics.

The research presented here has two main objectives. We first demonstrate the functional and economical effectiveness of sacrificial approach embankments in significantly reducing bridge scour. The second objective illustrates the benefits of reconnecting a stream to its floodplain during large flow events with sacrificial embankment installation by reducing the stream stage and velocity. To incorporate uncertainty in streamflow return periods, a Bayesian approach was used to estimate the confidence intervals associated with the return periods. We also interviewed practicing professional engineers to assess the feasibility of implementing this concept in practice; a summary of these interviews is also included.

6.2 Methods

To analyze the effectiveness of the sacrificial approach embankments in reducing bridge scour, we made some reasonable assumptions to simplify the hydraulic model. First, we assumed that when a flood wave hits a bridge, a well-designed sacrificial embankment immediately erodes away. Using stream gauge data from the United States Geological Survey (USGS), we developed a Bayesian estimator to generate a distribution of possible streamflow return periods to test the efficacy of incorporating a sacrificial embankment fuse under non-stationary climatic conditions. We evaluated three existing bridges that cover a broad range of structural and hydraulic characteristics and analytically tested the effectiveness of sacrificial embankments to reduce scour at these bridges. The study is designed as a “proof of concept” and is not meant to make specific recommendations for the select bridges at each study site. Although the study used data from the Northeastern United States, specifically the state of Vermont and the 2011 extreme flooding event of Tropical Storm Irene, the methodology presented here is applicable to other settings.

6.2.1 Study Sites

We used three example bridge sites in Vermont for our analysis. The relevant characteristics of each bridge are summarized in Table 6.1. Note that the “Federal Sufficiency Rating” is based on the United States National Bridge Inventory inspection program, where bridges are given a score from 0 - 100 based on their condition. A score of 100 is considered to be in perfect condition; and a 0 represents a bridge that is unusable or entirely deficient. According to the FHWA, “any bridge with a sufficiency rating of 50.0 or less is eligible for replacement or rehabilitation, while bridges with a sufficiency rating of 80.0 or less are eligible for rehabilitation” (Burrows et al. 2015).

The first bridge, labeled “Bridge 1”, was built in 1992 and is considered at lower risk of failure due to scour at the 100-year storm design because of its age, geometry, and foundation type and depth. The second bridge (Bridge 2) was built in 1985 and is a general example of a bridge with a “moderate” risk of failure due to scour at the design storm. In addition, the Federal Inspection report noted that the stream has a slight chance of overtopping the roadway during the 100-year storm event. The third bridge (Bridge 3)

was built in 1928 with a steel pony truss and simple slab foundation at an unknown elevation below the original streambed surface. The foundation depth was assumed to be 1.8 m below the original streambed elevation as per standard Vermont Agency of Transportation practice (Wark et al., 2015). The bridge is considered functionally deficient by federal standards. Significant repairs are needed for both the superstructure and substructure. One abutment is cracked, rotated and in need of repair; the other abutment is also cracked. This structure represents some of the worst-case bridge scenarios – those in need of repair and also having unknown foundations.

Table 6.1 - List of bridges used in the analysis with relevant characteristics

Bridge	Year Built	Foundation Type	Foundation Depth (m)	Drainage Area (km ²)	Span (m)	Deck Area (m ²)	Federal Sufficiency Rating
1	1992	H-Pile	6.9	1,740	41.5	1,226	96.4
2	1985	H-Pile	12.2-13.4	331	30.5	1,486	83.8
3	1928	Slab Footing	Unknown (assumed 6 feet)	385	30.5	209.7	50.9

6.2.2 Streamflow Return Period Estimates Under Non-Stationary Conditions

Bayesian statistics, first proposed in a hydrologic context by Wood and Rodriguez-Iturbe (1975), has become an increasingly popular method for accommodating uncertainty in streamflow return period estimates. The Bayesian estimation of streamflow return periods allows uncertainty to be incorporated into designs because it provides a range of possible values for design parameters compared to single estimates (Botto et al., 2014).

According to Bayes theorem (Equation 1), we can find the probability of observing an event A given a new piece of evidence B (known as the conditional probability) by multiplying the reverse conditional probability of B given A , with the probability of A , and dividing by the probability of B .

$$P(A|B) = \frac{P(B|A)P(A)}{P(B)} \quad (1)$$

For this paper, A is defined as one of the log-normal distribution parameters, μ or σ associated with the measured maximum annual streamflow measured over a period of n years; and B is defined as the maximum streamflow in each year. Using measured annual stream flow maxima, we may estimate the log-normal distribution parameters, μ and σ of the annual maximum streamflow. A two-parameter log-normal distribution was used over the more conventional Log-Pearson Type III three parameter distribution based on research by Laio et al. (2009). They suggest that if the aim of flood frequency analysis is extrapolation to rare events with the smallest possible estimation error, then it could be convenient to select a two-parameter distribution even when the parent is a three-parameter distribution. We utilized an analytical

solution to the Bayesian estimation of the log-normal distribution parameters, μ and σ , to develop our Bayesian return period estimates. The data passed the Shapiro-Wilk W Goodness of Fit test for normality using JMP Pro Version 12.

For the purposes of this paper, an example dataset was tested using streamflow information from the USGS National Water Information System (NWIS). This data is openly available and often have instantaneous, daily statistics, monthly statistics, and annual statistics. The NWIS annual maximum streamflows were the primary data used for the Bayesian return period estimator. We used the maximum streamflow recorded in a given water year (October 1st to September 30th) for 100 years measured from the USGS Montpelier stream gauge on the Winooski River (USGS Site Number 04286000) and the Lamoille River (USGS Site Number 04292000).

The Bayesian estimator was then run for the length of the datasets (77 and 89 years for the Winooski and Lamoille Rivers, respectively). The estimated Bayesian outputs contained distributions of μ and σ for each year. Based on observed changes in the distributions with respect to time, we assumed the μ parameter was stationary with respect to time, and that σ could change. We then developed confidence intervals for the σ parameter, and used these as inputs into the lognormal distribution to estimate the potential return periods associated with each confidence interval. The associated flows for each confidence interval for both the Lamoille and Winooski Rivers are shown in Figure 6.2.

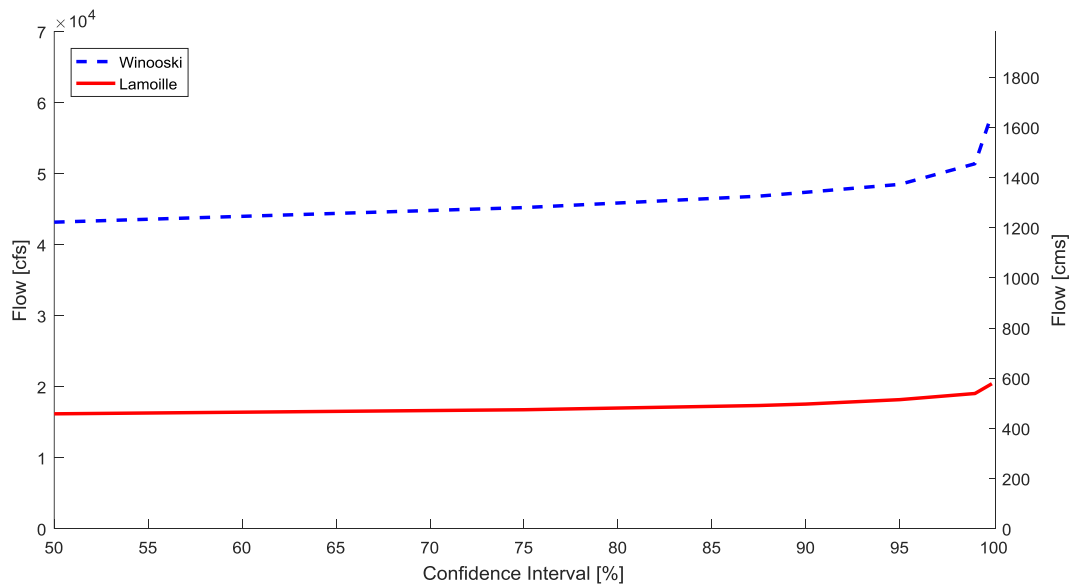


Figure 6.2: Confidence intervals vs corresponding flows for Winooski and Lamoille Rivers

6.2.3 Estimation of Scour Depths for Sacrificial and Non-Sacrificial Embankments

A review of inspection photographs of Vermont bridges damaged in Tropical Storm Irene revealed that 34 bridges experienced erosion of the soil behind the bridge abutments (flanking), and did not show

significant signs of scour (around and under pier and/or abutment foundation). Two photographs, highlighting the differences between scour damage and flanking damage, are provided in Figure 6.3. Flanking damage is very similar to the type of damage that a bridge with a sacrificial embankment might experience. The primary difference between flanking and scour damage is that flanking primarily occurs around a bridge abutment and tends to destroy the road and embankment, but does not threaten the structural integrity of the bridge. According to HEC-18, scour damage results from high velocity due to flow contraction, erosion along abutments, erosion along piers, or the long-term downcutting of the channel.



Figure 6.3: Example of flanking (a) and abutment scour (b) damage to bridge embankment and abutment due to Tropical Storm Irene (source: Vermont Agency of Transportation, 2014)

Scour depths at the studied bridges were calculated using the most current methods recommended in HEC-18 (Arneson et al. 2012). For the embankment without a fuse, we used both methods (NCHRP and Froehlich’s Abutment Scour Equation) without any modifications. The equations for the Froehlich method are shown in Equation 2.

$$\frac{y_s}{y_a} = 2.27K_1K_2 \left(\frac{L'}{y_a}\right)^{0.43} Fr^{0.61} + 1 \quad (2)$$

where y_s is the scour depth, y_a is the average depth of flow in the floodplain, K_1 is the coefficient for abutment shape, K_2 is the coefficient for angle of embankment to flow, L' is the length of active flow obstructed by the embankment, and Fr the Froude number of the approach flow upstream of the abutment (Arneson et al., 2012). Each parameter is an output from the HEC-RAS model, and used as input into a MATLAB (Version 2016b) script to calculate y_s .

For the sacrificial embankment, we used the National Cooperative Highway Research Program (NCHRP) method (Arneson et al. 2012) for the situation when a bridge embankment is flanked (“Scour Condition C”), which is analogous to a sacrificial embankment scenario. In addition, we assumed that when

the embankment is removed, the abutment could be treated as a pier and accordingly used the relevant pier scour equations (CSU equation) as a way of verifying the NCHRP method.

6.2.4 Scour Repair Cost Estimates

Anderson et al. (2017a) reported that 328 bridges were damaged in Tropical Storm Irene, which deposited between 127 mm and 254 mm of rain and had an estimated return period in excess of 100 years in most areas of Vermont and in excess of 500 years in some areas. Of these 328 bridges, 313 bridges had span lengths longer than 6 m. Anderson et al. (2017a) had access to repair/replacement cost estimates for a total of 103 bridges, and clustered the observed damage into four categories – slight, moderate, extensive, and complete (Figure 6.4). Descriptions of these damage categories are summarized in Table 6.2. The horizontal line and asterisk in each box plot represent the median and mean, respectively; the edges of the box are the 25th and 75th percentiles, and the whiskers extend to the most extreme data points not considered outliers. Outliers are plotted individually. We fit curves through the means and upper and lower quartiles of each damage category. These curves, presented in Figure 6.5, provide reasonable estimates of the mean, upper and lower bound of repair costs per deck area for typical Vermont bridges for each of the four damage categories. For the purpose of this study, we redefined the level of damage in terms of the estimated scour depth compared to the depth of foundation, as reflected in the horizontal axis of Figure 6.5 so we could relate calculated scour depth to remediation cost estimates. The mean repair costs along with the upper and lower quartile costs for each category are best fit using curves (Figure 6.5) to estimate corresponding scour damage repair costs for the example bridges considered in this work.

Damage due to flanking had an estimated average repair cost of \$108,000, and that the average cost of flanking-induced repair per square meter of the deck area of \$120 per square meter. In comparison, scour damage was estimated to cost \$260,000 on average to repair with an average repair cost of \$318 per square meter of deck area.

Complete bridge replacement can cost hundreds of thousands of dollars or even millions, and take months to years to complete; whereas washed-out approaches require a simple backfill and leveling, and can be reopened temporarily for emergency service hours or days after the flood subsides. This research treats flanking damage as an analogous substitute of a sacrificial embankment for the purposes of cost estimates. In this work, we assume the cost of constructing a sacrificial embankment to be similar to the estimated repair costs of flanking damage for bridges damaged in Tropical Storm Irene. We estimate cost using the methods described previously in this section and then add a cost for installation and replacement of the sacrificial embankment to the estimated scour costs. These additional installation and repair costs are estimated using the repair costs associated with bridges that experienced flanking damage during Tropical Storm Irene.

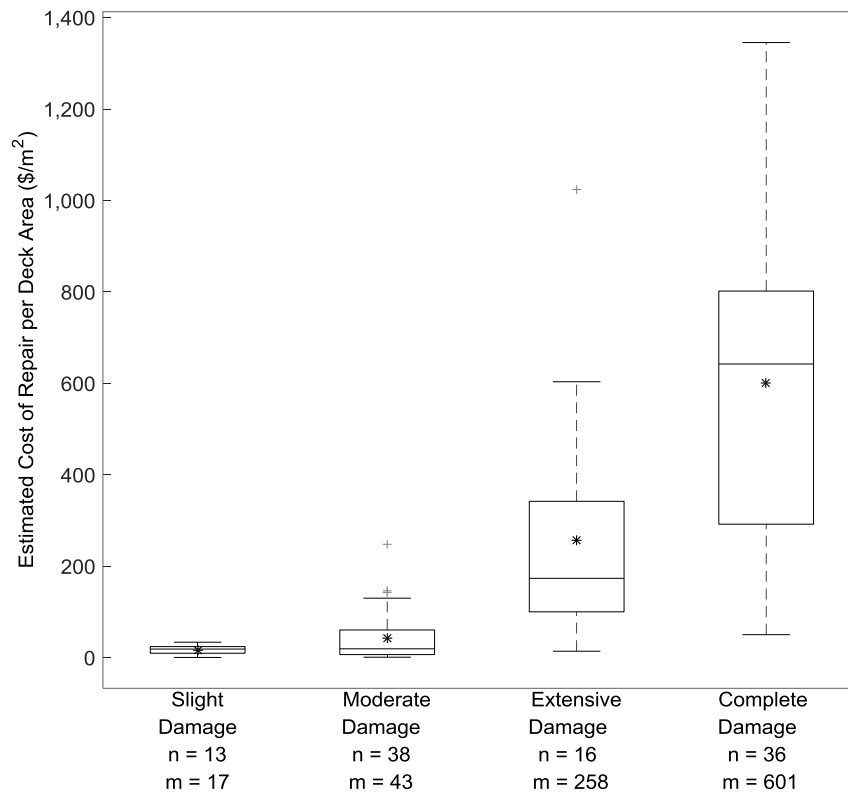


Figure 6.4: Estimated cost of repair for bridges damaged in Vermont during Tropical Storm Irene. The star represents the mean, bar the median, the box the 25th and 75th quantile, the whiskers the 95% confidence interval, and +’s are outliers (data source: Anderson et al., 2017a).

Table 6.2 - Description of damage categories used in analysis (Anderson et al., 2017a).

Damage Category	Depth of Calculated Scour (%)	Description
Slight	0-10	Channel erosion that does not affect the bridge foundation, superstructure and guardrail damage and debris accumulation without scour present.
Moderate	10-75	Scour that affects the foundation, but not to a crucial state, bank and approach erosion, heavy aggradation and damage to the superstructure, but not to a crucial state.
Extensive	75-100	Crucial scour, with some settlement to a single foundation, but not to the point of collapse, full flanking of both approaches, and superstructure damage that makes it structurally unsafe.
Complete	100-105	Bridge washed away, collapsed, or has significant foundation damage that requires replacement.

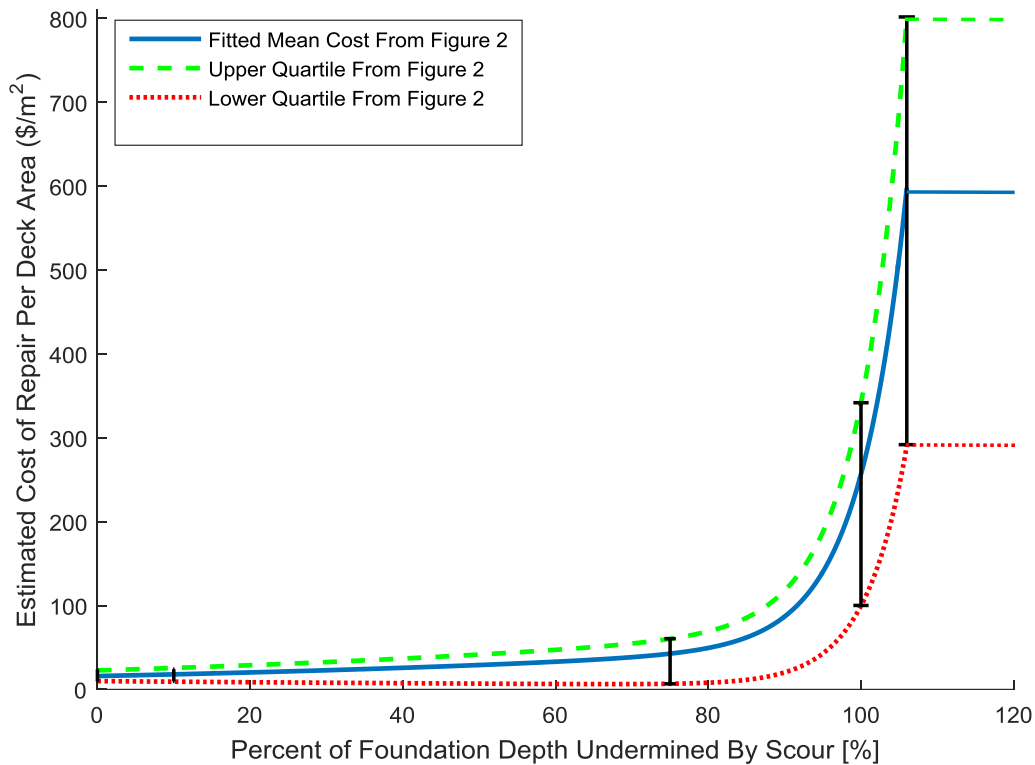


Figure 6.5: Smoothed curve estimate for cost of repair using data from Figure 4

6.2.5 Hydraulic Modeling Techniques

Hydraulic modeling for the selected bridges was performed using the Hydrologic Engineering Centers River Analysis System Version 4.1.0 (HEC-RAS). HEC-RAS is a one-dimensional river modeling software package that uses streamflow, channel geometry, and estimates of Manning’s n values to solve the one-dimensional St. Venant’s equations to develop stage, discharge, and water velocity estimates. The original models were developed and calibrated by the USGS; and we modified them to incorporate nonstationary flows and sacrificial embankments. Storm modeling was performed in a steady state HEC-RAS model using the 100-year streamflow return period confidence intervals. The confidence intervals corresponding to the streamflow inputs for the Winooski and Lamoille Rivers are shown in Figure 6.2. The HEC-RAS streamflow simulation was performed for each bridge scenario with and without a fuse; and the appropriate model outputs (i.e., stage height, velocity, and bridge geometry) were extracted and subsequently used to estimate scour using the methods described earlier; the latter was performed using MATLAB (Version R2015b).

6.2.6 Interviews with Professional Engineers

To guide future work, we interviewed eleven practicing professional engineers from Vermont and New Hampshire including some with experience in post-disaster recovery and interactions with the United States Federal Emergency Management Agency (FEMA). The engineers were interviewed both over the phone and through email to assess the feasibility of using sacrificial approach embankments in practice; their responses are summarized later.

6.3 Results and Discussion

6.3.1 Stream Flows

Comparisons between the USGS and the Bayesian streamflow estimates for the 10, 25, 50 and 100-year return periods for the Winooski and Lamoille Rivers are presented in Figures 6a and 6b, respectively. For both rivers, the Bayesian estimates of the “most likely return period” are similar to USGS estimates, and therefore, help validate the modeled results. It is important to note that these are just point estimate predictions used to verify the relative accuracy of the Bayesian estimator. The Bayesian estimator also provides a range of possible streamflows for both rivers based on the confidence intervals, which are reported in Figure 6.6.

6.3.2 Hydraulic Model Results and Scour Predictions

Figure 6.7 shows a flood stage profile of the Winooski River under a 100-year design with and without a sacrificial embankment. The x-axis represents the distance along the modeled section of the main channel (in meters); and the y-axis is the modeled elevation of the stage (in meters). There is a significant scale distortion of 500-unit horizontal to one-unit vertical. The streambed and location of Bridge 1 are labeled for clarity. The solid line represents the sacrificial embankment scenario water elevation for the USGS 100-year flow; and the non-erodible embankment scenario is represented with a solid line and triangles. Replacing the south embankment with a sacrificial embankment resulted in a stage reduction of 0.66 m just upstream of the bridge and significant reduction for another 3.2 km upstream of the bridge. Bridges 2 and 3 showed similar results when installing a sacrificial embankment, with 0.87 m and 0.091 m reduction in stage at Bridges 2 and 3, respectively.

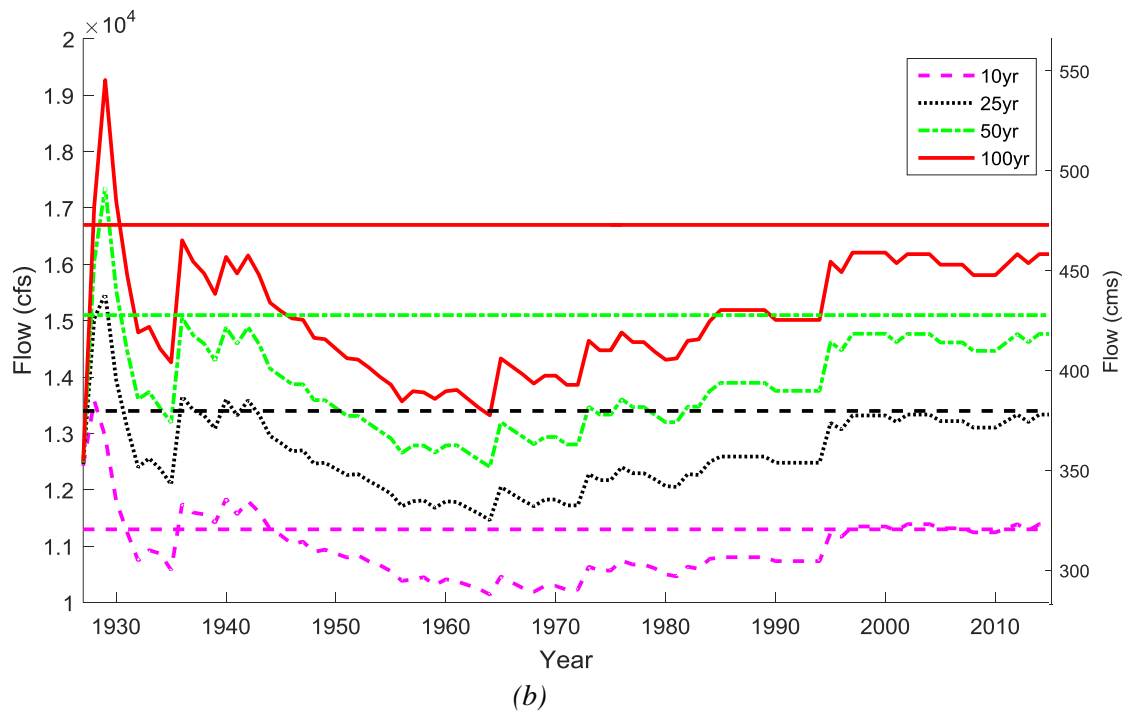
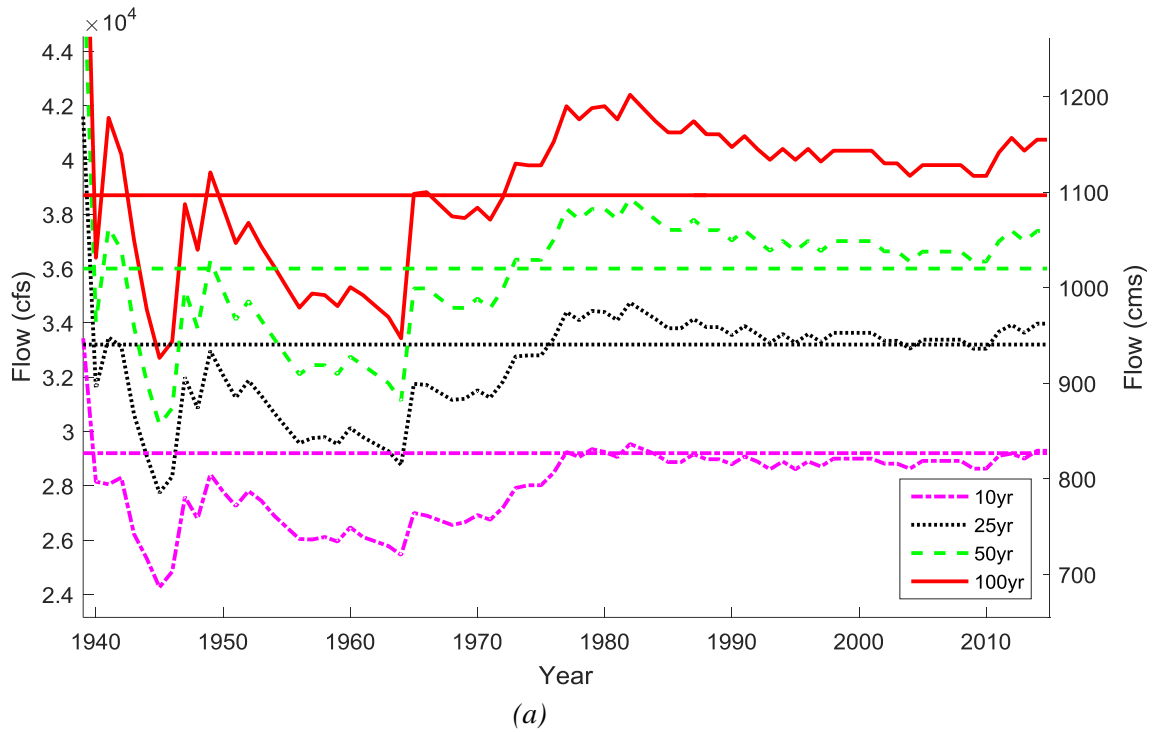


Figure 6.6: Streamflow return period estimates using a Bayesian Estimator (jagged line) vs. USGS estimates (straight line) for stream gauge on (a) the Winooski River, and (b) the Lamoille River.

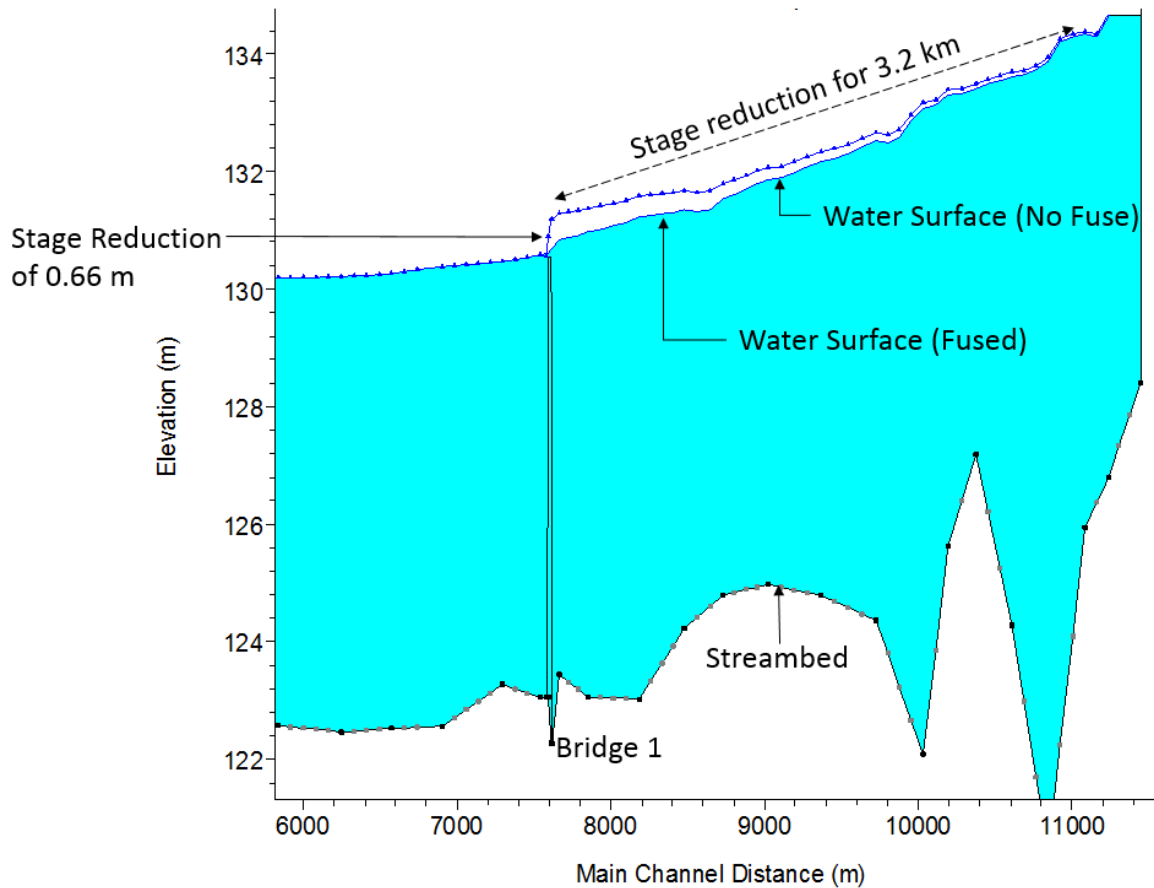


Figure 6.7: Profile view of river comparing fused vs non-fused embankment for “Bridge 1”

In addition to reducing the stage at a given bridge location, a sacrificial embankment can significantly reduce channel velocities by allowing floodplain access during an extreme streamflow event. For Bridge 1 and the 100-year storm design, the main channel velocity reduced significantly, from 3.3 m/s to 2.2 m/s, a 33% reduction in velocity. For Bridge 2, the main channel velocity was reduced from 3.6 m/s to 1.0 m/s (72% reduction); and Bridge 3 had the main channel velocity reduced from 3.3 m/s to 3.0 m/s (9.1% reduction).

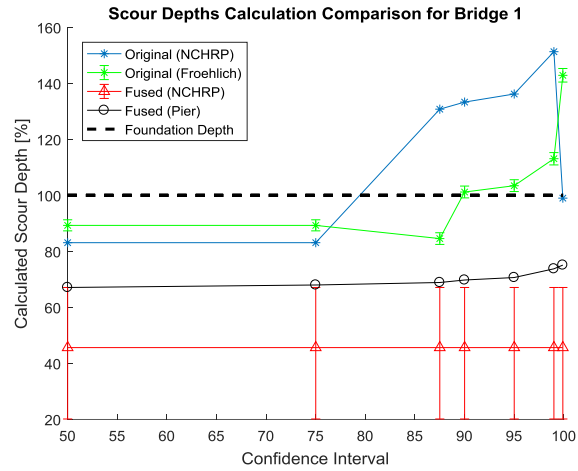
6.3.3 Cost Estimates and Scour Predictions

The scour depths calculated for a 100-year flow and the equivalent Bayesian estimated flow (Figure 6.8a) show that scour depth was significantly reduced when a fuse was installed at Bridge 1. However, under current flow conditions, it is not likely that the bridge would collapse due to scour from a 100-year flow. Figure 6.9a compares the costs of the bridge with and without a sacrificial embankment under changing flows, with 50% representing the maximum likelihood flow. The range of costs is due to the variability in estimated scour depths and damage cost categories calculations. Figure 6.9a shows that Bridge 1 is not an ideal location for sacrificial embankment under the current design flow. Therefore, installing a

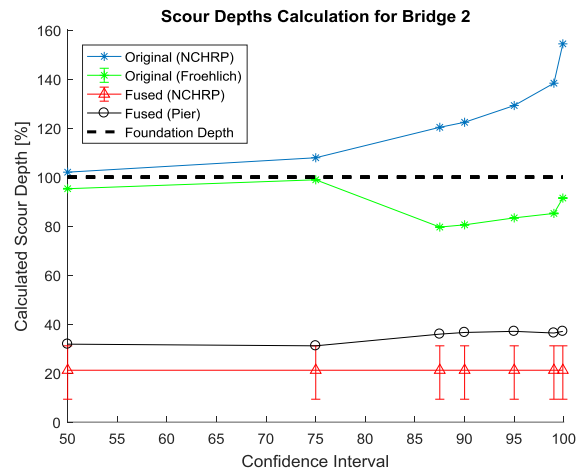
sacrificial embankment for Bridge 1 is not economically rational because the mean cost of repairing the damage after a 100-year storm is significantly lower than the cost of installing and repairing a fuse. However, the location provides insight into how sacrificial embankments may become cost effective over time as the magnitude and frequency of extreme storm events may increase. There is a “cross-over” point at a confidence of ~80% when the cost of the sacrificial embankment system becomes less expensive than the repair costs associated with doing nothing. Statistically this means that there is a 20% chance that installing a fuse is more economically rational than leaving the bridge as is. This result could be helpful to policy makers as it quantifies the risk and uncertainty involved when a fuse is not installed and helps determine the best course of action based on a range of possible scenarios. Based on these results, this site would require careful monitoring of streamflow over time to ensure that the statistical trends used to estimate the original 100-year return period are stationary. If the statistical trends drift over time to more extreme and/or frequent flow events, installing a sacrificial embankment at that location may become worthwhile.

The results of the cost analyses for Bridges 2 and 3 (Figures 6.9b and 6.9c) are presented in similar format to Bridge 1 (Figure 6.9a). Once again, the calculated scour depth for Bridge 2 was reduced when a sacrificial embankment was installed, and never exceeded the 50% threshold for any calculation method. Based on current streamflow estimates, the scour equations predict that Bridge 2 might suffer major damage or collapse during a 100-year flow event because the calculated scour depth meets or exceeds the foundation depth (Figure 6.8b). Figure 6.9b shows it is cost effective to install a sacrificial embankment under the current and future estimates of extreme streamflow; costs are approximately \$600,000 less per “100-year storm” than the cost of doing nothing after the 90% confidence interval. In addition, the removal of the bridge abutment reduces the stage at the bridge by about 0.87 m, which could noticeably reduce upstream flooding damages, cost savings from which are not included in this analysis.

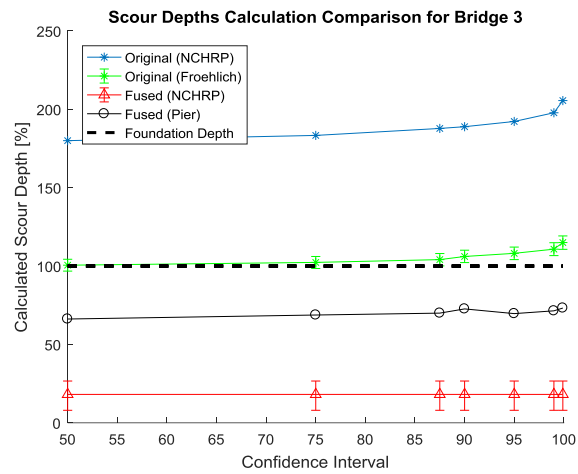
Figure 6.8c shows that Bridge 3 has the greatest risk of failure due to scour, and that at the 100-year stage, failure due to scour is almost certain. However, the estimated sacrificial embankment scour depth is significantly lower; and it is more likely that the bridge would survive the 100-year storm event. On average, it would cost about \$95,000 to leave the bridge “as is” compared to installing a sacrificial embankment (Figure 9c). A secondary benefit of sacrificial embankments is stage reduction; this was not incorporated in the cost analysis. Depending on the geography of the area, the stage reduction could significantly reduce the flooding potential on the town upstream of the bridge.



(a)

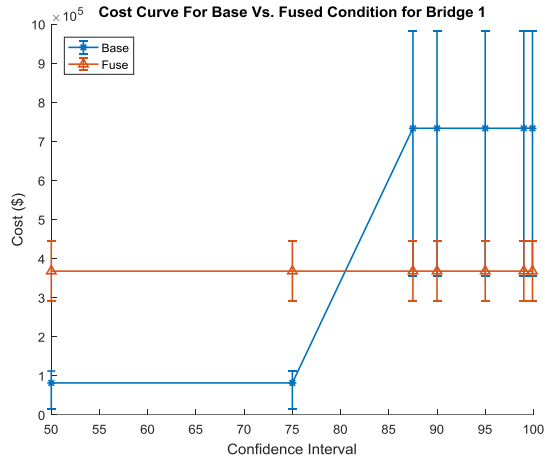


(b)

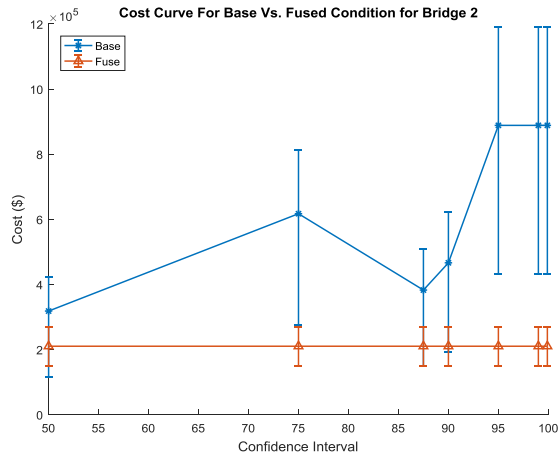


(c)

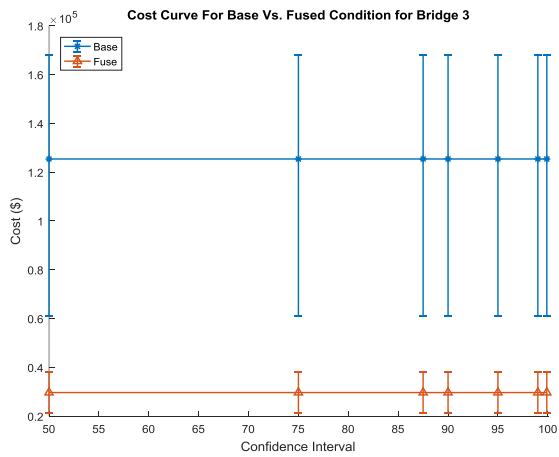
Figure 6.8: Calculated scour depth as a percentage of total foundation depth for various storm conditions (a) Bridge 1, (2) Bridge 2, and (3) Bridge 3



(a)



(b)



(c)

Figure 6.9: Cost curve estimate under different 100-year storm conditions for (a) Bridge 1, (2) Bridge 2, and (3) Bridge 3

The above results suggest that sacrificial embankments are an effective scour mitigation technique even if current climatic conditions are stationary under the general conditions presented in Bridges 2 and 3. Sacrificial embankments may be effective for the situation presented in Bridge 1, especially if precipitation and corresponding streamflows become more extreme. In addition, sacrificial embankments are effective in reducing stream stage and velocity during high flow events and may also help reduce flooding upstream of the bridge.

6.3.4 Practicing Professional Engineers' Opinion on the Feasibility

In general, all engineers we interviewed agreed that sacrificial embankments are an innovative idea; and to the best of their knowledge, they were not aware of any bridges where a sacrificial embankment was intentionally designed. Most engineers expressed a willingness to consider using a sacrificial embankment as a scour countermeasure in practice if trial test cases prove its safety and cost effectiveness. At the top of the list was the need for sufficient studies proving that the sacrificial embankment would only wash away during the design flow event, and not simply during a heavy rainstorm, traffic loadings, or normal high water event. The pavement over the sacrificial embankment would need to support traffic loads adequately, yet wash away with the embankment. All engineers interviewed suggested the need for pilot studies, and that the best place to start may be rural bridges spanning smaller streams with low average daily traffic and unpaved approaches. For widespread consideration, it would be helpful if design manuals incorporated this as a viable mitigation/countermeasure strategy. The engineers strongly suggested that further work assuring the cost effectiveness of installing a fuse, particularly the life-cycle costs, is critical.

The following potential issues were identified: (1) a washed away embankment would contribute a large volume of sediment to the stream negatively affecting water quality; (2) right-of-way and archeological aspects may prevent this solution at some sites; (3) public perception of an engineered fuse that is intentionally designed to fail may be negative; and (4) ability to ensure public safety. Each interviewed engineer emphasized the importance of Item 4 – ensuring public safety. In this regard, outreach and education of practicing engineers and the general public would be of paramount importance. In terms of safety, they suggested signage and warning systems that alert drivers and pedestrians to not use the bridge when near-critical flows are expected.

6.4 Conclusions

The following conclusions are drawn from the work presented in this chapter:

- 1) Bayesian estimation of confidence intervals on streamflow return periods can be useful in designing hydraulic infrastructure to account for non-stationarity.

- 2) Sacrificial embankments can significantly reduce bridge scour and provide a cost-effective scour countermeasure.
- 3) Sacrificial embankments provide the secondary benefits of reducing the flood velocities and stage upstream of the bridge site.
- 4) The approach adopted to compute costs based on available data from an earlier extreme event from the region is reasonable and prove to be an effective tool for policy makers and bridge designers in the decision-making process to account for streamflow return period uncertainty in designing mitigation strategies for bridges.
- 5) The interviewed practicing professional engineers suggested that the use of sacrificial embankment as a scour countermeasure is innovative. All engineers interviewed suggested the need for pilot studies, and that the best place to start may be rural bridges spanning smaller streams with low average daily traffic and unpaved approaches. Each interviewed engineer emphasized the importance of ensuring public safety through validated design of sacrificial embankments for their intended purpose, that they would only wash away during the design flow event and not prematurely under traffic loads and smaller storms. Additional research is needed before this solution could be implemented in practice.
- 6) Although the study used data from the Northeastern United States, specifically the state of Vermont and the 2011 extreme flooding event of Tropical Storm Irene, the methodology presented here is applicable to other settings.

CHAPTER 7

SCOUR MONITORING SYSTEMS

(A number of undergraduate students from Civil, Environmental, Mechanical and Electrical Engineering of the University of Vermont have participated in various aspects of the scour monitoring sensor development work and the literature review presented here. These students worked on the sensor development as their independent research or capstone design projects. The lead authors of this report thank and acknowledge the contributions of these students including Sebastian Downs, Caleb Fields, Joseph Hasselman, Heath Hescocock, Griffin Jones, Connor Lacasse, Albin Meli, Cameron Michaud, Trevon Noiva, Brendan Stringer, Adisun Wheelock and Roy Wu. Some of the excerpts included in this chapter are from these students' research/project reports).

Synopsis:

Due to potential severity of scour related damage to bridges, a monitoring system is desired to assess and record the progression of scour. Ideally, a scour sensor (or a collection of scour sensors) will measure the evolution (depth and extent as a function of time) of erosion and deposition, be robust enough to withstand the stream environment, be easy to install at a new or existing bridge, be inexpensive, require minimal energy, be activated as needed, and communicate the measurements to necessary personnel remotely, preferably with a built-in alert system. This chapter presents a review of available scour sensing/monitoring systems and summarizes their benefits and limitations. Proof-of-concept development and designs of two scour sensors developed as part of this project are also described.

7.1 Literature Review of Existing Technologies

FHWA guidelines suggest that bridges found to be vulnerable to scour could be monitored as an appropriate scour countermeasure (Lagasse et al., 2009). Scour countermeasures can be broadly divided into three categories: structural, hydraulic, and monitoring; and monitoring is usually the least expensive of the three options (Briaud et al., 2011). In a survey conducted of State Department of Transportations, 32 states use or have deployed scour monitoring on their highway bridges (Hunt, 2009). Available scour monitoring methods can be broadly categorized into three groups: visual monitoring, portable instrumentation, and fixed instrumentation (Briaud et al., 2011). Methods such as the scour rod, float out devices, sonar, time domain reflectometry (TDR), and optical sensors can be found in the literature. A number of relatively recent papers and reports include reviews of these scour monitoring methods; for example: Briaud et al. (2011), Cai et al. (2015), Hunt (2009), Khan and Atamturkur (2015), Prendergast and Gavin (2014), and Yu and Yu (2010). In the following sections, some of these technologies are briefly reviewed.

7.1.1 Visual Monitoring Methods

Visual inspection monitoring including underwater inspection can be performed at standard regular intervals. There are limitations on when inspectors can visit the bridges during storms. The scour hole that forms during a high-flow event is often filled in during the receding stage as the stream flow returns to normal (“scour-and-infill” or “scour-and-deposition”), is commonly not detected by visual inspection.

7.1.2 Portable Instrumentation

Portable instrumentation monitoring devices can be carried to and used at a bridge as needed, and transported from one bridge to another. Portable instruments are generally more cost-effective in monitoring an entire bridge or multiple bridges than fixed instruments; however, they are unable to offer continuous monitoring (Hunt, 2009).

An example of a portable instrumentation is a scour rod, which measures the depth of a scour hole at a given point. The scour rod can be considered a rigid tape measure. This measurement system is labor intensive, surveyors enter the stream, and manually measure the scour holes. The involvement of human travel and labor makes this process costly and inefficient. Another shortcoming of this scour measuring method is that it does not provide real-time monitoring of scour during high flow events. These instruments are not rugged enough to be used during high flow events and it is dangerous for an individual to go into the field during these events to make measurements (Yu and Yu, 2010). As a result, other methods of scour measurement are preferred.

7.1.3 Fixed Instrumentation

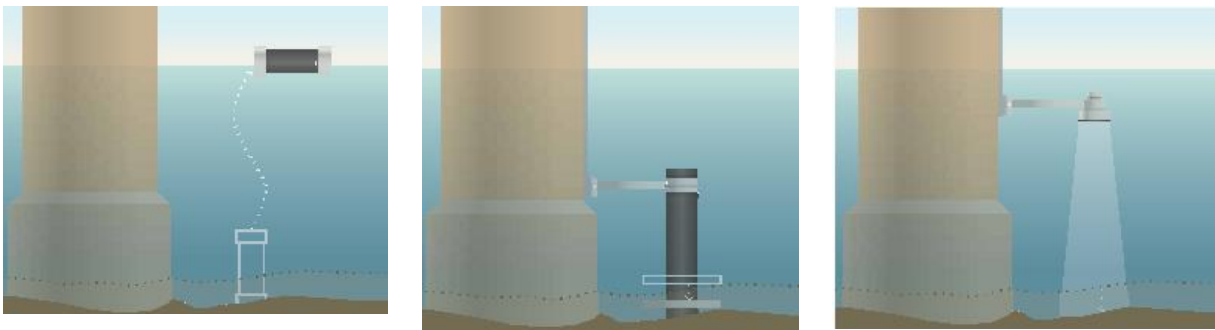
Fixed scour monitors can be placed on a bridge structure, or in the streambed or on the banks near the bridge. These often allow continuous measurement of scour and in some cases deposition. Below is a brief review of fixed scour sensors.

Float Out Devices

“Float out” means that when the embedded sensor is uncovered by removal of the overlying material, the device will rise to the water surface and act as an early warning system to indicate that scour has occurred on site. There are two types of these devices in use. One of them has the float out portion remaining attached to an object fixed into the riverbed (Figure 7.1a). These systems are reliable but they require a person to go out to the site and observe if the sensor has been deployed. Since an individual still needs to visually check these sensors, there is travel time involved, which often makes this method expensive and inefficient. The deployment of the sensor is also limited to single scour event.

Other float out devices travel down river with the current once exhumed from the sediment. This method is simple and removes the need to physically travel to the site. The data are recorded when the

device travels downstream. This is accomplished by a detector located at a specific location downstream. This makes the float out device a less feasible option. The early warning device could be lost during its journey downstream. Both variations require the device to be buried in the riverbed. This is an expensive and difficult process due to the amount of physical work and regulations for working in streambeds. Furthermore, excavating soil near a bridge pier may cause problems with the stability of the bridge foundation in the future, and has a one-time use limitation (Hunt et al., 2012).



(a) *Float-out device* (b) *Magnetic sliding collar* (c) *Sonar*
Figure 7.1: Examples of fixed scour instrumentation (Fondriest Environmental, Inc. fondriest.com)

Falling collar

Magnetic sliding collars are sensors which use a falling collar to measure the maximum scour depth (Figure 7.1b). As the flow creates a scour hole, the collar falls, registering its position on the rod, allowing for a measurement of the scour depth. Rods can be imbedded in the river bed, or attached to the bridge foundation. The sensor functions with a number of magnetic switches placed at various depths, which activate as the collar passes, are registered in a data logger, and determine the depth. A shortcoming of this technique is that while it will determine maximum scour depth, it will not accommodate the detection of redeposition.

Sonar Method

Alternatively, the ultrasonic method uses a Sonic Fathometer and can be described as a sonar method for monitoring scour (Yu and Yu 2010). These devices, much like sonar, send out an ultrasonic pulse to detect the riverbed (Figure 7.1c). These pulses hit a solid surface and reflect back to the recording device. The further away that object is, the longer the signal takes to get back to the recording device. This system has been used to successfully measure scour in the United States and is currently attached to an estimated 48 bridges (Fisher et al. 2013). This system has proven to be reliable and can measure the development of a scour hole from 0.28 to 1.2 meters in depth (Fisher et al. 2013). Sonar sensors can also be created to withstand hurricane force winds. One of the downfalls of this system is that it is not capable of accurately measuring scour during high turbulence events. This is a concern because turbulence is a characteristic feature of many of the high energy flows that lead to scour. Turbulent waters disturb the

ultrasonic pulse, and prevent reliable measures of the riverbed depth. Other problems can be caused when a large amount of air bubbles are present in the water. Figure 7.3 shows how the sensor can also miss the scour hole if the device is not deployed at the correct height. If the device is placed too low, then it will not be able to accurately measure the diameter or width of the scour hole. The presence of air bubbles has been known to cause up to 15 ft fluctuations in the data. Another problem with this system is that it cannot accurately take measurements when there is debris in the water. The sonar device will not be able to accurately measure the distance to the riverbed because the ultrasonic pulse will be reflected back to the system once it hits any debris. This causes the riverbed to appear to rise and lower suddenly over short periods of time (Fisher et al. 2013).

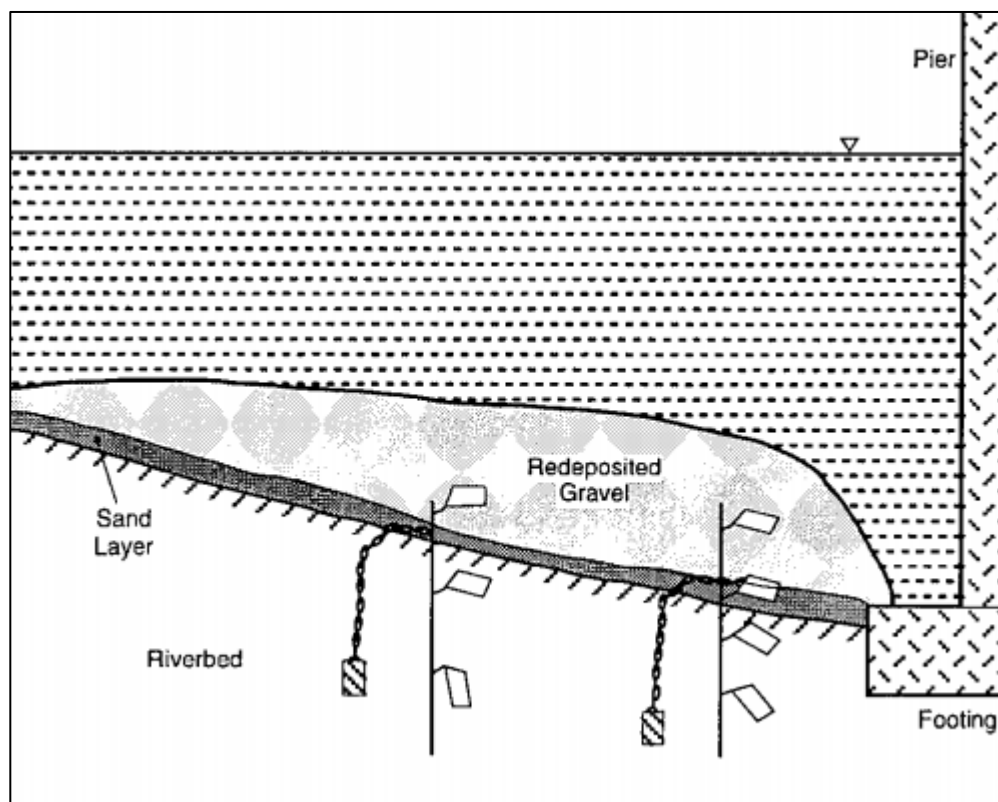


Figure 7.2: Examples of rod based float out transmitter (Zabilansky 1996)

Rod Based Float Out Device

A more advanced version of the float out sensor can use mechanical switches to make recordings of which floats were unburied, to notify practitioners of the corresponding depth of scour. Zabilansky (1996) in a study on ice and scour monitoring developed an array of float out devices, based upon wildlife movement tracking units (Figure 7.2). The units emit timing pulses that vary with motion. These transmitters are instrumented along a support rod that is then buried in the sediment. The transmitter based device has

the advantage of tracking refill events, which traditional float out systems would miss. As with any sensor placed in the flow field, float out devices are prone to damage by debris.

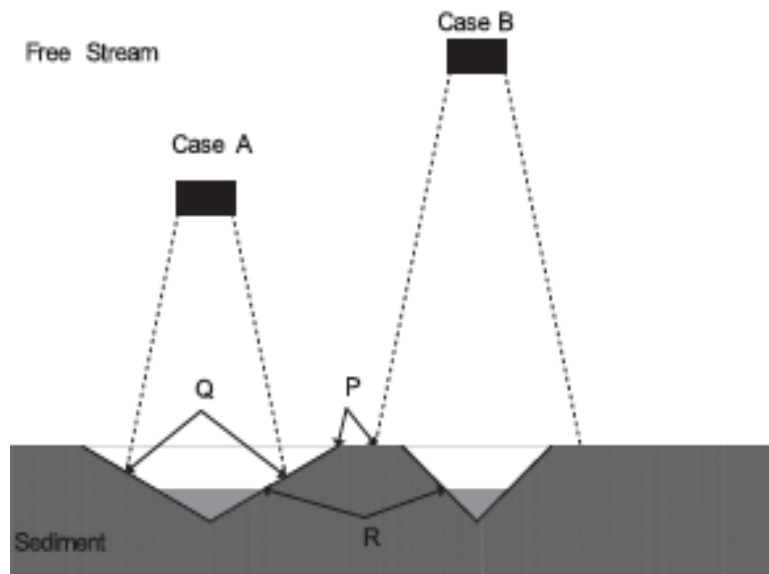


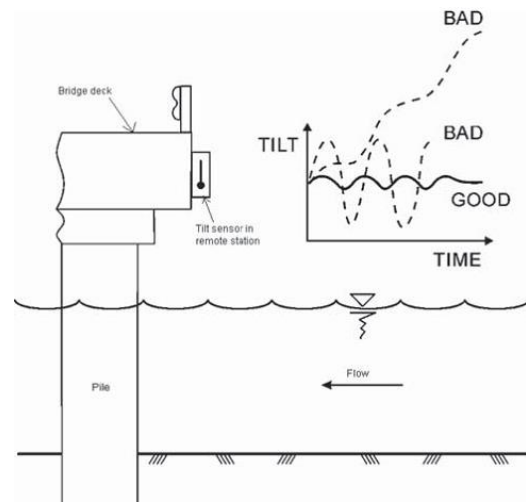
Figure 7.3 - Example of one of the limitations of the ultrasonic sensing methods (Fisher et al, 2013)

Tiltmeter

Tiltmeter, also known as inclinometer or tilt sensor, is used to measure the change in angle of the member it is attached to with respect to an axis or a level (Briaud et al., 2011). It can be single-axis or dual-axis tiltmeter (Figure 7.4) hardwired to a data acquisition system and the output is positive if the tiltmeter rotates clockwise (facing the tiltmeter). Briaud, et al. (2011) note that tiltmeters are compact, rugged and lightweight; measurement is a direct tilt angle, which is simple and easy to interpret; the operation is reliable; and power consumption is low. They also note that the key issue during installation is to make sure that the tiltmeter is set to a level reading with respect to which the change in angle is measured. The main disadvantage of the tiltmeter is that it does not provide a direct measurement of scour depth and deposition.



(a) An installed tiltmeter

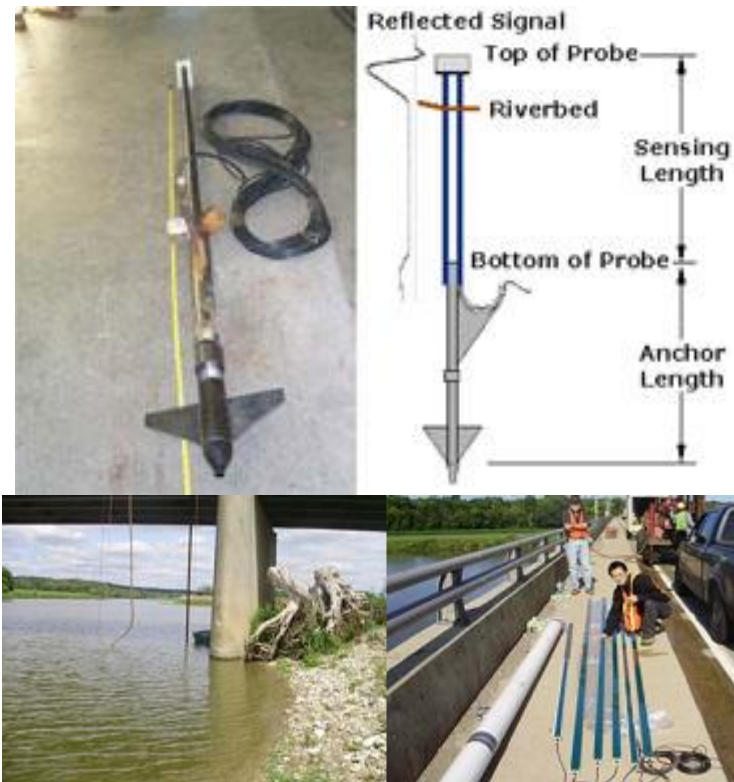


(b) Schematic of tiltmeter concept

Figure 7.4 – Tiltmeter (source: Hunt, 2009)

Time Domain Reflectometry

Scour can also be monitored using a technique called time domain reflectometry (TDR) (e.g. Yankielun and Zabilansky, 1999, Yu et al. 2013). TDR uses electromagnetic waves to determine the location of the sediment layer (Figure 7.5). TDR is a common measurement technique for locating damage to power and telecommunications cables, and has appeared in some geotechnical applications, but remains relatively unproven as a scour monitoring technique in the field. The technique uses metal rods to act as waveguides for electromagnetic pulses. The wave speed depends on the dielectric properties of the surrounding medium. This allows the device to measure the interaction between the water and soil. Laboratory testing has been done correlating TDR signal with scour depth to within 5% (Yu and Yu 2011). Testing has been performed on the accuracy of the TDR under varying conditions, including the salinity of water. An increase in the salinity of the water created a decrease in measurement accuracy. The salt in the water will cause the electromagnetic waves to move more slowly. Slowing of the waves allows a greater chance for the wave to encounter interference, leading to an increased chance of error. Temperature has a similar effect on the electromagnetic wave of the TDR and can render the device inaccurate over varying temperatures (Fisher et al. 2013).



(a) A TDR scour sensing system developed by U. S. Army Corps of Engineers Cold Regions Research and Engineering (source: <http://techlinkcenter.org/summaries/dr-bridge-scour-monitoring-system>)

(b) A recent installation of a TDR probe at a bridge in Ohio (source: Yu and Yu, 2010)

Figure 7.5 – TDR scour monitoring

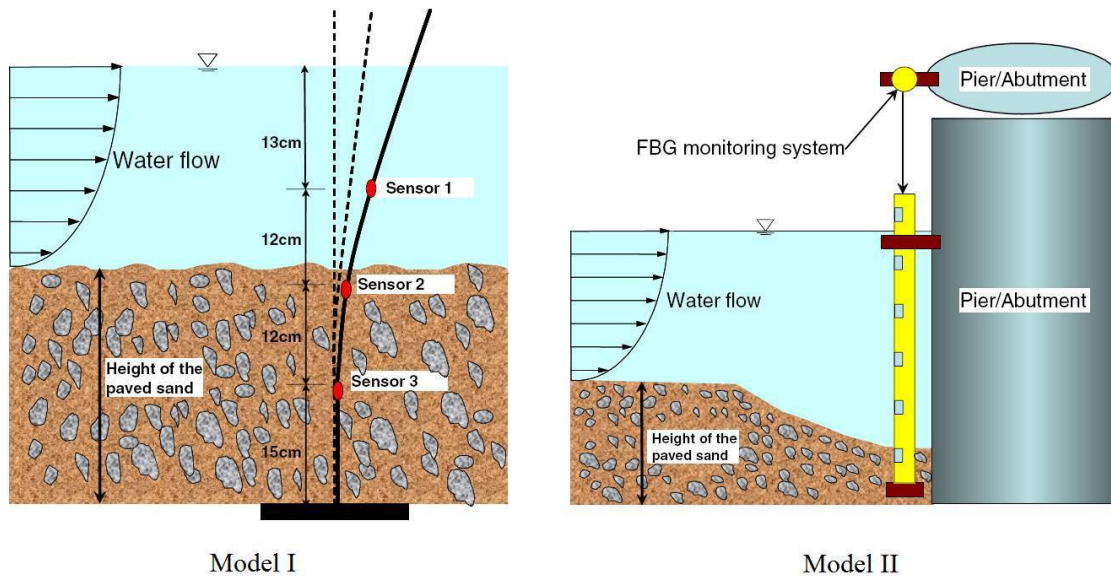
Thermometry

Thermometry sensors are another type of scour sensor that uses a rod as a measurement device. Thermometry devices are often placed in locations with little change in temperature and over long distances, such as the ocean floor along pipelines (Zhao et al. 2012). The thermometry measurement device can be placed into the riverbed or ocean bed horizontally or vertically. The device is designed to measure temperature at different segments of the rod. The sensor can be used to infer scour as follows. There is a difference in temperature or conduction properties between soil and water. When the recorded temperature differs from the norm, assuming the sensor device was initially in soil, it would mean that scour has occurred at that location. Some benefits of the thermometry device are that it is a simple concept to understand and the device has no moving parts that may be lost during high flows. The shortcoming of this type of device is that temperature-reading devices may not be accurate enough to read temperature changes over small intervals. Another problem with the device is that it takes time to set up base data before it can sense a difference between water and soil temperatures. Measuring scour in real time can also be difficult.

Fiber Optic Sensors

Optical scour depth measurement has been conducted with fiber optic wavelength and intensity sensors. Fiber Bragg Grating (FBG) sensors measure strain in the fiber optic cable through wave length shifts of the light signal passes through it (Guemes and Menendez, 2006). Intensity based measurements

compare the amount of light emitted and reflected back. The refractive index of the core and surrounding environment are used to predict the soil/water interface. Based on these principles, several sensor configurations have been developed. An example of the fiber optic sensor can be seen in Figure 7.6 below. Ansari (2010) used FBG sensors as strain gauges to measure the vibration frequency of the buried and unburied rod. Lin et al, (2004; 2006) used the deflection of the FBG sensors to determine the depth of scour by measuring the strain of an array of cantilever plates along a rod. Isley et al (2006) used intensity based sensors that arrayed the terminated ends of the fiber optics against the surrounding material, and measured the refraction, to judge the material present at varying depths. Early results from the wavelength applications show that though the depth of scour was detectable in laboratory and field studies, the signal generated is often small compared to the apparent noise. Intensity based measurements appear to be able to determine the interface depth, but showed reduced performance in turbid conditions. Variations in temperature often interfere with fiber optic sensors, as the thermal strain will alter the signal.



Model I
Model II
Figure 7.6 - Fiber Optic Scour Sensor (Cai et al. 2014)

7.2 Development of a “Smart Rod” Scour Sensor

A robust, affordable, and low maintenance sensor to detect scour in fine bed streams and report back in real-time was pursued. The design and testing of such a sensor was conducted by a pair of groups of undergraduate engineering students as part of their capstone projects. The initial prototype was detailed in the UVM Transportation Research Center Report 15-002 (Anderson et al., 2015). The second round of work, is detailed in the following section. The system designed included a rod with embedded sensors to detect the progressing level of scour, and included real-time data transmission to offsite supervision.

Initial design objectives included the ability to remotely transmit signals from sensors placed in the bed of the stream that would be robust enough to survive extended deployment, and could be installed at

existing bridges. A rod based design was selected, in hopes that minimal excavation would allow for deployment in fine grain streambeds. The sensor would be buried below the current bed, with minimal disturbance to the existing conditions, and allow for several feet of scour monitoring. Two sensing technologies were selected and tested, an accelerometer-based motion detection and an optical sensor. The scour rod was connected to a communication hub placed onsite to receive, log, and transmit the data. The sensor's components are illustrated in Figure 7.8.

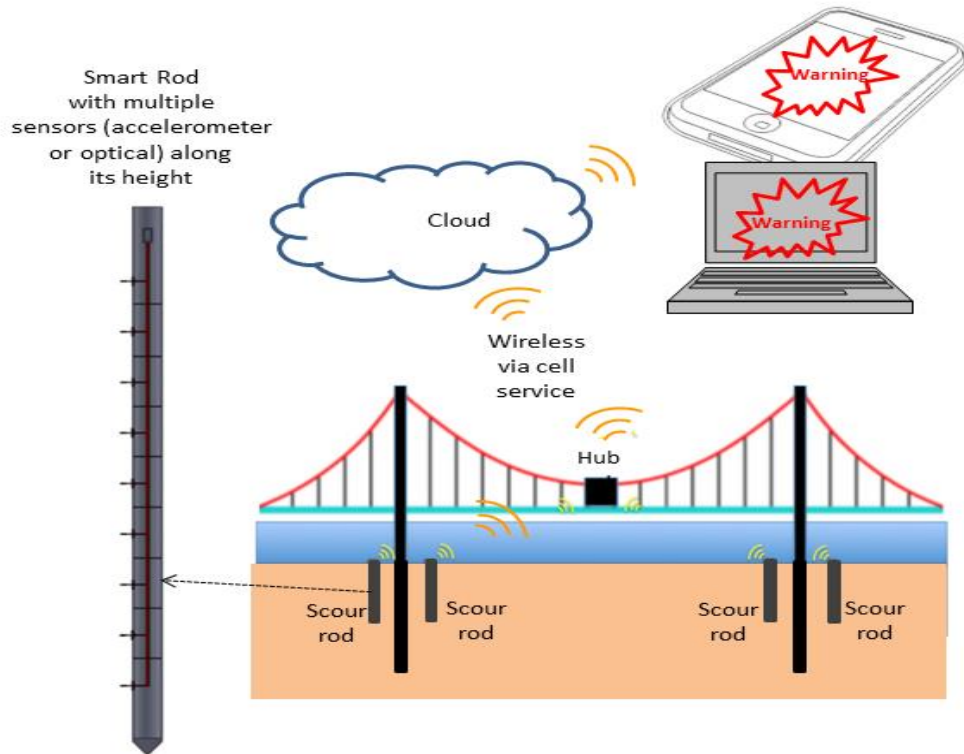


Figure 7.7 – Overall concept of the scour monitoring system

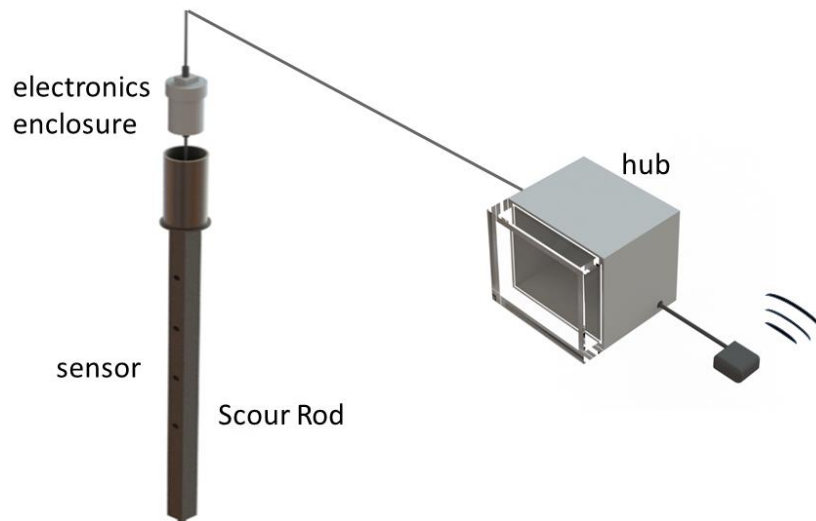


Figure 7.8 – Designed components

7.2.1 Data Acquisition and Communication

Data collection occurred in the onsite communications hub (Figure 7.8), which was wired to the onboard processing unit. The processor was programmable to sample periodically for changes to the scour state, allowing for reduced power demand, and increased lifespan. While in its low power state, multiple samples are collected and stored before being transmitted to the communication hub, further reducing power consumption. Upon sensing a change in the scour state, the unit would switch from its low power and interval sampling setting, to a higher frequency sampling and real-time data transmission.

Within the design process, low frequency underwater acoustic communication was attempted from the sensor to a communications hub located on site. The use of wireless communication would relieve a critical weakness of most in-bed sensors that is the cables required to relay the data transfer, which are prone to damage from debris. This idea was eventually abandoned, as the challenges outweighed the potential payoffs.

In addition to collecting and storing the data in the onsite communication hub, direct real-time communication was made possible through a satellite communication module, capable of connecting with the Iridium satellite network, facilitated by RockSeven Mobile Services. The satellite communication module allows the transition of short messages to and from the onsite hub. Data and alerts can be transmitted in real-time to an HTML endpoint or email address, and short commands can be related back. Commands were created that would allow a number of predetermined sampling regimes, triggered by short command messages sent from offsite users, related through the satellite communication module. Due to the often remote locations of bridges in the state, satellite communication was selected of mobile telephone based methods.

7.2.2 Accelerometer Sensors

Accelerometer based sensors were selected for their robust design, with few or no moving parts, and low power draw. Arms protruding from the rod would allow the accelerometer sensor to detect scour due to the turbulent motion of flowing water (Figure 7.9). Accelerometers are relatively inexpensive, capable of detecting fine deviations in position, and sensitive to small movements, making them a good candidate for application in sensing scour. As with any electronics deployed in a stream, waterproofing proved a key component of the design process.

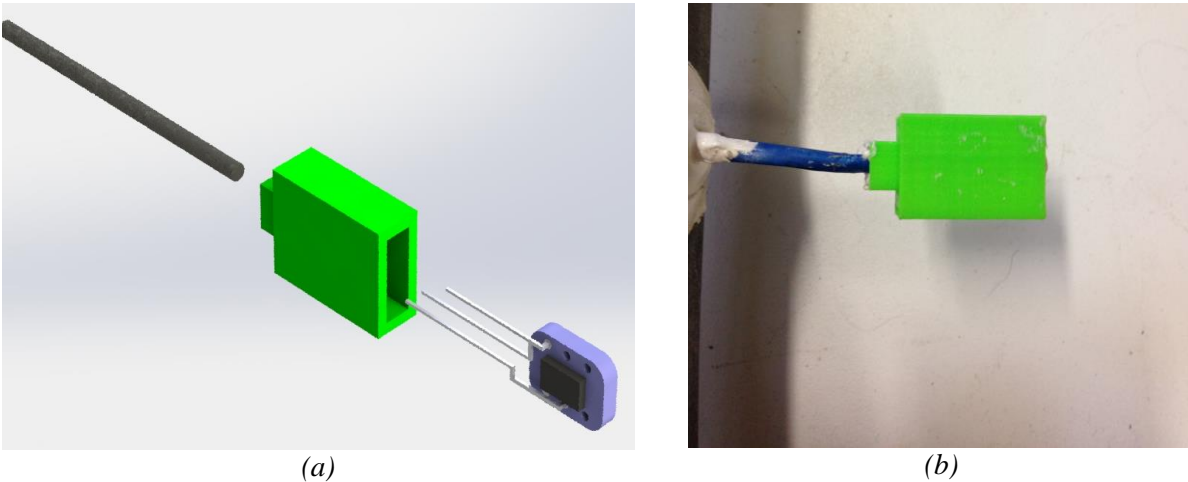


Figure 7.9: Design (a) and Prototype (b) of the accelerometer sensing arm

The bottom photographs in Figure 7.10 shows one of the latter versions of the accelerometer-based smart rod. An earlier version used a PVC pipe. Testing in the laboratory tank and flume showed the accelerometers were capable of detecting the difference between the buried and flowing state. Figure 7.11 shows the output of a test in the flume, in which the sensor is initially buried, and reporting zero output values. The large peak indicates the exposure of the sensor, followed by sustained non-zero output values indicating the continuous exposure to flow. A pair of accelerometers was tested in the field, and in a controlled weir with moderate flow. The sensors were outfitted on the scour rod, with the top sensor exposed to continuous flow, and the bottom sensor, buried beneath the bed. Over the course of the 80hr test window, scour was not observed in the lower sensor (Figure 7.12). The little disturbance experienced in the sampling of the bottom accelerometer is believed to be from movement and disturbance to the rod itself, not the sensing element. A deposition event was simulated (indicated with the arrow in Figure 7.12), which resulted in a significantly reduced signal from the top accelerometer.

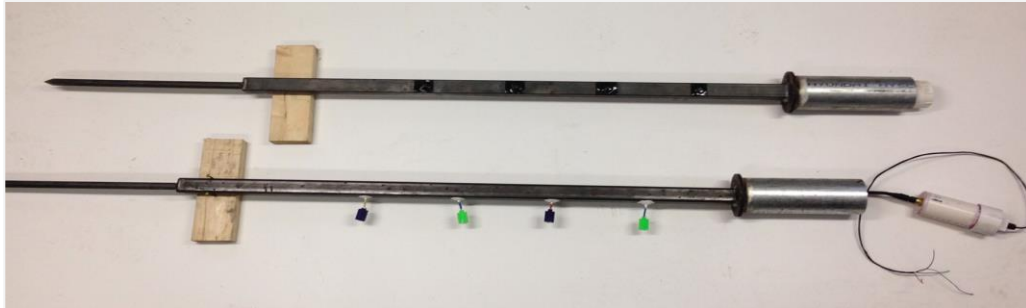


Figure 7.10: Two versions of smart rods – the photograph at the bottom is with accelerometers, and the photograph on top uses optical sensors

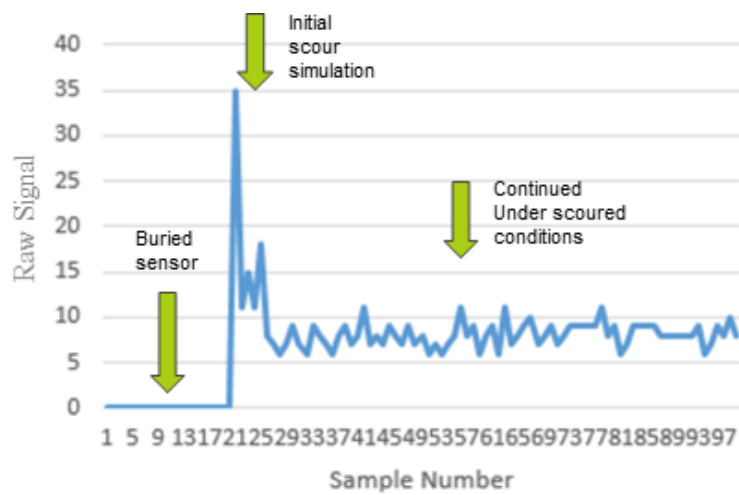


Figure 7.11: Laboratory flume testing results for the accelerometer sensor

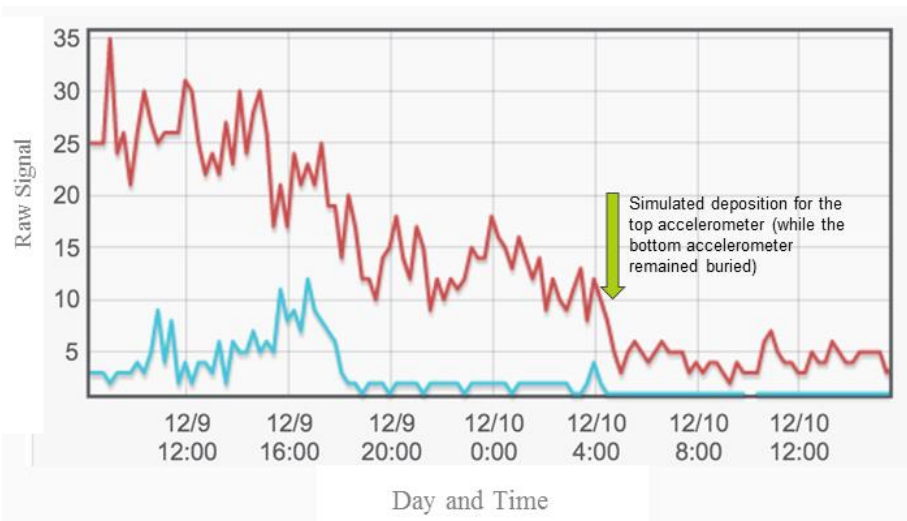


Figure 7.12: Field (in a stream) testing results for a pair of accelerometer sensors (red: top accelerometer, blue: bottom accelerometer)

7.2.3 Optical Sensors

An optical sensor was built in-house for the purposes of scour detection (top photograph of Figure 7.10). The conceptual idea behind an optical sensor relies on the differing refraction properties of soil and water. A sensor was constructed with a light source, a low power laser, that would project out a small window in the sensor housing. The light would pass through the transparent window and reflect off surrounding media. The reflected light is detected by the photoresistor. When the unit is buried in sediment, high reflection is detected, as most of the light is returns (Figure 7.13a). When exposed to water (by scour), the majority of the light leaves the photoresistor chamber, and is scattered with little reflection back to the photoresistor (Figure 7.13b). The sensors were imbedded in recesses within the rod, reducing the chance they may become obstructed or damaged by debris flow.

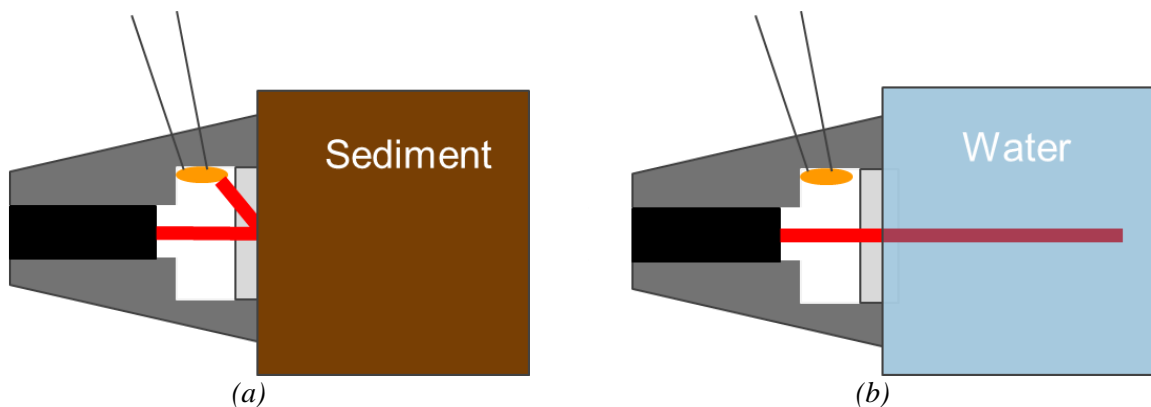


Figure 7.13: Optical sensor in sediment (a) and water (b)

Testing in the laboratory tank (Figure 7.14a), laboratory flume, and field (Figure 7.14b) showed the optical sensors work in both clean and turbid water, and are capable of determining when the surrounding sediment was removed. Figure 7.15 shows the results of laboratory testing, in which the top sensor was continuously exposed to water, while the bottom sensor was initially covered in sediment, and then uncovered. The resulting drop in refraction illustrates the successful observation of scour. Field deployment of the pair of optical sensors was also conducted, with observations during a total of 200 hr of use. Figure 7.16 shows a 48 hr window of the total test. With both sensors starting uncovered in water, daily sunlight exposure can be observed as an increase in measured resistance. Midway through the second daily cycle, the lower sensor was covered with sediment (simulated deposition), resulting in sustained high resistance.



(a)



(b)

Figure 7.14: An earlier version/prototype of optical scour rod made out of a PVC pipe being tested in very cloudy water and in relatively clean water at night in a stream.

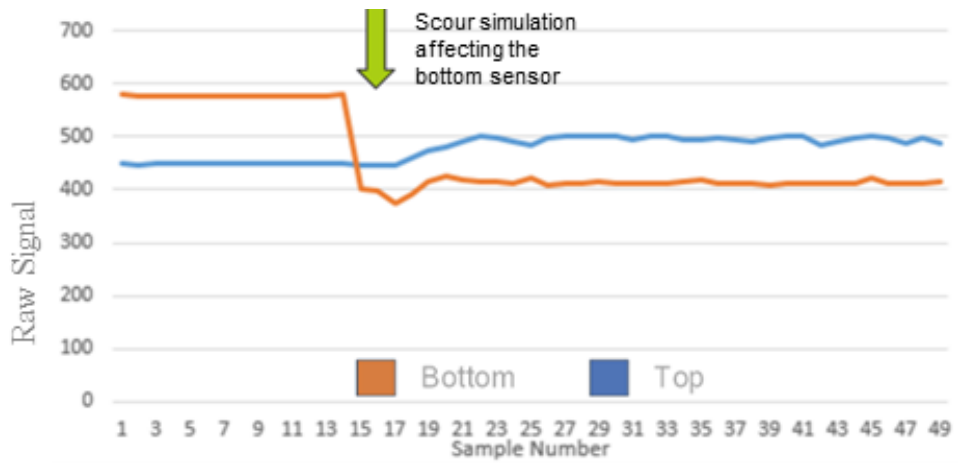


Figure 7.15: Laboratory testing results for two optical sensors on a scour rod

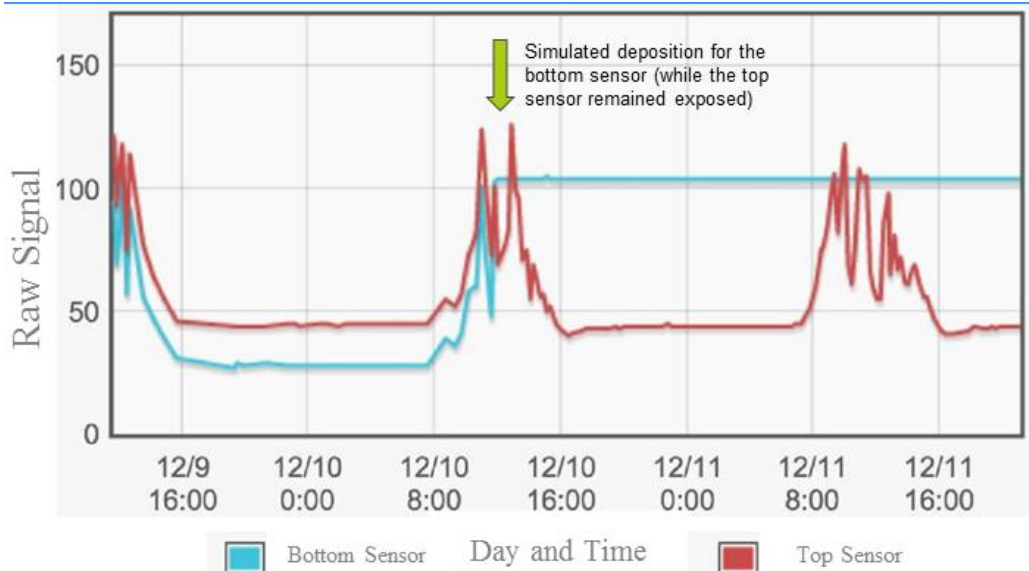


Figure 7.16: Field testing (in stream) results for two optical sensors on a prototype scour rod

7.3 Discussion and Conclusions

A device capable of remote monitoring and reporting of bridge scour was built and tested in both laboratory and field settings. Accelerometer and optical sensors were both successful in determining the change from sediment to water, and would allow for detection of both scour hole development, but also refilling. Though underwater communication was not successfully achieved, remote communication through satellite connection allowed for real-time monitoring and control of the sensing rods.

Accelerometer sensors are inexpensive, robust, and simple to program. Issues arise in their deployment in the field, as the current configuration could not be easily installed in an existing streambed, due to the vulnerability of the sensing arms. Disturbances to the scour rod are also registered by the attached sensor arms, potentially causing issues with false detection. An internal accelerometer should be used to help create a baseline observation of the excitation of the total system, so that the external measures can be corrected.

The optical sensor has the benefit of being installed flush with the rod, protecting them from debris, and allowing for simple installation. The optical sensors are relatively inexpensive, and with no moving parts, should increase the long life span of the sensor. One area of conflict is the interference of ambient daylight potentially interfering with the scour depth readings, as the refraction of sediments may be indistinguishable from full sun exposure. In addition to the lower power laser used, LED light sources should be tested, as they have the potential to further reduce the power demand of the unit.

This prototype study shows the feasibility of using both accelerometer and optical sensing for scour monitoring. Optical sensing using reflection of an emitted light registered with a photoresistor has great

potential for detecting the interface between the streamflow and sediment. Future work needed includes; additional testing under differing field conditions, testing in turbid water, and with differing sediment types. A new product recently discovered, the ‘Sedimeter’, which utilizes the same principles in detecting soil deposition, should be studied for adaptation to monitor erosion and scour. The ‘Sedimeter’ contains an array of LEDs and photoresistors to measure soil sedimentation, at very high resolutions. Though no testing has been done to show its ability to monitor scour and erosion, this type of sensor has a potential for adaptation, and deployment at bridge sites.

CHAPTER 8

CONCLUSIONS AND FUTURE RECOMMENDATIONS

A thorough review of bridge scour from Tropical Storm Irene, as well as an integration of available information from bridge and stream geomorphology datasets were conducted to identify features that relate to bridge scour. A comprehensive database of all bridges in Vermont including the damage records from Irene, FHWA bridge inspection records, stream geomorphic features, and watershed analysis of stream power was created to aid in the investigation. Additional efforts were made to test hydraulic models (HEC-RAS) with an optimization routine for floodplain encroachment, and a new countermeasure technique of a sacrificial embankment.

8.1 Conclusions from Tropical Storm Irene Case Study and Database Analysis Work

A total of 326 Vermont bridges were identified as damaged during Tropical Storm Irene, with damage ranging from minor streambank erosion to entire bridge collapse. Of these, 313 bridges with spans greater than 6 m had inspection records available and were considered further. The collection and georeferencing of hundreds of damaged and non-damaged bridges during a single extreme hurricane-related storm event, in combination with their inspection records and associated stream geomorphic assessments allowed assembly of a unique and significantly useful dataset. To the best of our knowledge such a database is not available elsewhere.

The damaged bridges included 55% steel beam, 34% concrete slab or beam, and the remaining 11% historical steel or wood truss superstructures. Single span bridges made up the vast majority, 82%, of bridges damaged, with 12% double span, and the few remaining including 3 and 4 span structures. About 55.6% of the damaged bridges had scour damage, 29.7% had channel flanking, 8.3% had debris damage, and the remaining 6.3% had superstructure damage. Scour damage resulted in the highest estimated cost to repair, followed by channel flanking, and then superstructure damage. When a bridge showed only flanking damage, the associated estimated costs of repair were substantially smaller than those associated with scour damage. The average estimated cost of repair for scour, flanking, and superstructure damage were about \$260,000, \$108,000, and \$18,000 per bridge, or \$318, \$120, and \$30 per square meter of deck area, respectively.

Characterization of the level and type of damage was also performed independent of any knowledge of the repair costs. Of the damaged bridges, 30% were categorized as having slight damage, 39% as moderate damage, 14.5% as extensive damage, and 16.5% as complete damage. Damage level correlated well with the estimated cost of repair and the cost of repair per deck area.

The bridge rating assessment characteristics were all strongly correlated to damage. Channel rating and waterway adequacy rating had strong discriminating power between bridge damage levels. The analysis

indicated that stream geomorphic data has the potential to be used to supplement and enhance the bridge rating systems, and may aid in identifying hydraulic vulnerability. Ratios such as entrenchment, incision, width to depth and straightening show significance at the watershed scale, and indicate that relative measures of a stream's geomorphic condition (disequilibrium) are more important than specific measurements. To the best of our knowledge, this is the first study that links hydrologic stream networks with performance of bridges. As geomorphic data become more widely available, the framework presented here could be applied elsewhere. The analysis identified individual features of the bridge and stream that correlate with underlying damage vulnerability, through comparisons at the stream reach and watershed scales, and outlines a framework to leverage these features to aid in the prediction of bridge vulnerability. Logistic regression identified correlations in the key features and levels of bridge damage, as classified through inspection reports and visual observation by the authors. Empirical fragility curves were created to depict the exceedance probability for a given damage level against the channel and waterway adequacy ratings, creating insights that can aid in evaluating bridges' vulnerability to extreme events.

Through the creation of a GIS script to generate stream power measures statewide, it was found that Specific Stream Power, and the event-based, Irene Specific Stream Power were both statistically significant at discriminating between damaged and non-damaged bridges, as well as between bridge damage levels from Tropical Storm Irene. The resulting spatial probability maps allowed for visual display of vulnerable reaches, for which bridge placement would be at increased hazard. Further application of event-based SSP probability maps could be generated using rainfall ARI in future climate simulations to produce the probability of bridge damage for a hypothetical climate scenario. The approach presented here could be implemented in other geographic regions. The method of estimating SSP and ISSP, and the calculation and expression of bridge hazard through fragility curves and probability maps could be useful in creating a screening tool for damage prediction. The methodology, and automated scripts used allow for rapid implementation in future applications, thus not limiting this work to Vermont. The Tropical Storm Irene database used here for the 313 damaged bridges experienced rainfall recurrence intervals ranging between 10 and 500 years, indicating that this methodology could be evaluated for a wide range of design flows for any watershed beyond the borders of Vermont. As far as we know, this is the first investigation comparing site-specific stream power to observed bridge damage at a network level, and represents a fundamental breakthrough in the prediction of flood related bridge damage.

Future studies expanding upon this work could apply the probability maps to create a risk-based inventory screening tool, to aid in decision making relating to transportation infrastructure planning. The complex interactions between the inherent bridge and site vulnerability cannot solely be explained through stream power, channel rating, or any single variable. The total cause of bridge damage also very likely includes a combined occurrence of high stresses, hydrogeologic instability, and vulnerable bridge

infrastructure. Future research seeks to leverage the full database of features to identify which underlying characteristics play the most significant role in bridge damage vulnerability. Identifying these features requires the development of new feature selection techniques (i.e., genetic algorithms, learning system classifiers), which until recently were not widely available.

8.2 Conclusions from Hydraulic Modeling Work

The first part of this work presents a new approach to applying differential evolution (DE) optimization to engineering challenges, and tests that approach on a real bridge with scour issues. A multi-objective solution was found in a constrained optimization problem, representing bridge scour with respect to floodplain access. The use of DE on constructed cost functions representing different weightings of the two objectives provided the same rank-order of reach locations with respect to their floodplain access impact on predicted bridge scour; ancillary testing using a finite difference scour gradient supported the proposed interpretation. Also of interest is that the sensitivity analysis is somewhat independent of objective weighting, which potentially reduces the stakeholder burden of deciding how to weight competing objectives. Instead, this approach focuses analysis on elements of the system's behavior that can be used to guide the design of floodplain infrastructure, remediation efforts, or the placement of new bridges. Applying this approach to other rivers would focus attention on locations where increased floodplain access would result in the most efficient use of resources and reduced scour at bridges, and applying it to other systems with spatially-variable components which have functional relationships with objectives of interest to stakeholders may provide similar decision support information.

The second component of the modeling investigation included the use of non-stationary streamflow predictions, and sacrificial embankments to reduce bridge scour. A Bayesian estimator was used to determine the confidence intervals for streamflow return periods, allowing hydraulic modeling to incorporate non-stationarity into the design flow estimates. A sacrificial embankment, similar to those used in dam spillways, is proposed for bridge scour failure prevention. Hydraulic modeling of the sacrificial embankment concept showed significant reductions in bridge scour, reducing the likelihood of complete failure. The sacrificial embankment model also lowered upstream stage and velocity, potentially reducing the hydraulic stress at additional sites with a single remediation site. A guideline for determining the cost-effective use of sacrificial embankments was proposed, to aid practitioners in determining if the likelihood of an extreme event warranted the use of a sacrificial embankment.

8.3 Conclusions from Scour Sensor Development Work

A “smart scour rod” device capable of remote monitoring and wirelessly reporting of bridge scour with an alert system was built and tested in both laboratory and field (in stream) settings. Accelerometer

and optical sensors were both successful in determining the change from sediment to water, and would allow for detection of both scour holes development, but also refilling. Though underwater communication was not successfully achieved during the project time, remote communication through satellite connection allowed for real-time monitoring and control of the sensing rods.

Accelerometer sensors are inexpensive, robust, and simple to program. Issues arise in their deployment in the field, as the current configuration could not be easily installed in an existing streambed, due to the vulnerability of the sensing arms. Disturbances to the scour rod are also registered by the attached sensor arms, potentially causing issues with false detection. An internal accelerometer should be used to help create a baseline observation of the excitation of the total system, so that the external measures can be corrected.

The optical sensor has the benefit of being installed flush with the rod, protecting them from debris, and allowing for simple installation. The optical sensors are relatively inexpensive, and with no moving parts, should increase the lifespan of the sensors. One area of concern is the interference of ambient daylight potentially interfering with the scour depth reading, as the refraction of sediments may be indistinguishable from full sun exposure. In addition to the laser used, LED light sources should be tested, they have the potential to further reduce the power demand of the unit.

Overall, this work showed the feasibility of using both accelerometer and optical sensing for scour monitoring. Optical sensing using refraction of an emitted light registered with a photoresistor has good potential for detecting the interface between the streamflow and sediment. Future work needed includes; additional testing under differing field conditions, testing in turbid water, and with differing sediment types.

8.4 Specific Conclusions and Recommendations to VTrans based on the Literature Review and Research

Following our literature review on the state of the practice in bridge scour design, the following recommendations are suggested:

- 1) A review of the application of the NCHRP 24-20 abutment and contraction scour calculation method is expected to be useful. The NCHRP 24-20 method has the benefit of incorporating both abutment and contraction scour and includes three scour conditions that closely resemble the apparent scour observed in Tropical Storm Irene.
- 2) A review of the application of the ABSCOUR program would be useful. ABSCOUR technique has the benefits of considering pressure scour, evaluates slope stability of the embankment, degradation and lateral channel movement. ABSCOUR has the benefit of offering a user-friendly computer application, which utilizes HEC-RAS outputs to compute scour for multiple methods, including NCHRP 24-20.

3) As recommended by both NCHRP 24-20 and ABSCOUR, treat contraction scour as a reference scour depth, and abutment scour as some multiple of contraction scour, rather than additive to it.

4) An update to the FDOT pier scour method, outlined in NCHRP 24-36, proposes the Sheppard/Melville method, which is recommended to be investigated for possible implementation.

5) It would be useful to add specific recommendations for armorings countermeasures for bridge scour in the Vermont Hydraulics Manual.

6) Partially grouted riprap has the potential to significantly improve the durability of scour countermeasures, while minimizing the need for intensive construction practices, as it can be applied in thinner layers, with smaller aggregate, and grouted in place with minimal effort. Partially grouted Type II riprap has the advantage of forming larger effective aggregates with greater stability, while remaining flexible.

7) Geotextile filter fabric should be incorporated in all countermeasure armorings applications, to reduce winnowing of the underlying material, and undermining of the armorings.

8) Applications which require underwater application of armorings should use geotextile laden with sand ballast, or sand filled geocontainers to ensure proper placement of filter layers.

9) This work showed the feasibility of using both accelerometer and optical sensing for scour and subsequent deposition monitoring. Optical sensing using refraction of an emitted light registered with a photoresistor has good potential for detecting the interface between the streamflow and sediment. Future work needed includes; additional testing under differing field conditions, testing in turbid water, and with differing sediment types. It is possible to develop scour rods with an array of optical sensors, which could be installed at existing or new bridges. A product containing an array of optical sensors developed for tracking sedimentation in streams is now available in market. It would be worthwhile to assess if this product could register soil removal and deposition reliably, and possibly adapt it as a scour sensor.

10) A link between stream power and channel geomorphic change in Vermont would greatly benefit the bridge design process. It is recommended that stream power calculations be conducted as part of the bridge design process, so future studies will have the information available. A greater emphasis on hydraulic design records would allow for a more thorough review of individual bridges.

11) It is recommended that bridge inspections in Vermont should adopt a system to monitor a number of geomorphic parameters, including the bankfull width and depth of the stream, a measure of the freeboard distance to the top of the bankfull width height.

12) The Channel Rating and Scour Rating are both overly complex and compound too much into a single parameter because they attempt to describe the entire bridge condition of scour and channel erosion, and lack the ability to clearly track changes. For channel rating, individual parameters should be used for the banks upstream/within/downstream, armorings, and debris accumulation. A new metric should be

implemented that rates the amount affected and its percent failure, rather than just qualitative conditional codes. New scour parameters should include depth to known foundation termination, depth of scour, the percent of foundation affected, and the location on the bridge foundation. Regular observations of these parameters will allow for a history of channel erosion and foundation scour to be studied.

REFERENCES

- Anderson, R. S. (1994). "Evolution of the Santa Cruz Mountains, California, through tectonic growth and geomorphic decay". *Journal of Geophysical Research: Solid Earth*, 99(B10), 20161-20179.
- Anderson, I.A., Dewoolkar, M.M., Rizzo, D.M., Huston, D.R. (2014). "Scour related Vermont bridge damage from tropical storm Irene," *Structures congress*, pp 505–515.
- Anderson, I., Rizzo, D. M., Huston, D. R., & Dewoolkar, M. M. (2017a). "Analysis of bridge and stream conditions of over 300 Vermont bridges damaged in Tropical Storm Irene" *Structure and Infrastructure Engineering*, <http://dx.doi.org/10.1080/15732479.2017.1285329>.
- Anderson, I., Rizzo, D. M., Huston, D. R., & Dewoolkar, M. M. (2017b). "Stream Power Application for Bridge-Damage Probability Mapping Based on Empirical Evidence from Tropical Storm Irene." *Journal of Bridge Engineering*, [http://dx.doi.org/10.1061/\(ASCE\)BE.1943-5592.0001022](http://dx.doi.org/10.1061/(ASCE)BE.1943-5592.0001022).
- Ansari, F. (2010). "Simple Cost-Effective Scour Sensor." Report No. FHWA-ICT-10-070, University of Illinois at Chicago.
- Arneson, L. A., Zevenbergen, L. W., Lagasse, P. F., & Clopper, P. E. (2012). "Evaluating scour at bridges." (No. FHWA-HIF-12-003).
- Bagnold, R. A. (1966). "An approach to the sediment transport problem from general physics." *U.S. Geol. Surv. Prof. Paper*, 422, 37.
- Barker, D. M., Lawler, D. M., Knight, D. W., Morris, D. G., Davies, H. N., and Stewart, E. J. (2009). "Longitudinal distributions of river flood power: the combined automated flood, elevation and stream power (CAFES) methodology." *Earth Surface Processes and Landforms*, 34(2), 280-290.
- Bartholomew-Biggs M, Parkhurst S, Wilson S (2002). "Using direct to solve an aircraft routing problem." *Comput Optim Appl* 21:311–323.
- Besaw, L. E., Rizzo, D. M., Kline, M., Underwood, K. L., Doris, J. J., Morrissey, L. A., and Pelletier, K. (2009). "Stream classification using hierarchical artificial neural networks: A fluvial hazard management tool." *J. of Hydrology*, 373(1), 34-43.
- Biron, P. M., Choné, G., Buffin-Bélanger, T., Demers, S., and Olsen, T. (2013). "Improvement of streams hydro-geomorphological assessment using LiDAR DEMs." *Earth Surface Processes and Landforms*, 38(15), 1808-1821.
- Botto, A., D. Ganora, F. Laio, and P. Claps. (2014). "Uncertainty compliant design flood estimation." *Water Resources Research*, 50(5), 4242-4253.
- Briaud JL, Gardoni P, Yao C (2014). "Statistical, risk, and reliability analysis of bridge scour." *J Geotech Geoenvironmental Eng* 140(2). doi:10.1061/ (ASCE)GT.1943-5606.0000989.
- Briaud, L., Ting, K., Chen, C., Gudavalli, R., Perugu, S., Wei, G. (1999). "SRICOS: prediction of scour rate in cohesive soils at bridge piers," *J. Geotech. Geoenviron. Eng.*, 125(4), 237246.
- Briaud, J.-L., Hurlbaeus, S., Chang, K.-A., Yao, C., Sharma, H., Yu, O.-Y., Darby, C., Hunt, B. E., and Price, G. R. (2011). "Realtime Monitoring of Bridge Scour Using Remote Monitoring Technology." FHWA/TX-11/0-6060-1, Texas Transportation Institute, the Texas A&M

University System.

- Brooks, G. R., & Lawrence, D. E. (1999). "The drainage of the Lake Ha! Ha! reservoir and downstream geomorphic impacts along Ha! Ha! River, Saguenay area, Quebec, Canada." *Geomorphology*, 28(1), 141-167.
- Brown, S. A., & Clyde, E. S. (1989). "Design of riprap revetment: Federal Highway Administration Hydraulic Engineering Circular No. 11." Publication FHWA-IP-89-016.
- Buraas, E. M., Renshaw, C. E., Magilligan, F. J., and Dade, W. B. (2014). "Impact of reach geometry on stream channel sensitivity to extreme floods." *Earth Surface Processes and Landforms*, 39(13), 1778-1789.
- Burrows, S., and Everett, M. (2015). "Bridges & Structures. Additional Guidance on 23 CFR 650 D." Federal Highway Administration, available at: <https://www.fhwa.dot.gov/bridge/0650dsup.cfm> (accessed July 30, 2016).
- Cai C.S., Kong X., Xiong W., Hou S., (2014). "Monitoring Bridge Scour Using Fiber Optic Sensors." Louisiana Transportation Research Center. FHWA/LA.10/535.
- Chang, F., & Davis, S. (1998). "Maryland SHA Procedure for Estimating Scour at Bridge Abutments Part 2-Clear Water Scour. In Stream Stability and Scour at Highway Bridges: Compendium of Stream Stability and Scour Papers Presented at Conferences Sponsored by the Water Resources Engineering (Hydraulics) Division of the American Society of Civil Engineers" (pp. 398-398). ASCE.
- Chang, F. and Davis, S. (1999). "Maryland SHA procedure for estimating scour at bridge abutments, Part II - Clear Water Scour." ASCE Compendium, Stream Stability and Scour at Highway Bridges, Richardson and Lagasse (eds.), Reston, VA., 1999, pp. 412-416
- Costa JE, O'Connor JE. (1995). "Geomorphically effective floods." *Natural and Anthropogenic Influences in Fluvial Geomorphology, Geophysical Monograph* 89: 45-56. DOI: 10.1029/GM089p0045
- Centre for Civil Engineering Research and Codes (CUR) (1995). "Manual on the Use of Rock in Hydraulic Engineering." A.A. Balkema Publishers, Brookfield, VT.
- Daly, C., Doggett, M., Gibson, W., and Smith, J. (2012). PRISM Climate Group Oregon State University.
- Deschaine LM, Lillys TP, Pinter JD (2013). "Groundwater remediation design using physics-based flow, transport and optimization technologies." *Environ Syst Res* 2(1):1.
- Dougherty DE, Marryott RA (1991). "Optimal groundwater management: 1. simulated annealing." *Water Resour Res* 27(10):2493-2508.
- Douglass, S. L., Hughes, S., Rogers, S., & Chen, Q. (2004). "The impact of Hurricane Ivan on the coastal roads of Florida and Alabama: a preliminary report." Rep. to Coastal Transportation Engineering Research and Education Center, Univ. of South Alabama, Mobile, Ala.
- Escarameia, M. (1998). "River and Channel Revetments: A Design Manual." Thomas Telford Ltd., London, UK, 245 p.

- ESRI (2011). "ArcGIS Desktop: Release 10." Redlands, CA: Environmental Systems Research Institute.
- Ettema, R., Melville, B. W., & Constantinescu, G. (2011). "Evaluation of bridge scour research: Pier scour processes and predictions." Washington, DC: Transportation Research Board of the National Academies.
- Ettema, R., Nakato, T., and Muste, M. (2010), "Estimation of Scour Depth at Bridge Abutments," NCHRP Project 24-20, Draft Final Report, Transportation Research Board, National Academy of Science, Washington, D.C. (Ettema, R., T. Nakato, and M. Muste).
- FHWA (1973). "A Statistical Summary of the Cause and Cost of Bridge Failures," Federal Highway Administration, U.S. Department of Transportation, Washington, D.C. (Chang, F.F.M.).
- FHWA (1978). "Countermeasures for Hydraulic Problems at Bridges," Vol. 1 and 2, FHWA/RD-78-162&163, Federal Highway Administration, U.S. Department of Transportation, Washington, D.C. (Brice, J.C. and J.C. Blodgett).
- FHWA, (1999). "Predicting Scour in Weak Rock of the Oregon Coast Range," Report No. FHWA-OR-RD-00-04, Washington, D.C., October (Dickenson, S.E. and M.W. Baillie).
- FHWA (2015). "Recording and coding guide for the structure inventory and appraisal of the nation's bridges." Federal Highway Administration Report No. FHWA-PD-96-01, U.S. Department of Transportation, Washington, D.C.
- Finlayson, D. P., and Montgomery, D. R. (2003). "Modeling large-scale fluvial erosion in geographic information systems." *Geomorphology*, 53(1), 147-164.
- Fisher, M., Chowdhury, N., Khan, A., Atamturktur, S., (2013). "An Evaluation of Scour Measurement Devices." *Flow Measurement and Instrumentation* 33, no. 0 (2013): 55 – 67.
<http://dx.doi.org/10.1016/j.flowmeasinst.2013.05.001>.
- Fondriest (2016). "Real Time Scour Monitoring." available at: <http://www.fondriest.com/environmental-measurements/environmental-monitoring-applications/monitoring-scour-bridges-offshore-structures/> (accessed November 30, 2016).
- Fonstad MA. (2003). "Spatial variation in the power of mountain streams in the Sangre de Cristo Mountains, New Mexico." *Geomorphology* 55: 75–96.
- Fowler, H.J., Ekstrom, M., Kilsby, C.G., and Jones, P.D. (2005), "New estimates of future changes in extreme rainfall across the UK using regional climate model integrations. 1. assessment of control climate." *Journal of Hydrology*, 300, 212-233.
- Fowler K, Jenkins E, Ostrove C, Chrispell J, Farthing M, Parno M (2015) "A decision making framework with mod ow-fmp2 via optimization: determining tradeoffs in crop selection." *Environ Model Softw* 69:280–291.
- Froehlich, D.C, 1989, "Abutment Scour Prediction," Presentation, Transportation Research Board, Washington, D.C. (Froehlich, D.C.).
- Frumhoff, P. C., McCarthy, J. J., Melillo, J. M., Moser, S. C., & Wuebbles, D. J. (2007). "Confronting climate change in the US Northeast. A report of the northeast climate impacts assessment." Union

of Concerned Scientists, Cambridge, Massachusetts.

- Fu, G., Yu, J., Yu, X., Ouyang, R., Zhang, Y., Wang, P., Liu, W., and Min, L. (2013). "Temporal Variation of Extreme Rainfall Events in China, 1961–2009." *Journal of Hydrology* 487, 48-59.
- Gartner, J. D., Dade, W. B., Renshaw, C. E., Magilligan, F. J., and Buraas, E. M. (2015). "Gradients in stream power influence lateral and downstream sediment flux in floods." *Geology*, 43(11), 983-986.
- Gee, K.W. (2008). "Action: Technical Guidance for Bridges over Waterways with Unknown Foundations." Federal Highway Administration, Washington, D.C., <http://www.fhwa.dot.gov/engineering/hydraulics/policymemo/20080109.cfm>. Accessed June 2014
- Goodell C (2014). "Breaking the HEC-RAS code: a user's guide to automating HEC-RAS." h2ls.
- Guerra-Gómez I, Tlelo-Cuautle E, de la Fraga LG (2013). "Richardson extrapolation-based sensitivity analysis in the multi-objective optimization of analog circuits." *Appl Math Comput* 222:167–176.
- Guilbert, J., Betts, A.K., Rizzo, D.M., Beckage, B., and Bomblies, A. (2015). "Characterization of increased persistence and intensity of precipitation in the northeastern United States." *Geophysical Research Letters* 42(6):1888-1893.
- Harsha Choday S, Roy K (2013). "Sensitivity analysis and optimization of thin-film thermoelectric coolers." *J Appl Phys* 113(21):214906.
- Heibaum, M.H. (2002). "Geotechnical Parameters of Scouring and Scour Countermeasures," *Mitteilungsblatt der Bundesanstalt für Wasserbau Nr. 85, Journal of Federal Waterways Engineering and Research Institute*, No. 85, Karlsruhe, Germany.
- Homer, C.G., Dewitz, J.A., Yang, L., Jin, S., Danielson, P., Xian, G., Coulston, J., Herold, N.D., Wickham, J.D., and Megown, K., (2015). "Completion of the 2011 National Land Cover Database for the conterminous United States-Representing a decade of land cover change information." *Photogrammetric Engineering and Remote Sensing*, v. 81, no. 5, p. 345-354
- Hornby GS, Lohn JD, Linden DS (2011). "Computer-automated evolution of an x-band antenna for Nasa's space technology 5 mission." *Evolut Comput* 19(1):1–23.
- Horton, R., Yohe, G., Easterling, W., Kates, R., Ruth, M., Sussman, E., Whelchel, A., Wolfe, D., and Lipschultz, F. (2014). "Ch. 16: Northeast, climate change impacts in the United States." *The Third National Climate Assessment*, edited by J. M. Melillo, T. C. Richmond, and G. W. Yohe, pp. 371–395, U.S. Global Change Research Program, Washington, D. C., doi:10.7930/J0SF2T3P.
- Hunt, B. E., Shields G. M., and Price, G. (2012). "New Directions in Scour Monitoring." AECOM, August 27, 2012. http://vzb.baw.de/publikationen.php?file=icse6/0/7_249_ICSE-6_Hunt_Scour_Monitoring_For_Posting-vreduite.pdf.
- Hunt, B. E. (2009). "Monitoring Scour Critical Bridges (Vol. 396)". Transportation Research Board.
- Isley II, J., Saafi, M., and Julius, J., (2006). "MEMS-based sensor networks for bridge stability safety monitoring during flood induced scour." *Bridge Maintenance, Safety, Management, Life-cycle*

Performance and Cost: Proceedings of the Third International Conference on Bridge Maintenance, Safety and Management, Ed: Cruz, P.J.S., Frangopol, D.M., Porto, Portugal, July 16-19, 2006.

- Jaffe DA, Sanders BF (2001). "Engineered levee breaches for flood mitigation." *J Hydraul Eng* 127(6):471–479. doi:10.1061/ (ASCE)0733-9429(2001)127:6(471).
- Jain, V., Preston, N., Fryirs, K., and Brierley, G. (2006). "Comparative assessment of three approaches for deriving stream power plots along long profiles in the upper Hunter River catchment, New South Wales, Australia." *Geomorphology*, 74(1), 297-317.
- Jaquith, S., and Kline, M., (2001). "Vermont regional hydraulic geometry Curves." River Management Program of the Vermont Department of Environmental Conservation, Waterbury, Vermont.
- Jeongwoo H, Papalambros PY (2010). "Optimal design of hybrid electric fuel cell vehicles under uncertainty and enterprise conditions." *J Fuel Cell Sci Technol* 7(2):021020.
- Karl, T. R., B. E. Gleason, M. J. Menne, J. R. McMahon, R. R. Heim, M. J. Brewer, K. E. Kunkel, D. S. Arndt, J. L. Privette, J. J. Bates, P. Y. Groisman, and D. R. Easterling. (2012). "U.S. temperature and drought: recent anomalies and trends." *Eos Trans. AGU Eos, Transactions American Geophysical Union* 93(47), 473.
- Kattell, J., & Eriksson, M. (1998). "Bridge scour evaluation: Screening, analysis, & countermeasures" (No. 9877 1207--SDTDC).
- Khan, A. A., and Atamturktur, H. S. (2015). "Real Time Measurement of Scour Depths Around Bridge Piers and Abutments." Report FHWA-SC-14-05, Clemson University.
- Kiah, R.G., Jarvis, J.D., Hegemann, R.F., Hilgendorf, G.S., and Ward, S.L. (2013). "Hydrologic conditions in New Hampshire and Vermont, water year 2011." U.S. Geological Survey Open-File Report, 2013–1135, 36 p., <<http://pubs.usgs.gov/of/2013/1135>> (Accessed June 2014)
- Kim, Y. J., Marshall, W., & Pal, I. (2014). "Assessment of infrastructure devastated by extreme floods: a case study from Colorado." USA. In *Proceedings of the ICE-Civil Engineering* (Vol. 167, No. 4, pp. 186-191). Thomas Telford.
- Kline M, Alexander C, and Pytlik S. (2007). "Vermont stream geomorphic assessment protocol handbooks." Resources VAoN (ed). Waterbury, Vermont.
- Kline, M., and Cahoon, B. (2010). "Protecting River Corridors in Vermont." *Journal of the American Water Resources Association*, 46(2), 227-236.
- Knighton, A.D. (1999). "Downstream variation in stream power." *Geomorphology* 29, 293 – 306.
- Koerner, R.M. (1998). "Designing with Geosynthetics." Fourth Edition, Prentice-Hall, Inc., Englewood Cliffs, NJ, 761 p.
- Kouchakzadeh S, Townsend R (1997). "Maximum scour depth at bridge abutments terminating in the floodplain zone." *Can J Civil Eng* 24(1):996–1006.
- Kruskal, W. H., & Wallis, W. A. (1952). "Use of ranks in one-criterion variance analysis." *Journal of the*

American Statistical Association, 47(260), 583-621

- Kurek W, Ostfeld A (2013). "Multi-objective optimization of water quality, pumps operation, and storage sizing of water distribution systems." *J Environ Manag* 115:189–197.
- Lagasse, P. F., Zevenbergen, L. W., Spitz, W. J., & Arneson, L. A. (2012). "Stream stability at highway structures." (No. FHWA-HIF-12-004).
- Lagasse, P.F., Clopper, P.E., Zevenbergen, L.W., Girard, L.W., (2007). "Countermeasures to protect bridge pier from scour". NCHRP Report-593. Transportation research board, Washington D.C., United States.
- Lagasse, P. F., Zevenbergen, L. W., Schall, J. D., & Clopper, P. E. (2009). "Bridge scour and Stream Stability Countermeasures: Experience, Selection, and Design Guidance-Third Edition. Hydraulic Engineering Circular 23 (HEC-23)." Report FHWA-NH1-01-003. Federal Highway Administration, Washington, DC.
- Laio,F., G. Di Baldassaree, and A. Montanari (2009). "Model selection techniques for the frequency analysis of hydrological extremes." *Water Resour. Res.*, 45, W07416, doi: 10.1029/2007WR006666
- Lane, E.W. (1955). "Design of stable channels," Transactions of the American Society of Civil Engineers, Vol. 120, p. 1-34.
- Laursen, E.M. (1960). "Scour at Bridge Crossings." Journal Hydraulic Division, American Society of Civil Engineers, Vol. 86, No. HY 2. 11.4
- Laursen, E.M. (1963). "An Analysis of Relief Bridge Scour." Journal Hydraulic Division, American Society of Civil Engineers, Vol. 89, No. HY3.
- Laursen, E.M. (1980). "Predicting Scour at Bridge Piers and Abutments." General Report No. 3, Arizona Department of Transportation, Phoenix, AZ.
- Lecce, S.A., (1997). "Nonlinear downstream changes in stream power on Wisconsin's Blue River." *Annals of the Association of American Geographers* 78 (3), 471 – 486.
- Li, FF, Schoemaker CA, Qiu J, Wei JH (2015). "Hierarchical multi-reservoir optimization modeling for real-world complexity with application to the three gorges system." *Environ Model Softw* 69:319–329.
- Lin, Y.B., Chang, K.C., Lai, J.S., and Wu, I.W., (2004). "Applications of optical fiber sensors on local scour monitoring." *Proceedings of the IEEE: Sensors*, Vol. 2, 832–835.
- Lin, Y.B., Lai, J.S., Chang, K.C., and Li, L.S., (2006). "Flood scour monitoring system using fiber bragg grating sensors." *Smart Materials and Structures*, Vol. 15, 1950–1959.
- Liou CD, Wang KH, Liou MW (2013). "Genetic algorithm to the machine repair problem with two removable servers operating under the triadic (0, q, n, m) policy." *Appl Math Model* 37(18–19):8419–8430.
- Liu, H.K., Chang, F.M., and M.M. Skinner, (1961). "Effect of Bridge Constriction on Scour and

- Backwater.” Department of Civil Engineering, Colorado State University, Fort Collins, CO.
- Luke A, Kaplan B, Neal J, Lant J, Sanders B, Bates P, Alsdorf D (2015) “Hydraulic modeling of the 2011 new Madrid floodway activation: a case study on floodway activation controls.” *Nat Hazards* 77(3):1863–1887.
- Magilligan, F.J. (1992). “Thresholds and the spatial variability of flood power during extreme floods.” *Geomorphology* 5, 373 – 390.
- Marsden AL, Wang M, Dnnis JE Jr, Moin P (2004). “Optimal aeroacoustic shape design using the surrogate management framework.” *Optim Eng* 5:235–262. 841 pp. Doi: 10.7930/J0Z31WJ2.
- Melillo, J. M., Richmond, T.C., and Yohe, G. W. (Eds.) (2014), “Climate Change Impacts in the United States: The Third National Climate Assessment”. U.S. Global Change Research Program, 841 pp. Doi: 10.7930/J0Z31WJ2.
- Melville, B.W., (1992). “Local Scour at Bridge Abutments.” *Journal of Hydraulic Engineering*, American Society of Civil Engineers, Hydraulic Division, Vol. 118, No. 4.
- Melville, B. W. (1997). “Pier and abutment scour: integrated approach.” *Journal of hydraulic Engineering*, 123(2), 125-136.
- Melville, B. W., and Coleman, S. E. (1973). “Bridge Scour.” *Water Reosurces Publications*, LLC.
- Mesfin G, Shuhaimi M (2010). “A chance constrained approach for a gas processing plant with uncertain feed conditions.” *Comput Chem Eng* 34(8):1256–1267.
- Miller, A. J. (1990). “Flood hydrology and geomorphic effectiveness in the central Appalachians.” *Earth Surface Processes and Landforms*, 15(2), 119-134.
- MSHA (2010). “Manual for Hydrologic and Hydraulic Design.” Maryland State Highway Administration, Baltimore, MD Report available at www.gishydro.umd.edu.
- Mueller, D.S., and Wagner C.R. (2005). “Field Observations and Evaluations of Streambed Scour at Bridges.” Report FHWA-RD-03-052, Federal Highway Administration.
- Mugunthan P, Shoemaker CA, Regis RG (2005). “Comparison of function approximation, heuristic, and derivative-based methods for automatic calibration of computationally expensive groundwater bioremediation models.” *Water Resour Res* 41(11):n/a–n/a, w11427.
- National Weather Service (2011). “Preliminary Hurricane/Tropical Storm Irene weather summary for the North Country.” National Weather Service Forecast Office, Burlington VT, <<http://www.erh.noaa.gov/btv/events/Irene2011/>> (Accessed July 2014).
- NOAA (2016). “Mean annual temperatures at Burlington Vermont international airport: 2000–2015.” <http://w2.weather.gov/climate/xmacis.php?wfo=btv>.
- Okada, S., Mitamura, H., Ishikawa, H., & Hokkaido, S. R. (2006). “The collapse mechanism and the temporary restoration of Omori Bridge damaged by the storm surge of Typhoon No. 18 in 2004.” *Technical Memorandum of Public Works Research Institute*, 40(9), 185-192.
- Okeil, A. M., & Cai, C. S. (2008). “Survey of Short-and Medium-Span Bridge Damage Induced by

- Hurricane Katrina.” *Journal of Bridge Engineering*, 13(4), 377-387.
- Olson SA (2002). “Flow-frequency characteristics of Vermont streams.” *Water- Resources investigations report 02-4238*, USGS.
- Olson S (2014). “Estimation of flood discharges at selected annual exceedance probabilities for unregulated, rural streams in Vermont, with a section on Vermont regional skew regression, by Veilleux, a.g. Scientific Investigations Report 5078.” US Geologic Survey.
- Padgett, J., DesRoches, R., Nielson, B., Yashinsky, M., Kwon, O. S., Burdette, N., & Tavera, E. (2008). “Bridge damage and repair costs from Hurricane Katrina.” *Journal of Bridge Engineering*, 13(1), 6-14.
- Padgett, J. E., Spiller, A., & Arnold, C. (2012). “Statistical analysis of coastal bridge vulnerability based on empirical evidence from Hurricane Katrina.” *Structure and infrastructure engineering*, 8(6), 595-605.
- Parker, Gary; Toro-Escobar, Carlos; Voigt, Richard L. Jr. (1998). ”Countermeasures to Protect Bridge Piers from Scour.” St. Anthony Falls Laboratory. Retrieved from the University of Minnesota Digital Conservancy, <http://hdl.handle.net/11299/112995>.
- Prendergast, L. J., and Gavin, K. (2014). “A review of bridge scour monitoring techniques,” *Journal of Rock Mechanics and Geotechnical Engineering*, 6, 138-149.
- Pugh C (1985). “Hydraulic model studies of fuse-plug embankments.” Tech. rep., Hydraulics Branch, Division of Research and Laboratory Services, Engineering and Research Center, US Dept. of the Interior, Bureau of Reclamation, Denver, CO.
- Rajeevan, M., Bhate, J., and Jaswal, A. K. (2008). “Analysis of variability and trends of extreme rainfall events over India using 104 years of gridded daily rainfall data.” *Geophysical Research Letters* 35.18: 1-6.
- Richardson, E.V., D.B. Simons, and P.F. Lagasse, (2001). “River Engineering for Highway Encroachments - Highways in the River Environment.” FHWA NHI 01-004, Federal Highway Administration, Hydraulic Design Series No. 6, Washington, D.C.
- Rios LM, Sahinidis NV (2012). “Derivative-free optimization: a review of algorithms and comparison of software implementations.” *J Global Optim* 56(3):1247–1293.
- Rizzo DM, Dougherty DE (1996). “Design optimization for multiple management period groundwater remediation.” *Water Resour Res* 32(8):2549–2561.
- Rosenbloom, N. A., & Anderson, R. S. (1994). “Hillslope and channel evolution in a marine terraced landscape, Santa Cruz, California.” *Journal of Geophysical Research: Solid Earth*, 99(B7), 14013-14029.
- Scawthorn, C., Flores, P., Blais, N., Seligson, H., Tate, E., Chang, S., Mifflin, E., Thomas, W., Murphy, J., Jones, C., and Lawrence, M. (2006). “HAZUS-MH Flood Loss Estimation Methodology. II. Damage and Loss Assessment.” *Nat. Hazards Rev.*, 10.1061/(ASCE)1527-6988(2006)7:2(72), 72-81.

- Schmocker-Fackel, P. and Naef, F. (2010). "Changes in flood frequencies in Switzerland since 1500." *Hydrol. Earth Syst. Sci.*, 14, 1581-1594, doi:10.5194/hess-14-1581-2010, 2010.
- Schmocker L, Höck E, Mayor PA, Weitbrecht V (2013). "Hydraulic model study of the fuse plug spillway at Hagneck canal, Switzerland." *J Hydraul Eng* 139(8):894–904. doi:10.1061/(ASCE)HY.1943-7900.0000733.
- Schultz, M. T., Gouldby, B. P., Simm, J. D., and Wibowo, J. L. (2010). "Beyond the factor of safety: Developing fragility curves to characterize system reliability." *Geotechnical and Structures Laboratory, Engineer Research and Development Center, Vicksburg, MS.*
- Seidl, M. A., and Dietrich, W. E. (1992). "The Problem of Channel Erosion into Bedrock." *CATENA SUPPLEMENT*, 23, 101-124.
- Sheppard, D. M., Demir, H., & Melville, B. W. (2011). "Scour at wide piers and long skewed piers (Vol. 682)." *Transportation Research Board.*
- Sheppard D, Melville B, Demir H (2014). "Evaluation of existing equations for local scour at bridge piers." *J Hydraul Eng* 140(1):14–23.
- Sheppard, D.M. and W. Miller, (2006), "Live-bed Local Pier Scour Experiments," *Journal of Hydraulic Engineering - ASCE*, 132(7), 635-642.
- Shlomi S, Ostfeld A, Rubin H, Shoemaker C (2010) "Optimal groundwater contamination monitoring using pumping wells." *Water Sci Technol* 62(3):556–569.
- Siegel, S. (1956). "Nonparametric statistics for the behavioral sciences." *International Student Edition-McGraw-Hill Series in Psychology*, Tokyo: McGraw-Hill Kogakusha.
- South Mountain Research and Consulting, Milone & MacBroom Inc (2010) "Quinlan bridge area alternatives analysis to reduce flood and erosion risks." *Tech. rep, Lewis Creek Association.*
- Somerville, D.E. and B.A. Pruitt. (2004), "Physical Stream Assessment: A Review of Selected Protocols for Use in the Clean Water Act Section 404 Program." Prepared for the U.S. Environmental Protection Agency, Office of Wetlands, Oceans, and Watersheds, Wetlands Division (Order No. 3W-0503- NATX). Washington, D.C. 213 pp. Document No. EPA 843-S-12-002.
- Springston, G. E., Underwood, K.L., Robinson, K., and Swanberg, N. (2012), "Tropical Storm Irene and the White River Watershed of Vermont: flood magnitude and geomorphic impacts in guidebook to field trips in western New Hampshire and adjacent Vermont and Massachusetts." 104th meeting of the New England Intercollegiate Geological Conference edited by P. Thompson & T. Thompson, University of New Hampshire and T. Allen, Keene State College (330 pages).
- Stager, C., & Thill, M. K. (2010). "Climate change in the Champlain Basin: What natural resource managers can expect and do." *Nature Conservancy, Adirondack Chapter.*
- State of Vermont (2012), "State of Vermont Tropical Storm Irene after action report/improvement plan final draft." p. 242 <https://gmunitedway.files.wordpress.com/2012/04/ts-irene-aar-ip-2012_0409_final.pdf> (Accessed July 14, 2015)
- Storn R, Price K (1997). "Differential evolution—a simple and efficient heuristic for global optimization

- over continuous spaces.” *J Global Optim* 11:341–359.
- Straub, L. G. (1934). “Effect of channel-contraction works upon regimen of movable bed-streams.” *Eos, Transactions American Geophysical Union*, 15(2), 454-463.
- Sturm, T. W. (2006). “Scour around bankline and setback abutments in compound channels.” *Journal of Hydraulic Engineering*, 132(1), 21-32.
- Thomas, P., Jones, T., Azizi, S.C., (2013), “Jousting with bridges.” FEMA’s Historic Preservation Section, Joint Field Office, Essex Junction, VT.
- Troy A, Wang D, Capen D, O’Neil-Dunne J, MacFaden S (2014) “Updating the Lake Champlain Basin land use data to improve prediction of phosphorus loading.” Tech. Rep. 54, University of Vermont, Lake Champlain Basin Program.
- U.S. Geological Survey, (2010), “National Water Information System data available on the World Wide Web (USGS Water Data for the Nation),” accessed [June 10, 2015], at URL [<http://waterdata.usgs.gov/nwis/>]
- U. S. Geological Survey (2011), “High flows in New Hampshire and Vermont from Tropical Storm Irene estimated.” U.S. Geological Survey, <http://nh.water.usgs.gov/WhatsNew/Irene_aug2011.htm> (Accessed July 15, 2014)
- U.S. Geological Survey, (2013), “National hydrography dataset, high resolution: U.S. Geological Survey, The National Map, National Hydrography Dataset,” available at <http://nhd.usgs.gov/> (accessed October 18, 2013).
- U.S. Geological Survey and U.S. Department of Agriculture, Natural Resources Conservation Service, (2013), “Federal Standards and Procedures for the National Watershed Boundary Dataset (WBD)” Techniques and Methods 11–A3, p. 63, <<http://pubs.usgs.gov/tm/11/a3/>> (Accessed January 13, 2016).
- VCGI (2006), “Vermont Hydrologically Corrected Digital Elevation Model (VTHYDRODEM).” Vermont Center for Geographic Information, Burlington, VT. <http://www.vcgi.org/dataware/search_tools/moreinfo.cfm?catalog_id=1&layer_id=28&layer_name=ElevationDEM_VTHYDRODEM> (Accessed June 2014)
- Vermont Agency of Transportation (2014), “Engineering Image Archives.” Vermont Agency of Transportation, <<http://vtransmap01.aot.state.vt.us/rp/dpr/Diphotowebstore//dpr.asp>> (Accessed June 2014).
- Vermont Agency of Transportation. (2015). “Hydraulics Manual.” <http://vtrans.vermont.gov/sites/aot/files/highway/documents/structures/VTrans%20Hydraulics%20Manual.pdf> <Accessed November 1, 2016>
- Vesterstrom J, Thomsen R (2004). “A comparative study of differential evolution, particle swarm optimization, and evolutionary algorithms on numerical benchmark problems.” *Evolutionary computation*, 2004. CEC2004. Congress on, vol 2, pp 1980–1987.
- Vocal Ferencevic, M., and Ashmore, P. (2012). “Creating and evaluating digital elevation model-based stream-power map as a stream assessment tool.” *River Research and Applications*, 28(9), 1394-

- Walsh, J., Wuebbles, D., Hayhoe, K., Kossin, J., Kunkel, K., Stephens, G., Thorne, P., Vose, R., Wehner, M., Willis, J., Anderson, D., Doney, S., Feely, R., Hennon, P., Kharin, V., Knutson, T., Landerer, F., Lenton, T., Kennedy, J., and Somerville, R. (2014), "Chapter 2: Our Changing Climate. Climate Change Impacts in the United States: The Third National Climate Assessment," J. M. Melillo, Terese (T.C.) Richmond, and G. W. Yohe, Eds., U.S. Global Change Research Program, 19-67. doi:10.7930/J0KW5CXT.
- Wang, H., Hsieh, S.-C., Lin, C., and Wang C.-Y. (2014), "Forensic diagnosis on flood-induced bridge failure. I. Determination of the possible causes of failure," *Journal of Performance of Constructed Facilities*, 28(1), 76-84.
- Wardhana, K., and Hadipriono, F. C. (2003), "Analysis of recent bridge failures in the United States," *Journal of Performance of Constructed Facilities*, 17(3), 144-150.
- Wark, N., Smith, K., Kennedy, M., Widing, S., San Antonio, J., and Wildey, R. (2015), "Hydraulics Manual, Vermont Agency of Transportation," available at: <http://vtrans.vermont.gov/sites/aot/files/highway/documents/structures/VTrans%20Hydraulics%20Manual.pdf> (accessed July 30, 2016).
- Wood, E. F., and Rodríguez-Iturbe. I. (1975), "Bayesian inference and decision making for extreme hydrologic events," *Water Resources Research*, 11(4), 533-542.
- Xu Z, Lu S (2011) "Multi-objective optimization of sensor array using genetic algorithm." *Sens Actuators B Chem* 160(1):278–286.
- Yankielun, N.E., and Zabilansky, L.J., (1999). "Laboratory investigation of time domain reflectometry system for monitoring bridge scour." *Journal of Hydraulic Engineering, ASCE*, 125(12), 1279–1284.
- Yu, X., and Yu X. (2010). "Laboratory Evaluation of Time-Domain Reflectometry for Bridge Scour Measurement: Comparison with the Ultrasonic Method." *Advances in Civil Engineering 2010* (2010): 1-13. Hindawi. Hindawi Publishing Corporation, 2010.
- Yu, X., and Yu, X., (2011). "Development and evaluation of an automatic algorithm for a time-domain reflectometry bridge scour monitoring system." *Canadian Geotechnical Journal*, Vol. 48, 26–35
- Yu, X., Zhang, B., Tiao, J., and Yu, X. (2013), "A new time-domain reflectometry bridge scour sensor", *Structural Health Monitoring*, 12(2), 99-113.
- Zabilansky, L.J., (1996). "Ice force and scour instrumentation for the White River, Vermont." *Special Report 96-6*, U.S. Army Corps of Engineers, Cold Regions Research and Engineering Laboratory.
- Zhao, X., Li, L., Ba, Q., and Ou, J., (2012) "Scour Monitoring System of Subsea Pipeline Using Distributed Brillouin Optical Sensors Based on Active Thermometry." *Optics & Laser Technology* 44, no. 7 (2012): 2125 – 2129. doi:<http://dx.doi.org/10.1016/j.optlastec.2012.03.015>.